8-9-2011

Achieving grid parity for large scale photovoltaic systems in New Jersey

Ulrich Schwabe

ACHIEVING GRID PARITY FOR LARGE SCALE PHOTOVOLTAIC SYSTEMS IN NEW JERSEY

by
Ulrich Klaus Wilhelm Schwabe

A Thesis

Submitted to the
Department of Electrical & Computer Engineering
College of Engineering
In partial fulfillment of the requirements
For the degree of
Master of Science in Engineering
at
Rowan University
December 20, 2010

Thesis Chair: Peter Mark Jansson, PhD PP PE

Dedicated to

My parents, Dr. Stefan Klaus Friedrich Schwabe and Maria Elisabeth Schwabe, who have been stalwart role models and loving supporters all my life, and Dr. Peter Mark Jansson for being an encouraging mentor who gave me a chance to prove myself, while inspiring a greater thirst for knowledge.

Abstract

Ulrich Klaus Wilhelm Schwabe
ACHIEVING GRID PARITY FOR LARGE SCALE PHOTOVOLTAIC SYSTEMS IN NEW JERSEY
2010
Peter Mark Jansson, PhD PP PE
Master of Science in Electrical & Computer Engineering

With photovoltaic (PV) power systems becoming ever more prevalent in today's world, it is an inevitability that this renewable energy technology becomes more competitive from a price standpoint. Explored in this thesis are several engineering optimization and cost reduction methods that will enable large scale PV system costs to achieve grid parity in the next few years without requiring government subsidies or market support techniques. This research included actual data from numerous real world, large scale photovoltaic projects the author engineered in the northeastern United States and is informed by those design optimizations, best practice guidelines for proper photovoltaic system installation and parameter selection, as well as performance analyses of differing technologies. Incorporating historical data, a model is presented to help predict future photovoltaic system price-points and subsequently their associated electricity costs. Finally, an in-depth walk through of the engineering improvements required and their associated financial impacts requisite for the realization of grid parity for large scale photovoltaic systems in New Jersey brings clarity to an oft misrepresented and confounded topic.

Table of Contents

List of Figures

List of Tables

Chapter 1. The History of Photovoltaics & Technology Overview

1.1. The History of Photovoltaics

Ever since French physicist Alexandre E. Becquerel made the discovery that the presence of light affected conductivity in one of his selenium experiments, photovoltaics (PVs) have caught the interest of scientists and regular folks around the world. [3] Stalwarts of the scientific community such as Heinrich Hertz, Albert Einstein and Bell Labs' scientists continued to make headway in providing humanity with a truly sustainable means of energy generation. Hertz was first to discover the photoelectric effect, Einstein won the Nobel Prize for his discovery of the underlying theory. [73] For about half a century, selenium had been the only commonly known material to exhibit a photovoltaic effect, which individuals such as William G. Adams, Richard E. Day and Charles Fritts used to create the first photovoltaic cells. [74] Daryl Chapin, Calvin Fuller and Gerald Pearson at Bell Labs unintentionally discovered that one of their doped silicon transistors generated a useable amount of current in the presence of light, a breakthrough that set the stage for the future of PVs. Their efforts in the early 1950s produced cells that converted 6% of incoming sunlight into electric energy, but the immense costs associated with production kept them from becoming commercially viable for energy production. Applications were limited to expensive toys and gadgets until the late '50s when they proved a valuable source of energy for the satellites and spacecraft the U.S. deployed during the space race. Debatably the most prominent satellite instrumentation expert at the time, Hans Ziegler of Munich, Germany stood in opposition to the Navy's proposed chemical battery source for satellites and tried to push the use of PVs instead. He argued that any batteries would last only a few days to possibly weeks,

whereas an integrated PV system would keep supplying power for several years. The Navy relented and compromised on powering the next satellite with a dual supply of both batteries and solar cells. Dr. Ziegler was proven right within just a few days when the onboard batteries ceased to supply power to Vanguard I. However, the satellite remained operational for seven more years thanks to the four solar cells Ziegler managed to get on board. [74] This first satellite powered via PVs was only the fourth to be put into space from earth. It was dubbed the Vanguard 1, after the Vanguard rockets utilized as launch vehicles. Though NASA had launched several satellites utilizing PVs as their power source, there was still skepticism that such cells would be able to power their most ambitious and power-hungry projects. It saw solar power as a mere placeholder until small nuclear reactors would provide decade-long power for their spacecraft and satellites. Advancements in PVs ultimately made them the technology of choice for all but deep-space probes, as ever more ingenious and intricate systems provided ample amounts of power to meet increasing requirements. With a strong foothold as a power source for space vehicles and satellites, PVs secured their future and further investments that would increase their efficiency and versatility.

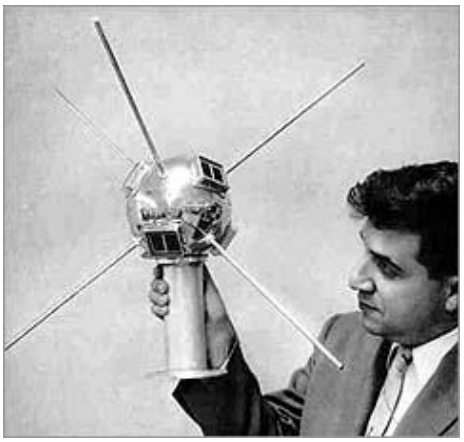

Figure 1-1. Vanguard I, the first Sattelite power by Photovoltaics [24]

This monopoly on providing space equipment with power did not, however, translate into cost effective generation on earth, with module costs remaining above $70/Watt. With size and weight being the most important factors to NASA due to the immense costs of placing payloads in orbit, the costs of PVs in comparison were

insignificant. It wasn't until the 1970s that the oil and gas giant Exxon began funding research that would lead to reductions in manufacturing costs of 80%, essentially making PV technology commercially viable and competitive for use with other remote power system options on earth. Exxon funded the work in order to replace the expensive battery setups required for warning lights on oil rigs and buoys. PVs were also used in cathodic protection systems that required little energy in remote locations, situations in which simple battery packs proved uneconomical. Over time more and more uses for PV power became evident, often being utilized in situations where small amounts of power were necessary yet utility interconnection or other means of supply were cost or maintenance prohibitive. (In some cases having to replace the expensive chemical batteries on set intervals actually cost more than the buoys they were mounted on.) Over the next decade into the late 90's, module prices decreased another 75% and stabilized at approximately $4/watt, a limit where costs would stagnate for almost another decade. Even though manufacturing costs continued in a slow but steady decline, a lack of competition in the market resulted in little change in consumer costs. At such a high price per watt, large scale energy production via PVs was economically unattractive. Exacerbating the situation were the record low oil and gas prices during the 1990's, which left PV technology non-competitive for most energy needs. This trend has undergone a radical reversal in recent years, spurred by technological advancements and increases in demand, creating manufacturing growth on a global scale.

1.2. Technology

On a very basic level, a standard silicon solar cell is merely a combination of two layers of doped silicon, one doped to be positive, the other doped to be negative, to form a PN junction. The most common materials used to dope these two layers are Boron and Phosphorous, having three and five valence electrons respectively. With Silicon's four valence electrons, Boron doping leads one cell layer to become a hole donor (p-type), while the addition of Phosphorus to the other creates an electron donor (n-type). Electrons from the n-type region move by diffusion to the p-type side, while leaving behind an accumulated positive charge in the n-type material. Diffusion only happens in a small area in the vicinity of the interface which, once equilibrium has been reached, creates what is known as the depletion region. It is this region that gives a solar cell the same behavior as a diode in that it creates a strong static E-Field at the junction, preventing electron drift with the absence of a bias voltage, light source, etc.

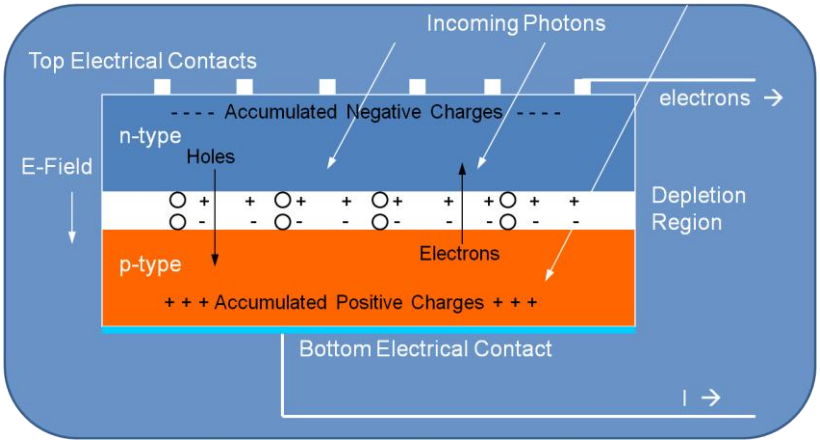

Figure 1-2. Illustration of PV cell cross section [36]

The electron drift that now occurs can be used to do work by creating a pathway through which the electrons (and in the reverse direction, current) can flow. Freed electrons move

toward the p-side where they are again caught by the E-field where they drift across the depletion region once more. Since this will only happen with electrons that have been freed by an increase in energy, an increase in photons (the energy equivalent of the valence electrons) striking the solar cell will cause an increase in current - while the voltage across the cell stays relatively stable. This happens due to the fact that a buildup of charge would cause the depletion region (just as in a diode) to become forward biased, at which point in time electrons drift across it instead of the outside current loop. This essentially limits the open-circuit voltage (Voc) to generally around 0.6V, depending on the type of materials and concentrations used in the manufacturing process. Current is limited by the number of available free electrons, which means it is theoretically only limited by the amount of incident solar radiation that the cell can convert.

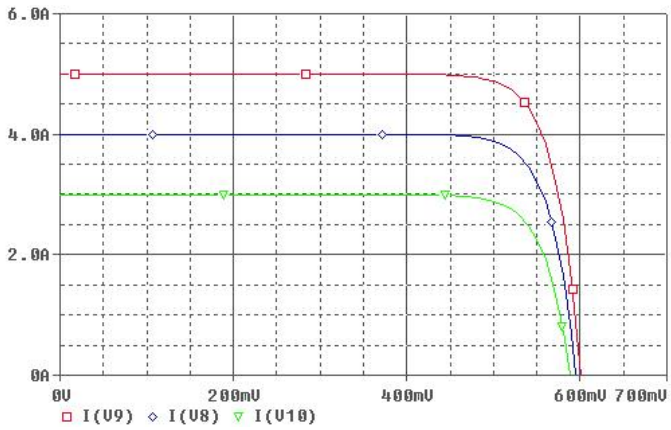

Figure 1-3. IV Curve of a PV Cell

The figure above gives a standard IV curve for an ideal PV cell, with current remaining nearly constant until the turn-on voltage of the p-n junction diode is reached. It would produce the highest current at 0V, giving the short circuit current (Isc). Maximum power lies somewhere within the knee, where both voltage and current remain high, and is called the maximum power point, comprised of a voltage (Vmp) and current (Imp).

1.3. Types of PV

1.3.a. Crystalline Silicon

Most photovoltaic cells today are based on silicon technology, a majority of which is crystalline silicon (c-Si). In terms of efficiency, commercially available c-Si PVs are the most efficient, but at a significant premium in costs due to expensive manufacturing processes and materials. Crystalline PV technology is divided into two major subgroups, single-crystalline Silicon (mono-Si) and multi or poly-crystalline Silicon (poly-Si). Single crystalline cells start out as silicon wafers identical to those used for the production of integrated circuits. The method, commonly known as the Czochralski process (illustrated in Figure 1-4), consists of melting a batch of high purity poly crystalline silicon, doped with either n- or p-type material, in a quartz crucible. A small seed crystal is dipped into the molten silicon and slowly rotated and pulled out. As the molten silicon molecules attach themselves to the existing structure they form an ever increasing rod consisting of a single crystal. [50] This 'ingot' is then cut into wafers, which can be textured to act as a sort of anti-reflective layer to increase the amount of light entering the cell. For the production of PV cells, the silicon is generally doped with boron to create p-type wafers which are then doped again with n-type material on one side in a later diffusion or ion implantation process. In most cases phosphor diffusion is be achieved by coating the surface of a wafer and heating it to specific temperatures, timing the diffusion process ensures desired penetration results. [9]

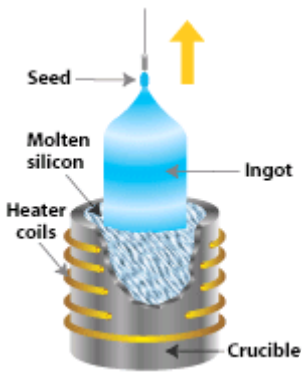

Figure 1-4. Single crystalline ingot. [10]

Once enough of the phosphorus has diffused, the wafer is brought back down to room temperature, after which the process is complete.

With single-crystalline silicon cells being the most efficient cells with today's technology, up to 24%, poly-Si cells are a close second having shown up to 20% efficiency. The price of poly-Si is brought down significantly by more economic manufacturing practices. Poly-Si ingots are made by simply pouring molten silicon into easily managed forms which, when cooled, solidify into a multitude of smaller crystals. It can then be processed in the same way that single crystalline modules are, being cut and textured in accordance with the customer's specifications. While it still relies on large quantities of expensive high purity silicon, it does not suffer from the sizeable costs and time consuming process of growing an ingot made of a single large crystal. Behavior of single and poly-crystalline cells are nearly identical, with the major exception being their efficiency differences. One thing to consider is their efficiency degradation with age, though this may not be as pronounced as with other cell types.

1.3.b. Other Silicon Types

The third most common type of PVs based on silicon are amorphous silicon (a-Si) thin film modules. Still a relatively new addition to the world of large scale solar power generation, a-Si cells have actually been around since 1976, used mostly on small electronics such as calculators. [5] The advantage of these types of cells is that silicon is usually deposited by chemical vapor deposition (CVD) and uses much less of the expensive high purity silicon than crystalline technology. For the average module this can be as little as 1/300th the amount necessary for c-Si production. Most crystalline PV cells are around 250–350 µm in thickness. [45] The amount of silicon being deposited on the substrate can also be tightly controlled without waste, leading to very thin, flexible layers that can be placed on a large variety of substrates. These can range from standard glass to sheet metal and plastics, and make a-Si modules anything from rigid to completely flexible. The ability to vary the thickness and flexibility of these cells has greatly increased the number of applications that are commercially available today. It has given rise to multi-junction techniques, utilizing several layers of different cell types, that widen the frequency band of light they react with, increasing their efficiency almost two-fold. Transparent modules are available as replacements to windows or can even be placed on greenhouses,

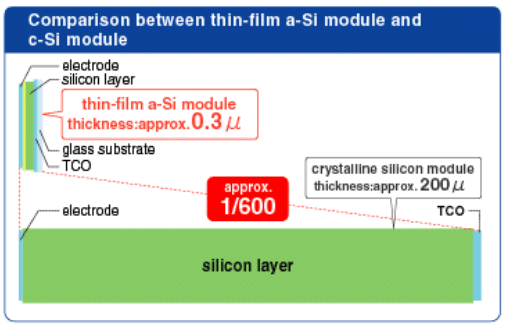

Figure 1-6. Silicon vs. thin-film cross sections [42]

Figure 1-5. Flexible thin film PV mat. [102]

where they produce power while also promoting healthier plant growth due to protection from UV rays. For households, farms and other buildings, solar shingles are available that can be nailed or screwed into place and integrate perfectly with the roof. Yearly production capacity has increased dramatically, since almost the entire process can be automated. Nominal output per cell does not vary significantly, as they do with crystalline PVs, and thus the matching of cells is no longer necessary. Unfortunately a-Si has a significant disadvantage, it still greatly lags behind c-Si in terms of conversion efficiency. When area is a concern and there is a need for substantial electrical production, crystalline technology still has strong market advantages over amorphous. The solar conversion efficiency for single cell a-Si currently ranges between 6-12%, with a theoretical maximum of ~15%. [95] With multi-junction cells, that number increases rapidly, in theory reaching close to 30%. [4] One serious issue with a-Si has been light induced degradation over time, an effect first observed by Staebler and Wronski soon after their creation of the first amorphous cells. [44] Degradation occurs due to the nature of the structural composition of a-Si, and the CVD use of silane gas (SiH_4) as the main carrier for silicon. In a crystalline structure, silicon atoms bond in tetrahedral fashion to four of their neighbors. Since amorphous silicon lacks this rigid structure, atoms throughout the deposition have dangling bonds (defects), which alter the electrical properties of the material. Filling these open bonds with hydrogen corrects much of the issue. However, the addition of hydrogen also introduces the light induced degradation from initial efficiencies, down to what is commonly known as the stabilized efficiency. This stabilized efficiency is the nominal efficiency that manufacturers can advertise for their module's performance, and has increased over the years with advancements in

manufacturing and technology. The dilution of the silane gas used for the CVD process with hydrogen has benefitted the efficiency retention significantly. [104] Various other thin film technologies have made their way to market. The sector itself is poised to grow significantly over the next few years, from a market share of 13% in 2007 to 34% by 2012, see Figure 1-7. [56]

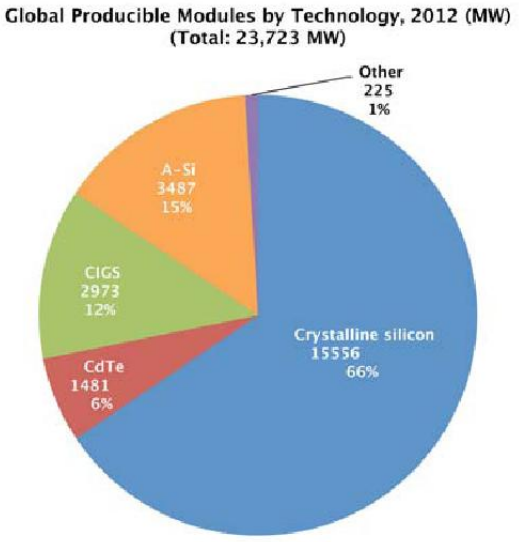

Figure 1-7.PV Tech forecast for technology in 2012 [56]

1.3.c. CdTe and CIGS

The most notable in terms of projected growth are copper indium gallium di-selenide (CIGS) and cadmium telluride (CdTe) cells, both of which are an improvement over amorphous silicon in terms of efficiency. CdTe cells are currently still the second most produced type of thin film, but they are expected to be overtaken by CIGS within the next two years. A very large part of the CdTe manufacturing capacity in the world comes from the U.S. company FirstSolar, as it has chosen to focus entirely on manufacturing CdTe modules. It has reached over 1.2GW manufacturing capacity by the end of 2009. [26] With a maximum efficiency of 11.1% , their modules are about half as efficient as the leading c-Si modules available to the consumer. [27] However, as with all

thin film technology prevalent on the market today, their cost effectiveness is a major seller. Manufacturing costs are already below $1/W, which gives them a significant advantage over manufacturers of crystalline modules, which are somewhere in the $1/W and $1.50/W range. It is expected that CdTe costs will decrease down to $.65-.7/W by 2012. [26]

CdTe cells are most commonly made by electro- or chemical vapor deposition. Unlike other cells, their manufacture starts with a superstrate, meaning deposition is made to the topmost part of the cell rather than the bottom most. This superstrate consists of a piece of glass coated with tin-oxide via CVD, which is commonly done to create an adhesion layer for various other coatings (as well as serving as a transparent conductor). Onto this superstrate, cadmium sulfide (CdS) is deposited via chemical bath deposition (CBD) as the n-type material. Cells may display a yellow tint depending on the thickness of the CdS layer. A layer of CdTe is then applied usually via chemical vapor transport (CVT), a method of applying crystallized layers of material, and chemically etched. This etching leaves its surface ready for the addition of a back contact, which can consist of a variety of materials ranging from carbon paste containing copper and tellurium and mercury tellurium to a combination of other metals and copper. Copper is the only essential part in the backing as it strongly affects the performance and stability of the solar cell. [101] The thickness of the CdS layer has been drastically reduced over the years, from several μm down to fractions of a μm. This was first proposed by Dr. Ting Chu at the University of South Florida after his findings that CdS layers thicker than .5 μm will block more than 20% of all incoming light. With this method it was possible to

create the first cell, which reached 15% efficiency. [105][46] Kumazawa et al. show that a thickness on the order of 60nm keeps a high V_{OC} while maximizing I_{SC}. [46]

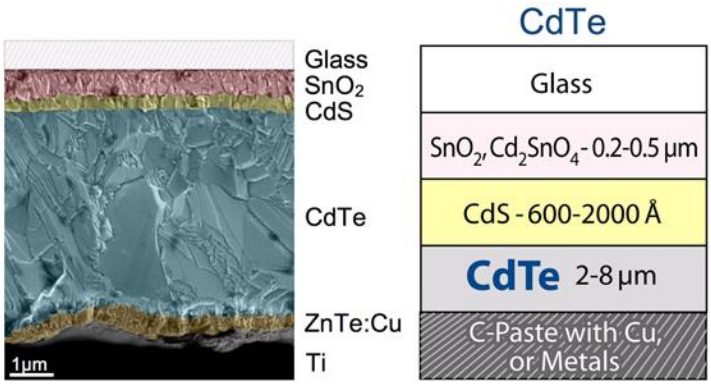

Figure 1-8. Cadmium Telluride cell cross section [66]

Since CdTe is the main component of these cells, reducing its thickness can reduce costs and eliminate waste. Some research suggests that 90% of all incident near infrared light is absorbed by a mere ~1µm of the material, while the standard thickness of CdTe at the time was between 2-13µm, leaving ample room for improvements. [30]

CIGS technology has been the focus of attention for many manufacturers due to their higher efficiencies, which rival poly-Si percentages, while production is relatively easy and cost effective. Their reliability is exceptional, in some cases no drops in efficiency have been observed over periods as long as 18 years and substrate applications are at least equally as versatile as other thin films. CdTe cells are currently still less expensive to produce per unit area due to highly efficient manufacturing processes, but this is expected to change in the upcoming years as semiconductor materials will be the most prominent drivers for costs. [66] CIGS will also benefit from innovative processes to hit the market soon. The company most often associated with CIGS and next generation technology is NanoSolar [59], which use nano-particle ink to print modules, and forecast selling modules for less than $1/W and efficiencies of nearly 15% [30]

Figure 1-9. Nanosolar ink and printing process [59]

Common methods for creating CIGS cells rely on standard manufacturing processes, which usually start by sputtering molybdenum on glass. This layer is "optimized for adhesion, sheet resistance and morphology where it allows sodium from the glass to diffuse through the CIGS layer." [66]

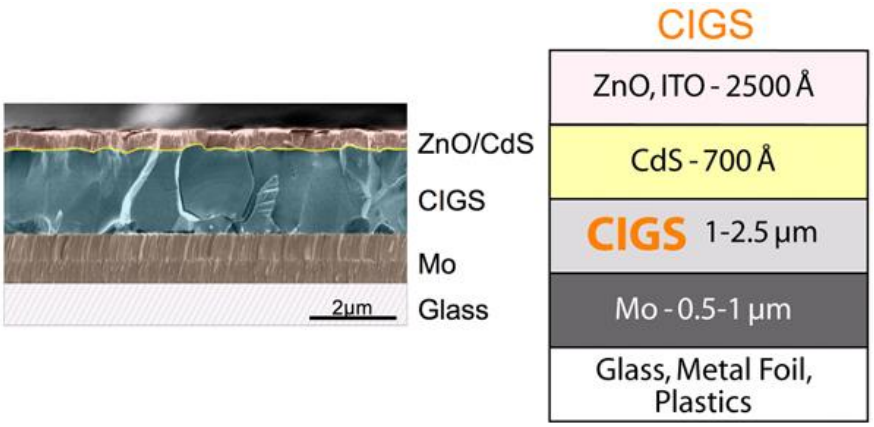

Figure 1-10. CIGS cross section [66]

A sodium content of about 0.1% is necessary to enhance grain growth, and with it carrier concentrations which ensures an additional conversion efficiency of around 3%. [66] After this Mo layer, the CIGS compound is placed either by evaporating all of the necessary elements at once (or in a specific order), sputtering of the metals and selenization thereafter, sputtering of metals with selenium vapor, or printing the metals and selenization as in the Nanosolar method. The n-type material used for this technology is the same as in CdTE, namely CdS. A very thin layer of CdS is placed via CBD,

ensuring that during operation a maximum of all freed electrons make their way to the CIGS side to optimize conversion efficiency. The final zinc oxide layer is placed on top via CVD, which acts as a transparent conductor and contact for the cell. [66] [72]

The biggest issue for non-ink manufacturing methods for CIGS (as well as CdTe) that include sputtering, are their reliance on a high vacuum, where the necessary elements are evaporated. These are hampered by a poor utilization of the materials, which in the case of indium for CIGS and tellurium for CdTe cells pose serious problems. [66] [101] LCD screens have grown to be the number one user of indium over the last few years, which has spurred worries of indium shortages for CIGS cells due to the LCD's competition and limited production of the metal. The reality of indium's abundance on earth however paints a much less gloomy picture for CIGS's future. Concentrations for indium in the earth's crust are higher than those of silver, and while silver is produced at a rate of 20,000 tons per year, indium is only extracted at a rate of about 400. [75] Indium has thus far only been extracted from zinc and lead concentrates due to its abundance in the metals. With an increase in demand, indium suppliers predict sustainable increases in production with new mining investments and increases in recovery yields from other substances. [75]

CdTe cells on the other hand seem not to share CIGS's fortune in terms of future prospects. First, some people predict CdTe cell producers will run into difficulties with their non-RoHS (the Restriction of Hazardous Substances Directive) compliant materials, as cadmium is the third of only six substances restricted by the directive. [1] Secondly, tellurium poses a serious issue especially due to its production limitations as it is the ninth rarest element on earth. A growing number of uses for the material will further

impact tellurium's availability for CdTe cell makers. These uses range from the media layers in rewriteable discs, memory chips and solid state electronics to thermoelectric devices, which have enjoyed an increase in use over the last few years. The limited number of Te producers in the world leads one to believe that CdTe cell production might not sustain the same rate of growth they have had thus far. [88][83] However, First Solar is confident about their Cd and Te supply for future growth in line with their expectations, and might even be able to benefit from their recycling guarantee in the future. [26]

1.3.d. Energy Conversion Efficiency

The most important characteristic of a PV cell is its effectiveness in converting sunlight into useable electricity. The various types of cells available today all vary greatly in their efficiency – both in theory and practice. Single-crystalline cells are by far the most efficient at one sun, having reached close to 25% efficiency in laboratory settings, while multi-junction cells have shown efficiencies over 40% when subject to concentrations of more than 200 times normal insolation. Polycrystalline technology has a maximum efficiency of approximately 20%, cheap CIGS thin film technologies are just below 20% efficiencies. Amorphous modules have the lowest efficiencies for existing technologies, with a maximum of about 12%, of nano- or microcrystalline modules have shown efficiencies of over 16%.

Figure 1-11. summarizes the efficiencies of PV technologies including the emerging dye-sensitized and organic PV cells, which have been found to have efficiencies of 11% and over 5%, respectively.

Energy conversion efficiency (η) is generally calculated by taking the ratio of the input and output power of a system according to (1).

(1) $$\eta = \frac{\text{Poutput}}{\text{Pinput}} * 100\% = \frac{\text{P}_{max}}{\text{W m}^{-2} \times \text{Area}}$$

Where P_{max} is the maximum power,
Wm^{-2} is derived from the solar irradiance, and
A is the area of the collector, in an environment of STC. (STC being the Standard Test Conditions of 25°C ambient temperatures and $1kW/m^2$ of insolation)

Instead of recording maximum power, or irradiance at specific intervals, a more practical way of calculating the actual efficiency of a solar module in the field is shown in (2), which uses insolation, system output energy, and collector area for a given day; i.e., η is computed as the ratio of output energy to input energy.

(2) $$\eta = \frac{E_{System}}{insolation \ *Area} \Longrightarrow \frac{kWh_{System}}{(kWh_{Sun}/m^2) \times m^2}$$

Where kWh_{System} and kWh_{Sun} can be recorded over any period of time, with varying degrees of accuracy due to the meteorological situation and temperature effects on the module efficiency.

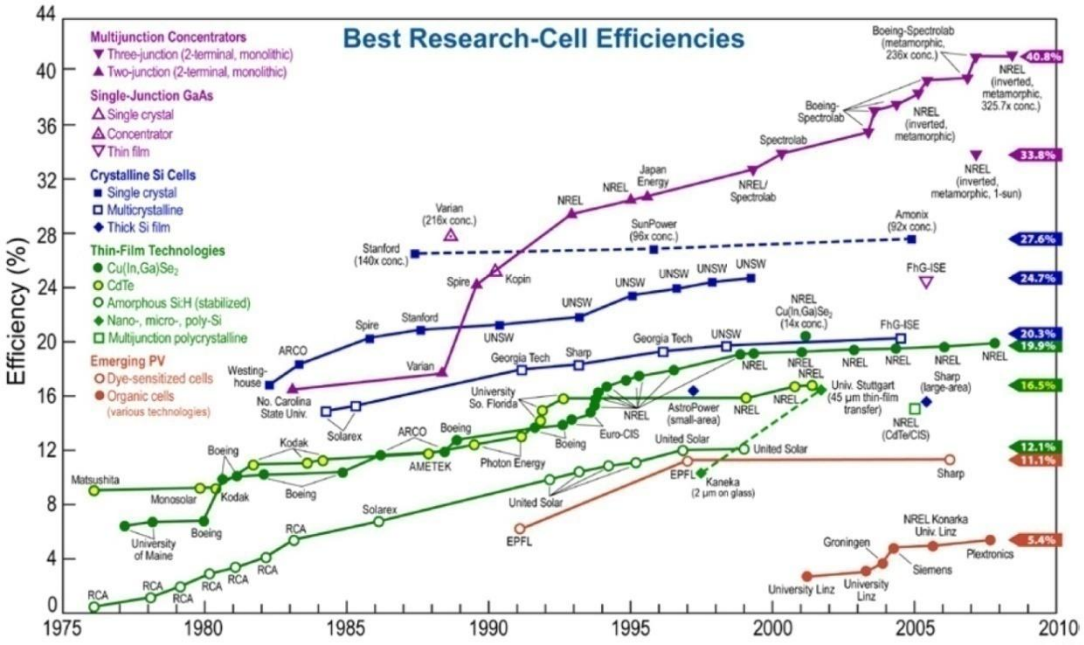

Figure 1-11. PV technology efficiency timeline [47]

1.4. Existing Generation Costs & Outlook

The main means of supplying electricity to the grid in the US consist of coal, natural gas, nuclear and hydro electric, ranked first through fourth respectively. Natural gas has climbed to overtake nuclear in 2006 with a total of 876 terawatt-hours (TWh) produced with gas in 2008, versus 806 TWh for nuclear. Coal holds a strong pole position with close to 2 petawatt-hours (PWh) having been produced in 2008, while hydroelectric means of generation have netted fourth place with approximately 250TWh. The US consumed a total of 4.11PWh in 2008. [12]

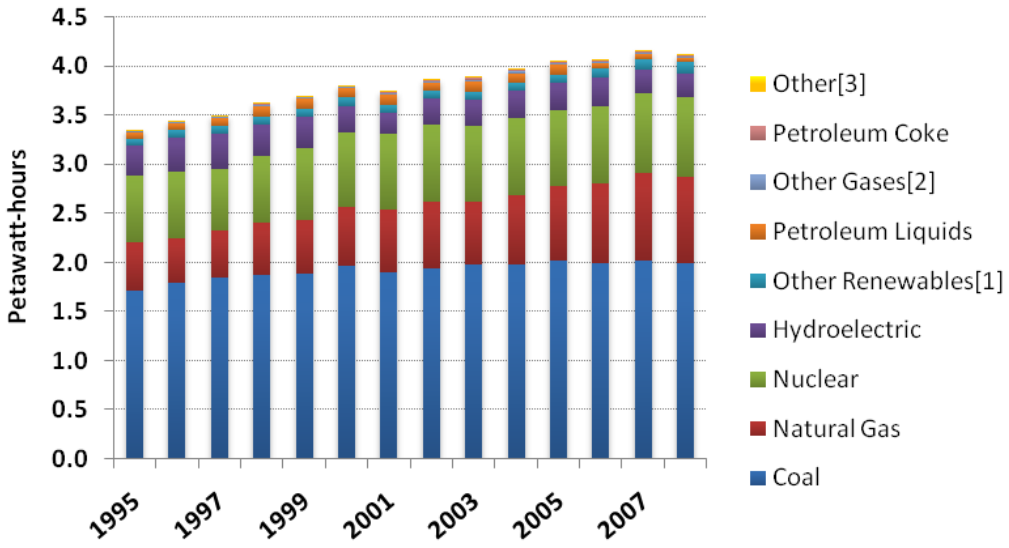

[1] Wood, black liquor, other wood waste, biogenic municipal solid waste, landfill gas, sludge waste, agriculture byproducts, other biomass, geothermal, solar thermal, photovoltaic energy, and wind.
[2] Blast furnace gas, propane gas, and other manufactured and waste gases derived from fossil fuels.
[3] Non-biogenic municipal solid waste, batteries, chemicals, hydrogen, pitch, purchased steam, sulfur, tire-derived fuel, and miscellaneous technologies. (Data source: EIA Aug 14, 2009)

Figure 1-12. Breakdown of electricity generators in the US

In New Jersey nuclear power plants the largest role with 50.4%, or ~32TWh, of its electricity use being generated by the four nuclear power plants in the state. Natural gas and coal are second and third with 32.7% (~20.5TWh) and 14.6% (~9.2TWh) respectively. [62]

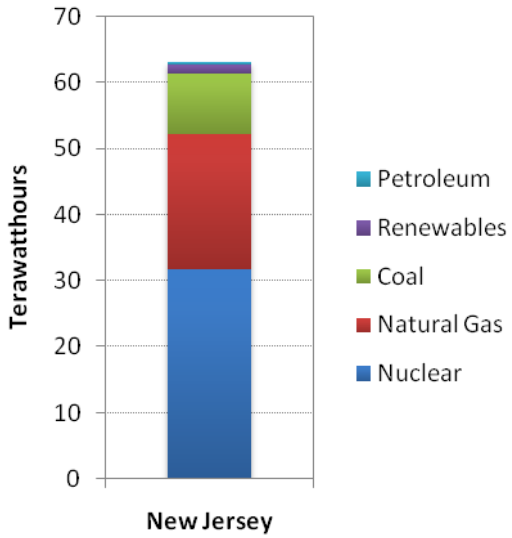

Figure 1-13. Breakdown of NJ electricity generators in 2008 [62]

The main suppliers of electric energy are generally referred to as baseline generators, since they account for over 90% of all capacity. Most of the plants designed to provide this bulk energy are very large-scale, they long periods of time to start up and require a great amount of planning to shut down without disrupting the grid, which makes their downtime expensive. This means baseline generators are designed to run continuously throughout the whole year, keeping the volume of generated supply high and energy costs for the consumer low. For this reason, nuclear, coal and other such large plants are designed to run as close to maximum capacity as possible, their sheer size rendering it difficult for them to significantly alter their output to meet large short term changes in consumer demand. Such changes occur frequently during specific times of the day, for example when many consumers turn on appliances at the same time. The most significant of these load peaks appears during the summer, when high usage of air conditioners creates large spikes in demand that cannot be met by baseline deliverers. These peak loads must be supplied by smaller power plants, often located locally, capable of ramping up and down quickly to respond to rapid changes in demand. Their small size, limited hours of use and expensive fuels make them costly to operate, which drive prices during peak demand periods to their maximum on most grids. This fact can make PV generation financially more attractive during the summer months, when peak PV generation is coincident with the highest demand, best insolation, and highest energy prices. Since the maximum generation of a PV system coincides very nicely with the increase in per kWh costs on the margin, PV can become competitive – especially as rising fossil fuel (and in the future, uranium) costs continue to drive consumer electric prices to new peaks. While the current economic climate caused a large drop in

commodity fuel prices, the laws of supply and demand tell us that we have yet to reach a maximum in their costs.

The availability of naturally occurring commodity fuels is a topic of heavy debate as there is no one perfect method of measuring and estimating available reserves. Most predictions rely on dispersed core samples which are then interpolated via mathematical models, which together with estimates on extraction costs, possible recovery percentages and future demand, create a wide range of future outlooks. A perfect example of this is an analysis on the uranium supply for the next 50 years by the international atomic energy agency (IAEA). The report focuses on three possible scenarios of uranium demand (low, medium and high) and evaluates models based on a number of variables, ranging from numbers based on reasonably assured resources, estimated additional resources of varying degree, to resources of an entirely speculative nature. It then theorizes on the cost justifications for the extraction of the resource based on the estimated prices willing to be paid for the recovery and also includes projections on uranium enrichment tails (the amount of re-enriched uranium recovered and reprocessed after initial processing). [34] What this creates is a very wide range of future possible costs for the nuclear power industry with its prices affected by changes in everything from potentially available resources to recovery efficiencies. Such reports have been written annually for quite some time and provide an insight into what can be expected for any given resource. While the availability of cheap oil is heavily scrutinized (with some saying that world oil production has reached its global peak already) adjustments in proven reserves seem to occur with every new report, a property illustrated in Figure 1-14.

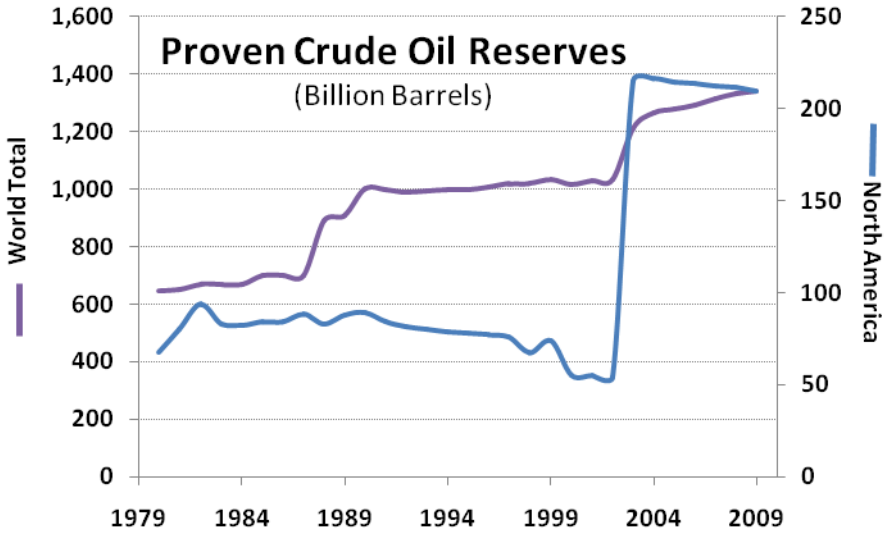

Figure 1-14. Proven oil reserves in the World and US (Data source: EIA)

While it seems that oil reserves are benefitting from newly found additions, coal may not be so lucky. Coal reserves have long been thought to be vast enough for 100 to 200 years supply, yet there may be some serious discrepancies in the resources and actual reserves around the world that these projections build on. [7][19] Much of the data has not been updated in several years, such as in the case of Vietnam whose assessments rely on 40 year old estimates. [19] China, while being the world's second largest supplier of coal, has not updated its numbers in over 20 years, a fact that poses a serious issue as they have since produced and used about 20% of their "then stated reserves". [19] Stark examples of overestimates exist in well developed countries as well, Germany and the UK have downgraded their proven recoverable reserves by over 90% - in 2004 Germany downgraded its hard coal reserves by 99%. [19] In the US, peak coal in terms of useable energy has already been reached, meaning coal prices and extraction costs will undoubtedly increase in the future. [17] [19]

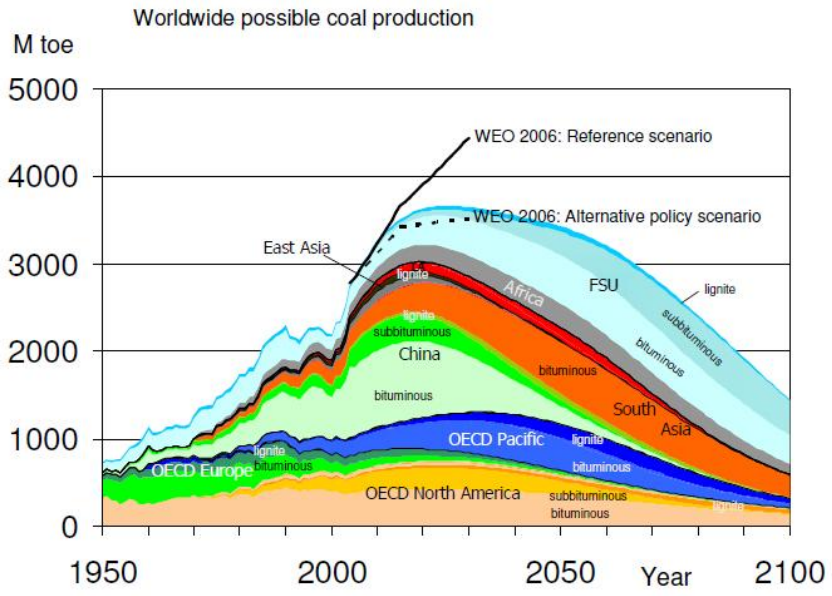

Figure 1-15. Coal production forecast [19]

The fact that these data are so unreliable and are usually overestimated could prove troublesome for the ever-increasing global demand. With China and other Asian countries ramping up significantly in terms of industrial growth and the US, Europe and former Soviet countries continuing their upward trend, coal may not be able to provide a cheap means of energy production for more than the next few decades. [8][19] For many, the most obvious solution to this problem would be the installation of renewable generators such as PV on a massive scale around the world. While a seemingly sound idea at a glance, in the current technological paradigm PVs are not likely to become a major replacement for fossil fueled and nuclear generation without some efficient means of inexpensively storing energy.

1.5. Overview of PV costs and Incentives

Grid connected PV systems are just beginning to be able to compete on a $/W basis with other means of energy generation, with government incentives playing a major role in the recent reduction of these costs. Of course the real measure of expense does not lie solely in the capital costs (expressed in $ per installed watt), but rather the fully loaded cost per unit of energy. In this case, the costs per technology for each generated kWh represent the most appropriate method of comparison. Table 1-1 gives a comparison of various types of generators. The numbers coincide with those seen in the early days of 2008 and are thus somewhat outdated, though they give a good indication of the wide spread between historical PV and standard means of electricity generation.

Table 1-1. Mean Price of Electricity per Technology

	Photovoltaic	Wind	Hydro	Geothermal	Nuclear	Coal	Gas
Cost ($/kWh)	0.240	0.070	0.050	0.070	0.067†	0.042	0.048

† According to NC WARN, Nuclear costs in NC have risen to $0.12-0.20/kWh, a staggering change from the sub-$0.10/kWh numbers usually estimated. [61] If true for NJ, PV will already have overtaken Nuclear generators in terms of its cost effectiveness.

Where other non-renewable sources of generation are able to supply energy needs day and night, solar power is only available for about a third of that time - increasing the overall cost per generated kilowatt-hour. While $/Watt numbers are starting to look very competitive, ¢/kWh costs tell a different story. Even though retail electricity prices from the utility have been increasing steadily over the last few years, the costs associated with PV per kWh still stand at more than double the current average of other generators. Policy changes in New Jersey and many other states are finally making renewable sources financially attractive, especially when supplemented by existing federal tax

incentives. A little over half of the 50 states have passed binding Renewable Portfolio Standards (RPS) which require that any utility operating within the state provide a fixed (and growing) percentage of their electrical generation through renewable sources. This indicates a growing future for renewables and lays the groundwork for PVs to become a means of adding substantial marginal capacity to the grid. In NJ the Energy Master Plan (EMP) [64] has provided guidelines and a plan of action to conserve energy, reduce peak demand, invest in renewable technology and develop an intelligent infrastructure to increase supply reliability. It also pushes to surpass RPS goals and achieve an electricity supply of 30% from renewable sources by 2020. Various methods have been implemented to generate interest in owning renewables, one of the most aggressive of which has been the infusion of money directly into the sector by way of setting (Solar) Alternative Compliance Payments ((S)ACPs) for the utilities. In order to achieve the goals set out by the RPS, every megawatt-hour generated through renewables is recorded and can be sold on an open market where utilities can purchase them. For PVs this unit is termed a Solar Renewable Energy Credit (SREC) and will openly be traded in the SREC market for a price not to exceed the SACP amount every year. Each SREC created by a PV system (after June 2009) will have a lifespan of two years. The SACP serves as a maximum price that the utility will pay for every MWh of their goal set out by the RPS that is not met by either offsetting generation through purchased SRECs or their own generation of electricity with PVs. This naturally sets an upper limit to the prices paid for SRECs, since utilities will never pay more for them than what it costs to pay the SACP. The NJ program set an SACP of $711 per MWh in June ’08, any generation before that point in time was set by the previous RPS SACP to not exceed $300/MWh. Every year

until energy year 2016, as the percentage of required PVs generation increases, SACPs will drop by 3% in price, see Figure 1-16, and market prices are expected to follow this trend closely (estimated at 70-80% of the SACP). If the SREC program is to be continued after 2016, the legislature will have to meet at least two years (by directive) before reinstating a new program and set new caps on SACPs. SRECs have played an instrumental role in the rapid growth of the PV market in New Jersey as they greatly reduce system payback periods and increase the rate of return on PV projects.

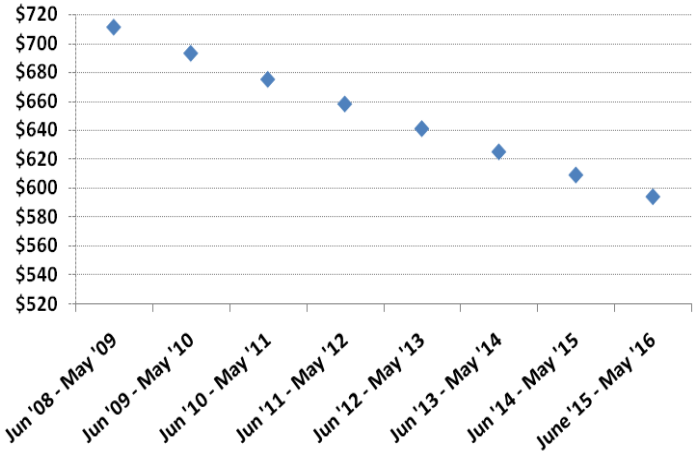

Figure 1-16. SACP limits, per energy year.

Chapter 2. Performance and System comparison for two Types of Modules

2.1. Introduction

Growth in the PV sector has spurred manufacturers, startups and researchers alike to come up with alternatives to standard crystalline silicon modules. While a few have already been mentioned, from c-Si to amorphous and CdTe to CIGS, there is even more technology on the horizon, from nano and micro crystalline thin film PV to dye-sensitized cells, organic cells and CIGS cylinders. With changes in materials used and manufacturing processes, applications can differ considerably. Approximately one and a half year's worth of data collected at the South Jersey Technology Park (SJTP) provides insight into the differences in performance between an amorphous silicon PV system and one consisting of single crystalline PV modules. While the efficiencies of the c-Si system were consistently superior to those of the a-Si system, some interesting trends were found where a-Si modules demonstrated some clear benefits The a-Si modules demonstrated superior performance in maintaining their efficiency during periods of time where modules exhibited temperatures above 30C° while c-Si modules showed serious drops. [37][87]

2.2. Two Types of Systems

The two systems being compared are both located on the roof of the SJTP, the larger 12.95kW c-Si system on the front facade and the 1kW a-Si system mounted on SolarDocks near the center of the flat roof of the building, (see Figure 2-1). Both are tilted at approximately 34° and share the same azimuth of ca. -24°. Meteorological

measurements are taken on the amorphous system only, as differences in insolation, ambient temperatures and wind-speeds are expected to be negligible. Module temperature is also measured solely on an a-Si module, though some discrepancy is expected to exist between the two for three reasons. First, the thermal mass of the a-Si modules is significantly lower, meaning that they will store less heat than their crystalline counterparts. Secondly, the backs of the c-Si modules are open, as compared to those of the a-Si modules. This gives the advantage to the c-Si modules, since they will benefit from better air flow on their back surfaces. The third difference could arguably be advantageous to either system; the lower module tilt of the reference c-Si system increases the amount of irradiance it receives during the summer months. However, this higher level of incidence with the sun could also lead to increases in module temperatures, benefitting the a-Si system in comparison. Since the change in tilt angle is slight (~2.5°), it is assumed to have less of an impact on the results than the other differences. Therefore only the first difference could be of benefit to the a-Si system. Though, since the comparison is done with respect to the a-Si module temperatures, any temperature increases which correspond to a decrease in performance of the c-Si modules are still valid, even if shifted by a few C°.

Figure 2-1. The c-Si and a-Si systems on the SJTP.

The a-Si system consist of 16 Kaneka [41] GSA-60W [43] modules, connected to a SMA [91] Sunny Boy 1800U Inverter. The c-Si system is composed of 74 Conergy S-175MU modules (rebranded SunTech Power STP175Ss) and is divided among three SMA inverters (two SB5000 and one SB 3000). [6] Both systems are monitored by the same SMA Web Box, which uploads hourly average values to the SMA SunnyPortal [96] website from the inverters, as well as data collected through the SMA Sensor Box. This allows for an hour by hour comparison of the two systems with respect to meteorological factors, module temperature and insolation.

2.3. Performance Characteristics

One of the most common methods of comparison for different types of modules is still the overall operational efficiency in terms of the amount of sun that is converted into electrical energy. This can be calculated relatively easily with eqn. (3), provided a reasonably accurate insolation reading is available.

$$\eta = \frac{\frac{kWh_{arrau}}{A_{array}}}{Solar\ \ Radiation} \tag{3}$$

Where kWh_{array} is the total output of the system
A_{array} is the total area of the system
Solar Radiation is the insolation incident with the surface

The efficiencies calculated with this equation give a good indication of the performance of one technology versus another, but the numbers are heavily dependent on the environment the modules are tested in. In some modules, efficiency will drop significantly with an increase in module temperature, a reason why almost all module datasheets list an expected drop in voltage, power and current per °C increase in

temperature. Since these values are determined in laboratory environments, it can be enlightening to see how various modules and technologies truly perform over extended periods of time, in varying outdoor environments. That was one of the main purposes of the analyses done on the data collected at the SJTP, where the relatively new thin-film amorphous silicon photovoltaic modules could be tested against a reference system composed of well known crystalline PV modules. The results were quite revealing during much of the summer; energy output per watt barely dropped for the amorphous system, whereas the silicon system lost more than 20% of its nominal capacity as modules reached temperatures around 60°C. Since the data were analyzed to be provided in technical reports to Kaneka, a method of comparison was developed that effectively compared the efficiency of both systems. Their difference is given as a gain which will either be positive or negative depending on the performance of the a-Si system with respect to the c-Si system (4).

$$\frac{\left(\frac{kWh_{a\text{-}Si}}{kW_{a\text{-}Si}}\right)-\left(\frac{kWh_{c-Si}}{kW_{c-Si}}\right)}{\left(\frac{kWh_{c-Si}}{kW_{c-Si}}\right)} = a\text{-}Si\ Gain\% \qquad (4)$$

Where $kWh_{a\text{-}Si}$ is the energy output by the amorphous system
$kW_{a\text{-}Si}$ is the nominal wattage of the amorphous system
$kWh_{c\text{-}Si}$ is the energy output by the crystalline system
$kW_{c\text{-}Si}$ is the nominal wattage of the crystalline system

Figure 2-2 gives the gain of the a-Si modules with respect to the c-Si modules. It shows the strong correlation between the drop in efficiency of the reference system in comparison to that of the a-Si system, indicating that the a-Si modules are much less affected by temperature increases than the 'thicker' crystalline types. It is especially intriguing to see differences as dramatic as those provided by the analysis. A "gain" of

20% represents a 20% drop in comparison to the output of the a-Si system by the c-Si system, this is a substantial amount of energy being lost due to the inefficiency induced by the operation and solar heating on the crystalline modules.

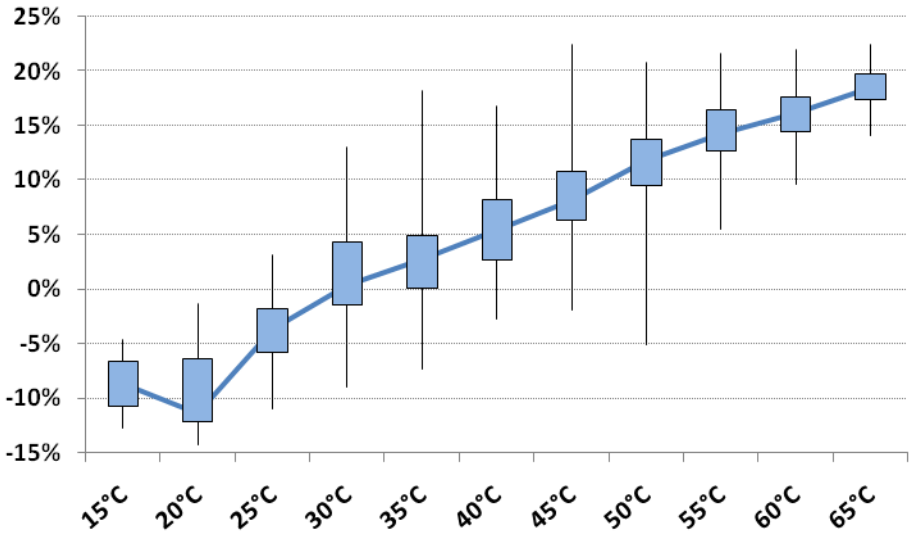

Figure 2-2. A-Si system gain, with respect to c-Si system.

The datasheet for the Conergy 175W modules provides a temperature coefficient of -0.48% Pmax for each C° of module temperature. The expected and actual data were very close, with outputs based on expected efficiency and real mean insolation data tracking actual generation precisely, Figure 2-3. Efficiency of the Conergy modules dropped to about 11.5%, coming from a maximum of almost 14.5% this represents a 20% drop in output, given in Figure 2-4.

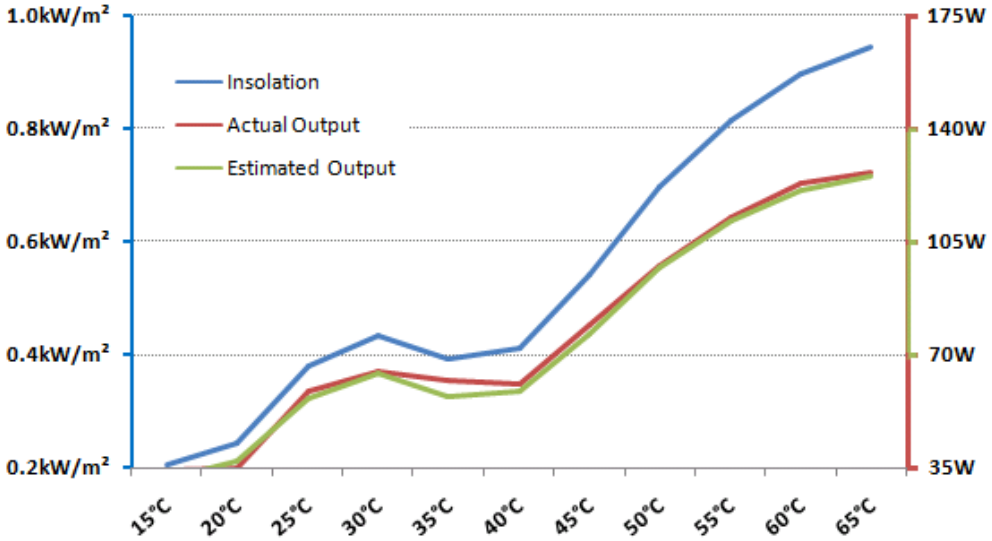

Figure 2-3. Actual versus estimated output per module temperature.

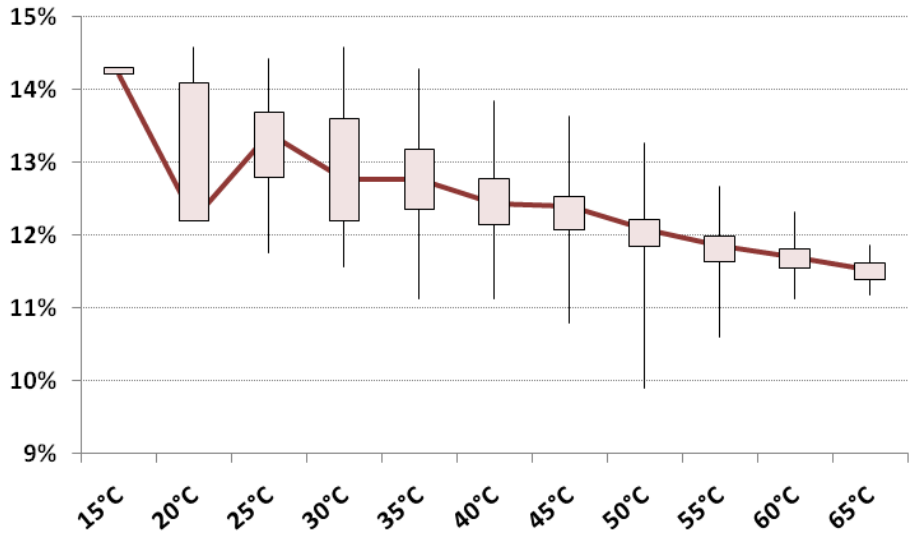

Figure 2-4. Efficiency of c-Si modules versus module temperature.

Kaneka's datasheet for their GSA-60 modules provides a -0.23% in Pmax for every 1C° increase in module temperature, starting at 0°C, which again gives a very good correlation to actual outputs during lower temperatures. A slight divergence between estimated and actual outputs can be observed at the highest temperatures, reaching 5W by 65°C. However, it should be noted that the literature speaks of amorphous module degradation and stabilization over the course of approximately a year, whereas Kaneka's

own datasheet states a 6 week period. [95][43] It is unknown if this will affect their resistance to high temperatures, but it is doubtful that the outputs will drop by the extent of those in the spec sheet based on these findings, Figure 2-5. By inspecting the efficiencies of the amorphous modules, there actually seems to be a slight up-trend in efficiency with an increase in temperature, this could be attributed to the high levels of insolation coincident with high module temperatures, Figure 2-6.

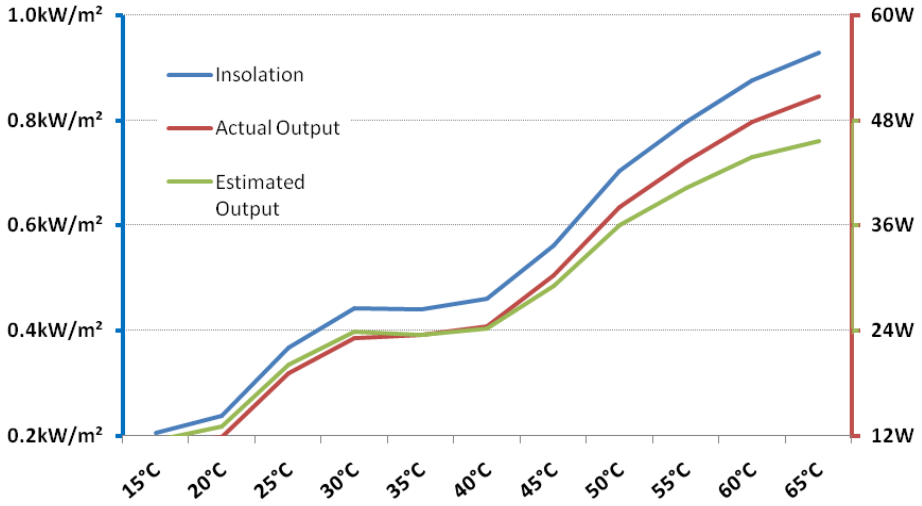

Figure 2-5. Module output comparison of modeled versus actual.

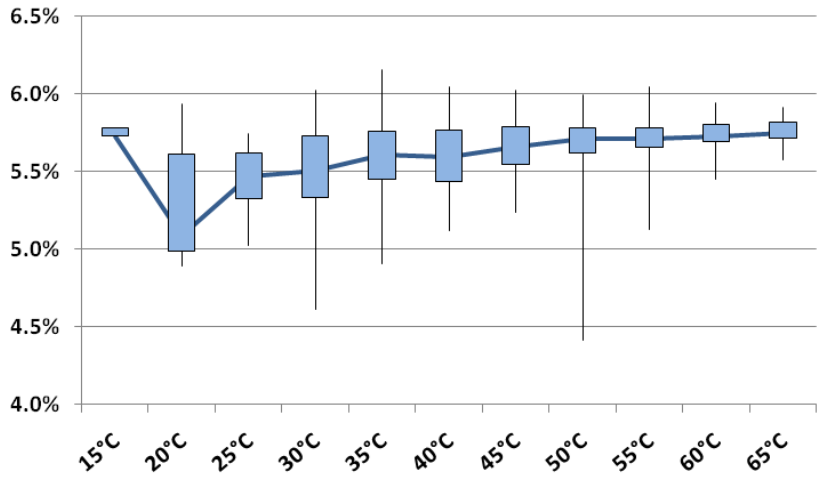

Figure 2-6. A-Si module efficiency versus module temperature.

A-Si modules are of course much less efficient in terms of their effectiveness to convert solar radiation into electric energy per module area. However, these results paint a very convincing picture of situations where amorphous photovoltaic modules could become a major player. Unless active (or maybe highly effective passive) cooling applications become widely and cheaply available for PV, areas around the world with high ambient temperatures, heavy insolation and low wind speeds would experience significant efficiency losses with c-Si modules. Since module prices are not determined by their area, but by wattage, it will be in the best interest of the investor or owner to retain the highest possible output throughout the expected spectrum of temperatures for a given project.

2.4. Cost Comparison

One major disadvantage of using a-Si modules, regardless of their performance during times of high module temperatures, is the fact that they are inherently less efficient. However, overall costs for a system could end up being much lower with a-Si modules for several reasons. A comparison based on racking and module costs given in Table 2-1Table 1-1 & Table 2-2 can be found in Table 2-3, taking standard module racking costs per watt and converting them to a basis per square meter.

Table 2-1. Comparison of module specs

	Module Specs	
Type	60W a-Si	230W c-Si
Length (m)	0.96	1.64
Width (m)	0.99	0.994
Area (m^2)	0.9504	1.63016
Cost ($/W)	1.5	2.5
Isc (A)	1.19	8.24
Voc (V)	92	37

The assumption with this approximation is that racking materials are the same for both types of modules per surface area. This skews the data to the benefit of the standard modules, as thin film modules in general are much lighter yet stronger due their reliance on dual panes of glass. Their strength also enables them to be considered part of the structural design, which gives additional possibilities of reductions in racking material. For these reasons one can expect to use about 10% less material for racking per area. [2]

Table 2-2. Racking Costs

Ground Mount Racking costs		
Min	0.45	$/W
Max	0.55	$/W

While the increased number of modules would seem to equal larger labor costs, new thin film racking is designed to let modules merely "snap" into place, making for a much faster installation than the screw down type for standard modules. This cuts labor costs per installed module, and may even reduce total installation costs. The increase in necessary wiring, though often utilizing only quick connectors, could even the costs. For the purpose of this example labor costs per are expected to be equal for both systems, though in reality they would seem to be in favor of thin-film systems. Wire sizes would, depending on the configuration, most likely be the same – so equipment and cable costs are also expected to be similar.

Table 2-3 System and Racking costs with differing module types for a 500kW system

		Theoretical 500kW System							
		# Modules	Racking $/Module	$/m²	Racking Total	Module Cost	Total Cost	Racking $/Watt	acres
Standard Modules (230W)	Low	2174	$104	$63	$225,000	$1,175,000	$1,400,000	$0.45	1.85
	ML		$115	$71	$250,000		$1,425,000	$0.50	
	High		$127	$78	$275,000		$1,450,000	$0.55	
Amorphous (60W)	Low	8333	$60	$63	$502,846	$646,667	$1,149,513	$1.01	4.14
	ML		$67	$71	$558,718		$1,205,385	$1.12	
	High		$74	$78	$614,590		$1,261,257	$1.23	
Amorphous Racking -10%	Low	8333	$54	$57	$452,562		$1,099,228	$0.91	
	ML		$60	$63	$502,846		$1,149,513	$1.01	
	High		$66	$70	$553,131		$1,199,798	$1.11	

Table 2-3 shows that even if racking costs are expected to be the same per square meter, the low cost of the amorphous modules per watt create at minimum a $140,000 savings in this 500kW example. If the 10% reduction in material costs is incorporated, these savings add up to around $200,000 in the worst case. This gives thin-film systems a serious advantage in terms of equipment & system cost. However, since this calculation does not include the cost of the land necessary for the installation of the system it is assumed that the land is owned by the owner of the system. If this is not the case, expensive land lease costs could spell difficulties in justifying the spatially larger amorphous system. In areas such as the south-west, where land is often inexpensive, ambient temperatures are high and strong insolation is available, amorphous may be a perfect fit. In New Jersey where farms have netted on average over $460 per acre annually, it may be difficult to justify more than doubling the necessary area at farms. [22] In all other locations, space utilization on the order of double that of crystalline systems would be no issue, as the cost of the land over the course of 25 years represents less than 4% of the entire cost of the system. The revenues in electricity alone would

equal over $90,000 per year, or more than $22,500 per acre-year for the thin film system and over $50,000 per acre-year for the crystalline system.

Of course the situation changes as thin film modules increase in efficiency. These 60W modules represent some of the least efficient, but also least expensive, options on the market today. 100W amorphous silicon and multi-junction modules are already available, which would cut racking costs as well as a system's footprint almost in half. As more variations come into play and technological advancements are made, thin film modules will become an ever larger share of the total market. The combination of inexpensive manufacturing, higher performance in hot climates and advanced framing, racking and installations could make thin film modules the least expensive option for large scale PV systems where inexpensive land is available.

Chapter 3. Optimizing engineering design to cut costs and increase efficiency

3.1. Introduction

The inception of economically attractive PV installations gave rise to a great number of installers, mostly existing electrical contractors that were well trained as residential and commercial electricians but often lacked a thorough understanding of the engineering principles that go along with creating efficient photovoltaic systems. A simple example being the wiring necessary to connect all components in such a system; federal regulations and guidelines, most notably the National Electrical Code (NEC), present a minimum requirement for everything ranging from cable gauges per maximum amperage to grounding loops. While strict adherence to these rules ensures the safety of the wiring and equipment, it does not account for deficiencies and losses in a system. The same applies to the actual placement of the modules; while placing more modules in a limited area will increase the nominal capacity, shading caused by insufficient spacing or failure to tilt the modules at appropriate angles reduces the effectiveness of the system and causes significant economic waste. Since the ultimate purpose of a PV system is to create a financial benefit for the owner, any losses incurred via inefficiencies in the wiring, equipment or short term savings will reduce the overall potential system benefits. For this reason, a crucial part of the engineering design for a PV system consists of guaranteeing minimal losses throughout the system while following federal and local guidelines for safety. Proper engineering design can also cut initial costs as well under certain conditions, as will be demonstrated in section 3.3.3.c. For applications where the amount of available roof or land area is limited, a host of other problems arise, e. g., what tilt does one specify for the modules, what kind of inter-row spacing is necessary,

optimal, or desirable, what kind of losses are acceptable due to shading, what type of module should be used, and finally where does one place combiner boxes, disconnects and inverters? It is for this reason that the engineer must make the necessary provisions and take the precautions for optimizing the system to achieve the highest value for the customer.

3.2. Basic Design & Wiring

One of the most straightforward examples in engineering optimization lies in the wiring. As noted, NEC guidelines and regulations were created to ensure the safety of the equipment and any individual interacting with the system. Though absolutely essential to proper engineering, the NEC does not list any provisions to account for wiring losses as they have no bearing on safety. Where the creation of value is pressing, however, the issue of eliminating deficiencies becomes one of great importance, as inefficient wiring design translates directly into losses of return on capital investments. Seemingly small loss factors can accumulate to represent large sums of money over time, especially when systems are of a considerable size and operate for 25+ years. Of course, safety still remains the number one concern for any engineer. To ensure compliance and efficiency, a design begins on the basis of being in accordance with NEC guidelines, and ends with being updated to reduce losses by the maximum extent for which there is economic justification.

To give a simple example, let us investigate the effects of a DC wire run which can be commonly found on a large rooftop system from a combiner box (CB) to an inverter. The next section goes through the entire process of calculating the maximum

voltage, current, losses and everything else that is necessary to create an efficient and safe system. Table 3-1 contains the specifications of the equipment used in the analysis.

Table 3-1. Example System Components

Modules		**Combiner Boxes**	**Inverter**	
Power	240W	16 Strings	Power	60kW
Voc	37V	600V Max.	Max Voltage	600V
Isc	8.3A		Max Current	191A
Vmp	30V		MPPT range	350-500V
Imp	8 A			

(MPPT being a maximum power point tracker)

3.2.a. Designing in Accordance with the NEC

Since the maximum voltage of the inverter (as is the case with most DC PV equipment) is set at 600V, it is a trivial feat to calculate the maximum possible number of panels per string. As with any first step in the design, in order to avoid any violations it is important to read the NEC handbook on the matter. In the photovoltaics section, article 690 of the handbook, clause 690.7 under *II. Circuit Requirements* is found, which gives directions as to the means to calculate the maximum voltage of a PV system. It states that the number of modules per string, multiplied by their Voc, and again multiplied by a temperature correction factor, will provide us with the maximum voltage of said string. Table 690.7 then provides a multiplication factor, which is dependent on the minimum ambient temperature expected at the location of the array. This correction factor is necessary to ensure safety due to the way that PV modules perform in lower temperatures. As the

Correction Factors for Ambient Temperatures Below 25°C (77°F). (Multiply the rated open circuit voltage by the appropriate correction factor shown below.)

Ambient Temperature (°C)	Factor	Ambient Temperature (°F
24 to 20	1.02	76 to 68
19 to 15	1.04	67 to 59
14 to 10	1.06	58 to 50
9 to 5	1.08	49 to 41
4 to 0	1.10	40 to 32
−1 to −5	1.12	31 to 23
−6 to −10	1.14	22 to 14
−11 to −15	1.16	13 to 5
−16 to −20	1.18	4 to −4
−21 to −25	1.20	−5 to −13
−26 to −30	1.21	−14 to −22
−31 to −35	1.23	−23 to −31
−36 to −40	1.25	−32 to −40

Figure 3-1. NEC Table 690.7 for Voltage Correction Factors. [63]

operating temperatures of most modules drop they, like most electrical & electronic systems, operate more efficiently. Their output power increases steadily mostly due to their voltage being incrementally higher with every degree Centigrade. Accounting for this change in output ensures that none of the equipment will fail, possibly causing dangerous conditions, due to being subjected to voltage levels higher than their maximum rating. In New Jersey, temperatures can be expected to stay above -30°C (-22°F), correlating with a correction factor of 1.21. With a 600V maximum voltage and the given correction factor, the maximum open circuit string voltage would be 495V. The modules chosen for this example have a Voc of 37V, giving a total of 13 modules per string. Such a string's maximum open circuit voltage with incorporated corrections will then be 582V, well within the requirements of the inverter. (With a Vmp of 30V for these modules, the system will be in the lower half of the inverter's MPPT capabilities making it less than optimal, but for the purpose of this example we will ignore this.) 13 modules per string will provide a maximum short circuit current of 8.3A and if the 16 string CB is used to its fullest extent, a maximum of 133A can be expected to be fed to the inverter. Even though Isc for this CB is 133A, 690.8(A) gives a clear requirement on the method of calculating maximum currents in a PV circuit, stating that the maximum current shall actually be 125% of the short circuit current. This is done to account for times during which reflections (e.g. from snow) cause higher insolation on the modules, which can push their output currents beyond nominal specs. Upon further reading, 690.8(B) makes clear that the conductors and over-current protection devices need to be sized at a current-carrying capacity, or ampacity, of 125% of this maximum current, meaning that any cable or fuse must be able to handle 125% of 125% of the short circuit current. Thus, we have a 1.56

(156%) multiplier for the Isc of this CB, giving an output current of 207A. This number must fall within the conductor's ampacity rating, which is also listed in the NEC under the tables in Article 310 as well as Annex B. Of course, the ampacity of the conductor depends heavily on the environment it will be placed in; the higher the temperature of the cable, the lower the amount of current it can safely carry. For this reason an accommodating correction factor, depending on the type of cable, conduit and ambient temperature, is found beneath each appropriate list of ampacities, insulation types and conductor gauges. In this example the conductor will be fed through a cable tray along the surface of the roof. The use of cable trays on roofs can be quite beneficial to the initial capital investment, as cables running in such a tray can be considered to be in free air and are thus not hampered by a very low derate factor. For instance, a simple note under 310.10 FPN No. 2 warns us of the increases in temperature one can expect inside a conduit exposed to the sun in proximity to a roof, stating that an increase on average of at least 17C° (30°F) can be measured under certain circumstances. Since this is an average, actual high temperatures may pose serious issues for a conductor, as the research behind this average number suggests. First, "during the peak period of July/August, average temperature *increases* ranged from 40F° to 58F°, depending on how the conduit was mounted to the roof surface." Secondly, "the maximum increase in temperature above ambient seen was 83F°." [94] Since the NEC requires that conductors are sized according to the maximum temperature they are expected to see, it is clear that rooftop conduits can create a serious safety risk, or a significant increase in conductor size if derated properly – a further benefit of choosing cable tray over conduits in roof applications.

To continue the example, the record high ambient temperature for New Jersey, recorded on July 10 1936, was 43C° (110°F) [60]. This, according to table 310.17, gives a correction factor of 0.87 for conductors rated at 90C°. To give an added degree of safety the next higher correction factor, or 0.82 for temperatures between 46 and 50C° (114-122F°), will be chosen. With 207A coming from the combiner box, a 1/0 90C° copper conductor will be necessary to handle the current safely, as it has an ampacity rating of 213 after being derated appropriately by 0.82. The resistance noted by the NEC for this type of wire and gauge comes in at 0.127Ω/ft, which for a run of 100ft will amount to a loss of around 0.82%. It is important to remember that the losses are based on twice the one-way length of the conductor, as a return path for the current on the negative side must be incorporated in the calculations. For a distance of 250ft we are already at 2.08% losses (2.5% at 300ft) for the entire system solely due to a pair of conductors. This makes it clear that even though NEC regulations have been followed, loss calculations should be performed in order to ensure an efficiently operating system.

Note: *While acceptable wiring losses are a topic of debate, those higher than 1% are deemed intolerable by the author and other engineers conferred with on the subject. The type of system, amount of energy produced and costs of the electricity produced may all impact the threshold for appropriate losses.*

To scrutinize the impacts of single digit percent losses from a monetary aspect, consider the historical SREC prices for NJ in Figure 3-2. The 16 strings being fed through the conductor total about 50kW, which if tilted at 30° at an azimuth of 180° would yield ca. 1250kWh per kW per year. This means it would generate a sizeable 62MWh per year totaling $9,300 with average electricity prices of 0.15¢/kWh. If SREC prices are included the value of the electricity generated is $46,376, meaning this percentage point of lost energy could cost the owner approximately $463 every year.

Over the course of the lifetime of the system, losses would come to over $11,500 for each percent, more than enough to justify a conductor size increase from 1/0 to 2/0, at a one-time cost of a mere ~$300.

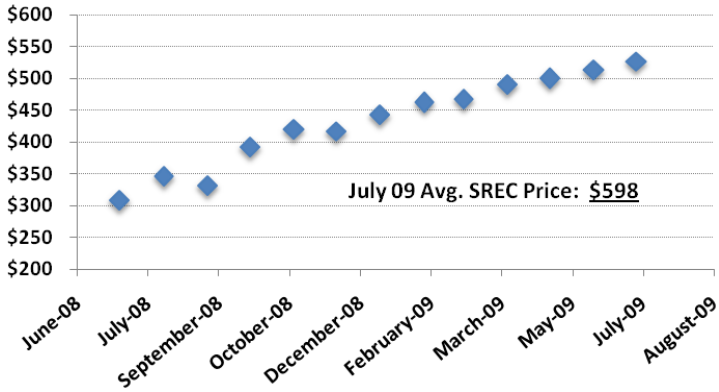

Figure 3-2. Cumulative, weighted average SREC prices

3.3. Large scale losses

The previous example gave insight into how some very simple engineering design changes can potentially save thousands of dollars over the course of the lifetime of a system. Considering the mentioned system consisted of only 50kW of PV, it is easy to give ballpark numbers for larger systems numbering in the megawatts. Losses become more and more financially problematic and great care must be taken to ensure all unnecessary losses are eliminated from the final design. Let us consider a 2MW PV array, ground mounted on a farm to offset usage of a nearby food processing plant, as presented in Appendix A. If we ignore SRECs for the moment and focus entirely on conservative electricity costs of 10¢/kWh, an inefficiency of one percent would create a loss of $2,000 per year. With SRECs expected to closely track SACPs, their prices will not likely fall below their current average. With that in mind, and using average SREC

prices at $500, each 1% loss for this 2MW will cost the owner a little under $15,000 per year.

It is not always easy to eliminate inefficiencies numerous connections, switches and pieces of equipment are involved. This holds especially true when reaching higher system voltage ratings connected to certain utilities, as the number of safety and disconnection requirements increase substantially. Though the high voltage ensures that losses are minimal, the cost of the equipment involved is quite significant. Relaying, which can be an expensive affair, is usually not required on PV systems as almost all solar inverters meet UL 1741 and IEEE 1547 for protective and installation settings. These standards include requirements for inverters to be anti-islanding, that they be able to detect voltage sag and frequency shifts, as well as a host of other situations where the system must automatically shut down to protect the public and utility personnel. The designation for an inverter to be anti-islanding essentially means that it cannot operate and supply the grid with electricity if utility generation has gone offline. This is important in keeping utility lines safe for linemen, which may be unaware that a small section of the grid is still under high voltage while the rest has been shut down. The fact that inverters are intelligent systems, able to be communicated with and operate safely autonomously, already gives PV a great advantage in simplicity and costs over many other means of generation. The entire system can be safely shut off and turned back on very rapidly through the inverter, without the need to manually disconnect various switchgear or installing expensive and complicated relay equipment.

However, there are still several ways of simplifying PV system interconnections to the grid and to make them more efficient. This section will focus on giving a few very

simple and yet extremely effective optimizations that can be applied to almost any large scale photovoltaic array. Much of this work has already been published and presented extensively by the author [86][39][37], but will be given here in shortened version. A comparison of two systems similar in capacity is presented, with differences lying mostly on the utility interconnection. The first of the two to be considered is a reference system to the second and has been commissioned on November 15th 2008 and been in operation reliably since. The second was a system proposed during the summer of 2008, for which funding became unavailable due to the economic downturn. It is expected to be built in the coming years.

3.3.a. Exelon 3MW

This system is comprised of 17,160 SunTech Power 175W modules [97], ground mounted on the water run-off site next to a large landfill owned by Waste Management [103] in Bucks County, PA. The project was conceived by SunTechnics [98] which was a subsidiary of the largest PV integrator in the world, Conergy [6] headquartered in Germany. Conergy's sister finance company Epuron [21] worked out the financial model for an energy purchase agreement with Exelon Generation Company LLC.[24] Exelon, through their Wholesale Power Marketing Division located in Kennett Square, Pennsylvania, USA is one of the most active companies within PJM [79] and Midwest ISO [57] in creating structured power marketing deals that can best optimize resources for the supply and demand portfolios (including renewable energy) of Exelon and other electric utilities. This 3MW system is at present the largest PV array east of Arizona, and the first to deliver multi-megawatt solar power directly to the PJM grid, which is the largest regional transmission organization in the world. [71] A group of investors,

connected by Epuron, took ownership of the project based on the cash flow and anticipated (not yet available at the time of the installation) RECs. The project developers benefitted greatly from the tax credits and depreciation created by the system. [37]

The focus of this discussion will be on the AC portion of the project as this is where the author designed efficiency and cost improvements. The major components of the AC side of the system are listed in Table 3-2, along with estimated prices for each component of the system. Figure 3-3 gives an indication of the percent costs for each of the components, with inverters constituting nearly 70% of all AC equipment costs.

Table 3-2. 3MW System Equipment List [86]

QTY	Equipment	Price ($US)
6	500kW Satcon Inverters	880,000
1	Puffer Gas Switch & 4-Way Triad	180,000
3	1MVA Cooper Transformers	110,000
3	Square D low voltage Switchgear	40,000
	Wire, Connectors & Conduit	11,000
8,100ft	1/0 Al Primary cable	17,000
1,800ft	600 Copper cable	17,000
	Pole & Feeder upgrades	30,000
	Total:	1,285,000

The inverters were chosen to be Satcon 500kW units, which come with built in isolation transformers that convert from 208Y to 480Y. Wire sizing varies greatly throughout the AC portion of the PV system to accommodate various loads. The AC side begins with six 500kW inverters separated into 3 pairs, each pair being housed on a common concrete pad. The interconnection between the inverters and the 1MVA step-up transformers

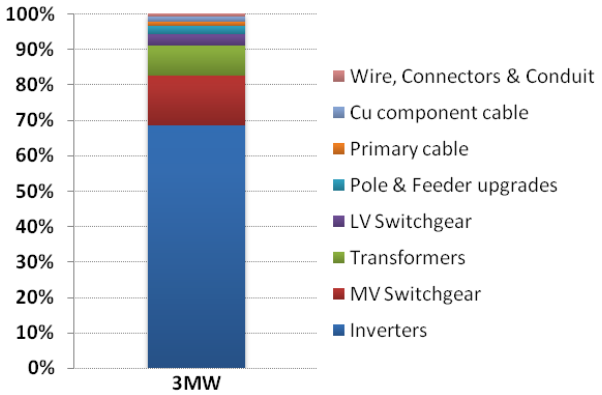

Figure 3-3. Breakdown of 3MW system

needed for the low-loss transmission of the generated power was done via a 480-volt switchboard connecting the pair of inverters into a common 3 phase circuit. Since the voltage coming out of the isolation transformer (and switchboard) is a low 277V per phase, current is high and requires the use of very large conductors. Various schemes were explored and the connection options were reduced to two, using two 600kcmil copper conductors or a single 1000kcmil copper conductor per phase. The final plans utilized the former option as installation difficulties, such as running the conductors through conduit bends, increase incrementally with the use of larger conductors. To illustrate the problem, 1000kcmil conductors are over 1.1" in diameter not including insulation. The 1MVA step-up transformers increase the voltage to 35kV and standard 1/0 Al TRXLPE conductors with concentric neutrals are run underground from them to a four-way triad switch. Very few losses occur over the maximum 1300ft run from the most distant inverter/transformer pad to the utility interconnection due to the run being at a high voltage and low current. The triad switch takes all three incoming feeds, combines them into a single three phase run and supplies the metering cabinets. After this the power is fed through the main puffer gas switch and finally, a riser pole with pole-top cutouts creates the interconnection to the utility overhead. The single line diagram for the entire AC side is given in Appendix B, which describes the major equipment and details. A partial single line for the switchgear pad is shown in Figure 3-4. [39] It is important to point out that the design for this system relies on a great number of switchgear, much of which may be redundant from a practical standpoint. Some of these can be eliminated with proper design, while others' inclusion comes from requirements by the utility – as is the case with the puffer gas switch. The PECO "Blue Book" of interconnection

specifications requires the use of such a heavy duty switch due to the project interconnecting with PECO's 34.5kV overhead system. A puffer gas switch is able to open and close a connection at high potential without creating potentially hazardous arcs and possibly electrical fire. It does this by introducing pressurized gas, usually Sulfur Hexafluoride (SF6), through the opening of the connection thereby cooling and extinguishing any electrical arc created in the process. While such requirements vary from utility to utility, they are generally not required for voltages under 12 to 15kV.

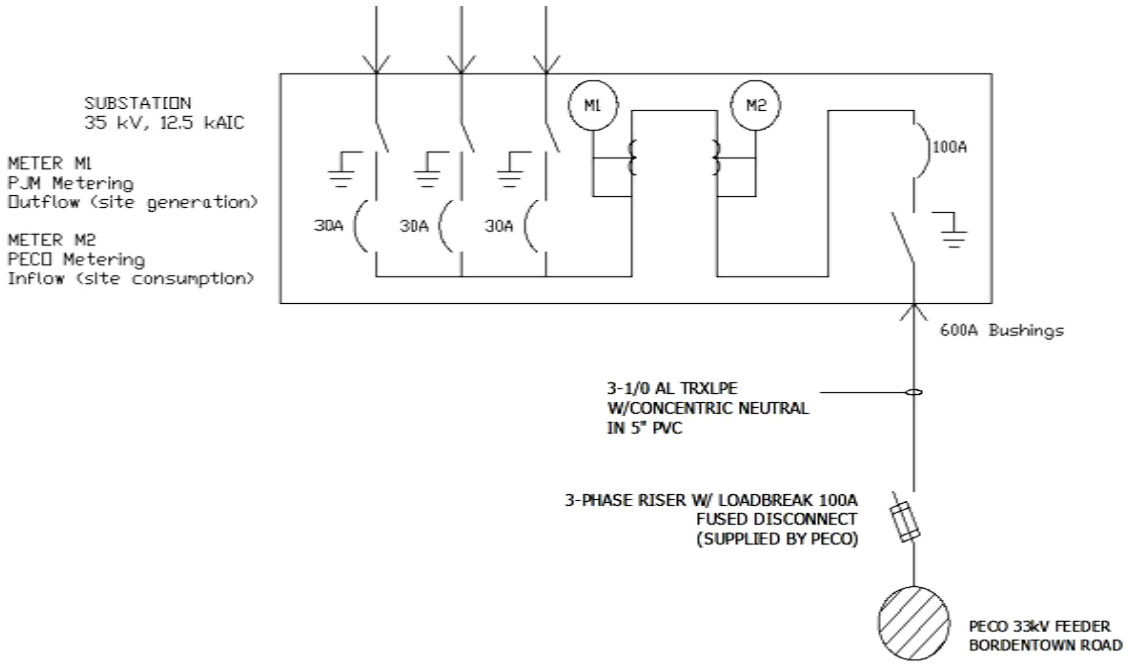

Figure 3-4. 3MW Switchgear pad single line, giving the 4 way switch on the left, down to the riser pole.

3.3.b. Seabrook Farms 2MW

With the availability of low 12kV overhead voltage at the Seabrook farms site, interconnection requirements changed significantly, and enabled an entirely redesigned system, which, when compared with the Exelon project, is quite minimalistic. This setup

shares common elements with the 3MW design; four independent DC sections (500 kW each) feed their own 500 kW inverter as well as a single interconnection provided to the grid. The primary difference with regard to the previous design lies in its effective use of less complex and more economic interconnection equipment and design, allowing for overall fewer components. [86]

Table 3-3. 2MW System Equipment List [86]

QTY	Equipment	Price (USD)
4	500kW Satcon Inverters	600,000
4	500kVA Cooper Transformers	62,000
	Wire, Connectors & Conduit	4,500
4000ft	1/0 Al Primary cable	8,200
320ft	600 Copper cable	3,000
	Pole-top Cutouts & Safety Equip.	2,700
	Total:	680,400

Similar to the previous system, half megawatt sections of PV are connected to 500kW inverters, but in this system each sub-section uses its own 500kVA step-up (480V to 12.47kV) transformer. However, in this design the inverters were specified to be provided without isolation transformers, as the step-up transformers bringing the output voltage to the required 12.47kV sufficed in galvanically isolating each sub-system from the grid. This not only reduces complexity but can also cuts losses by 1%, as any transformer will rarely be more efficient than 99%. [86] Since each inverter fed its own step-up transformer there was no benefit in using switchgear to combine the four outputs together, thereby eliminating another large cost for such a PV array. Combining the incoming 12.47kV feeds was also

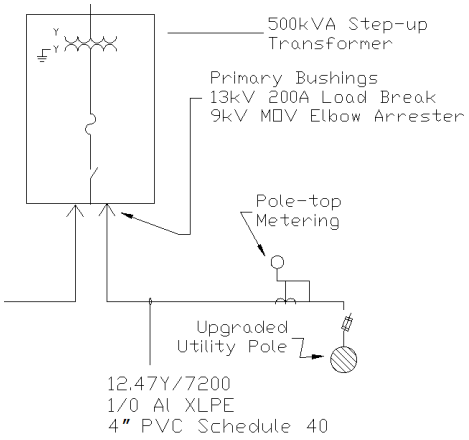

Figure 3-5. 2MW final transformer and interconnection to riser pole

handled in a simpler way. Instead of utilizing an expensive switch, such as the four way triad switch of the 3MW design, transformers were connected in loop feed fashion, putting all primaries in parallel and thus "hot". The final transformer closest to the pole was then outfitted with lighting protection and connected to a riser pole, as seen in Figure 3-5. Since the system employed 12.47kV, no expensive puffer gas switch was necessary and a set of pole-top cutouts sufficed as a means of disconnecting the array from the grid for maintenance. The final single-line diagram for this system, found in Appendix C, gives a good indication of the simplicity of the system in comparison to the 3MW design.

3.3.c. The Economics of Simplicity

While reducing several points of complexity and increasing the efficiency of such large scale systems are reasons enough to optimize PV arrays, economic factors provide a major benefit as well. The cost data estimated in Table 3-2 & Table 3-3 are for equipment only and do not incorporate any of the overheads and costs associated with the engineering design and labor for the installation of each of these systems. The estimates for project management and engineering fees for the purpose of this research were projected to be 10% of all equipment and setup. Stores and overheads for the items be directly shipped to the construction site were estimated to be 30% of their cost. Finally, installation costs for wiring and conduit installations are generally expected to be around 100% of the materials' price. This means project management, engineering, installation and various other overhead on the AC side come to a total of approximately $224,000 for the 3MW system and $95,000 for the optimized 2MW design. Approximately $40,000 of the larger system represents the setup and installation of the low and medium voltage switchgear components. The total procurement, installation, management and design

costs associated with the AC side of the 3MW will then have come to a total of approximately $1.5 Million, or 50¢/Watt. For the 2MW this totals approximately $775,000 or 39¢/Watt. This is an impressive 22% reduction in cost per watt, which when applied to such large systems can cut investment requirements by several hundreds of thousands of dollars. Much of these savings come with the elimination of the bulky switchgear, which represented almost $300,000 in end costs. By taking a simplistic and more minimalist approach to the design of large utility scale photovoltaic arrays, we have uncovered an 11¢/Watt (22%) savings for the AC interconnection portion of the system. System complexity was reduced significantly which will further reduce installation costs (not accounted for herein) and future maintenance as well as increasing the modularity of the AC side. Future site owners will have little difficulty when adding additional arrays to an existing interconnection, since the connection of step-up transformers (and with that inverters) is done through the daisy chain approach of a loop-feed setup. In areas where the local utility regulations allow it, utilizing these types of savings will keep investments to a minimum and increase value for the owner. [86]

Since much of the savings rely on the elimination of switch gear equipment, the decision of interconnecting at an appropriate voltage is crucial. The higher the grid voltage the more safety equipment and control features are necessary to comply with safety guidelines and utility regulations. These additions are costly and reduce the efficiency of a system, a factor that becomes increasingly important as systems grow in size. While an 11¢ reduction in cost seems insignificant when complete systems are in the $5/W range, these savings are "free" and can only become more important as module and inverter prices become lower. The equipment which is eliminated has been

standardized, is not PV specific and is in widespread use around the world with many different applications, meaning that its prices will not see significant reductions in the future - thus becoming an ever larger portion of system costs. Again, advancements in technology may have a large impact on the cost and the benefits of this equipment, though most likely not enough to warrant its inclusion when not necessary.

3.4. Module Installation Optimizations

Standards in wiring and system design such as the NEC give, provide at minimum requirements from which one may then adjust wiring and equipment to ensure optimal efficiencies. Unfortunately similar regulations or guidelines do not yet exist for the installation of photovoltaic modules and arrays to assure minimal output losses due to shading or generation effectiveness per installed capacity. Since most customers are not familiar with the various aspects of PV design, it has happened quite often that installers have sold large PV packages by encouraging the end-user with large capacity numbers and annual REC benefits without making clear the trade-offs between capacity and generation. This then resulted in panels being placed in regions where they may experience partial shade for extended periods of time. Practices such as these are not desirable as the customer pays large sums of money for a system that will operate inefficiently, causing extended payback periods and final costs per kilowatt-hour that are unnecessarily high.

3.4.a. Picking the right Orientation

One of the first things that should be considered when designing a PV system is the azimuth angle at which the system will be installed. For systems on existing roofs it is usually not possible to ensure a perfect azimuth direction, as it will be heavily dependent on the structure's existing orientation. The azimuth is essentially an angle measured on a horizontal plane between true north and any object in the distance, measured from the observers point of view. When referring to the azimuth in the realm of PV or when referencing a solar position, the azimuth is often taken to be the horizontal angle between the sun and true south, with it being positive in the eastward direction, see Figure 3-6

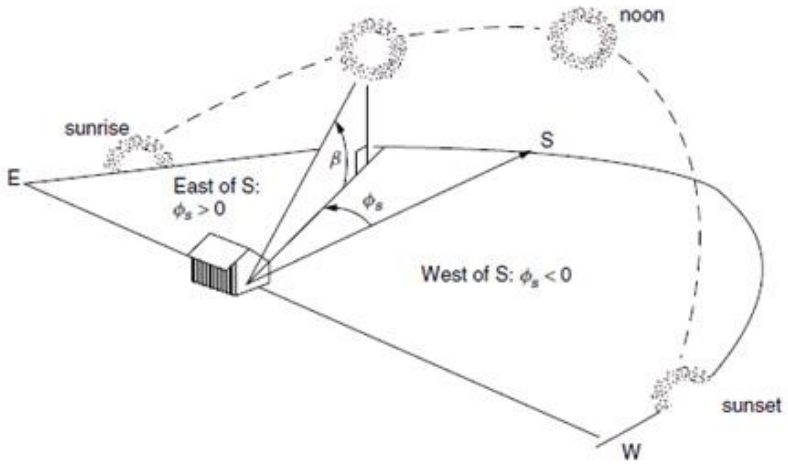

Figure 3-6. Sun position throughout a given day, in terms of β (solar elevation) and Φs (solar azimuth) [51]

As is well known, the Earth's rotation provides a sunrise in the east and a sunset in the west, with the solar path following along the equator relatively well. In the summer this path will be skewed towards the tropic of cancer, in the winter towards the tropic of Capricorn, while lying between the two extremes during spring and fall. This means that the optimal direction in which a collector must face to be incident with the maximum available insolation from the sun will depend on the hemisphere it would be located in. If

located in the northern hemisphere, it must face southward, if located in the southern hemisphere it would have to face northward. Figure 3-7 shows how the output of a theoretical 1kW system with a 30° tilt in New Jersey, is affected by changing its orientation (estimated via PVWatts) [82]. PVWatts is a PV generation estimation program provided by the National Renewable Energy Laboratory (NREL). [67]

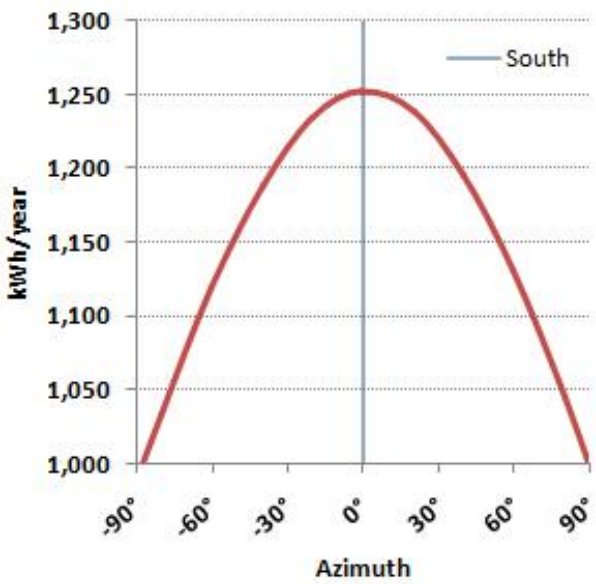

Figure 3-7. Theoretical output of a 1kW PV system located in NJ angled at 30°.

Figure 3-7 makes it quite clear that systems oriented east or west of the true southerly azimuth (0°) will not be incident with the solar radiation when it is most critical, causing a drop in electrical energy extraction, as high as 20% for true East and West orientations. The correlation of the output of the system per year and the azimuth in which it is installed is almost linear in either eastern or western directions. The maximum output lies at the point where system orientation is at 0° (south) azimuth, giving the oft quoted 1250kWh/kW for New Jersey.

3.4.b. Ensuring a Proper Module Tilt

One of the simplest yet most important aspects of designing a PV system lies in the choice of tilt angle for the modules. Too extreme of an angle and the system will not be incident with the incoming insolation, causing the system to extract less energy from the sun than is available. The general rule of thumb of the angle at which the module will be incident with the sun during the highest percentage of the year is to tilt it at the angle coinciding with the latitude of the location. This will ensure that the module is almost perpendicular to the incoming solar rays at noon during the spring and fall equinox, and receive sun during the summer and winter months at equal angles, see Figure 3-8. While it is true that this will give the highest percentage of incidence with the sun throughout the year, it does not guarantee the highest possible energy output. Depending on the location, more solar energy may be available either in the winter or summer months of the year. Additionally, local weather plays a role in optimizing tilt angles.

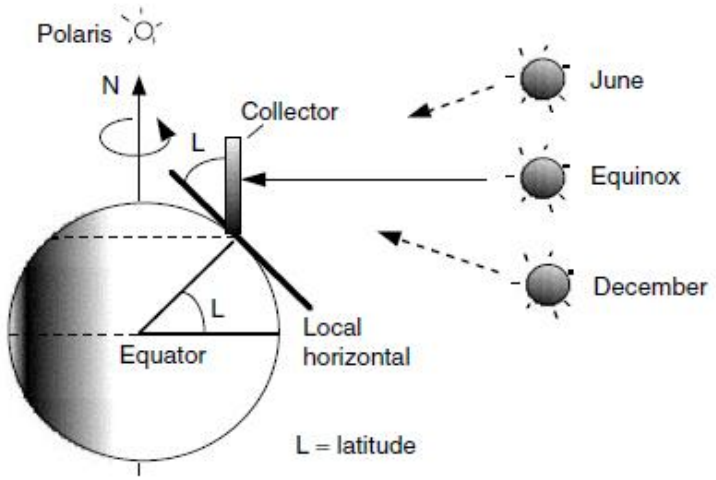

Figure 3-8. Collector tilt at latitude. [52]

For example, in New Jersey a large amount of the energy to be extracted from the sun will be available during the summer months, less in the winter months. The numbers pan out to be around 17% of the energy throughout the year being available during the winter and 33% in the summer, Figure 3-9. A quick estimation with PVWatts reveals that the maximum energy output of a 1kW system in NJ (ca. Latitude 40) will be 1254kWh extracted at a tilt angle of 35°. The numbers in Figure 3-9 were taken from the data collected via PV systems installed on the SJTP roof, and thus represent outputs that can be expected in the southern part of New Jersey.

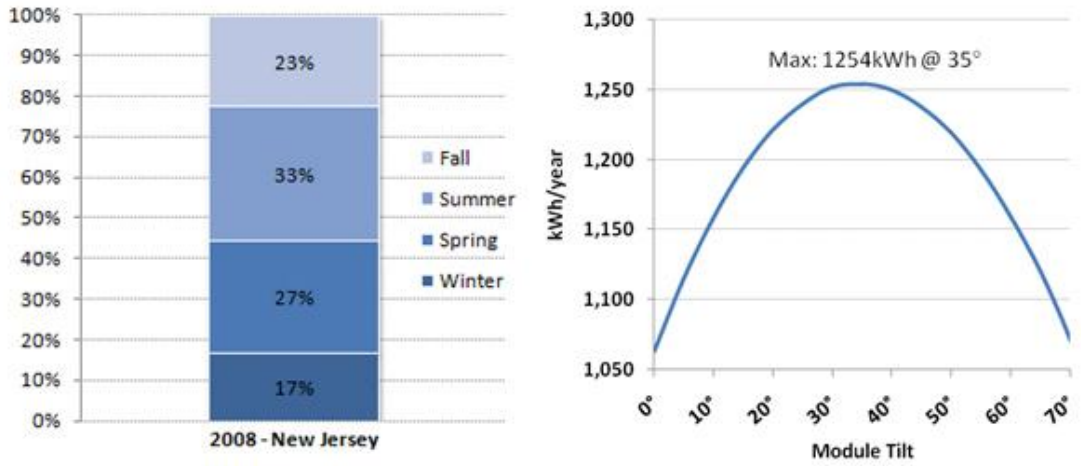

Figure 3-9. Percentage output per season and generated electricity per module tilt.

A look at average retail electricity prices reveals another reason to tilt the modules slightly lower still; average electricity prices peak during the summer. These averages already provide a strong argument to increase summer production, yet savings will most likely be even greater due to the immense price escalations during peak hours throughout which a PV system will be at maximum output (if the customer chooses to receive variable rates). Figure 3-10 shows average retail electricity prices throughout 2008 given by the Energy Information Administration (EIA) [12], and shows a clear trend of high electric prices during the summer throughout all sectors.

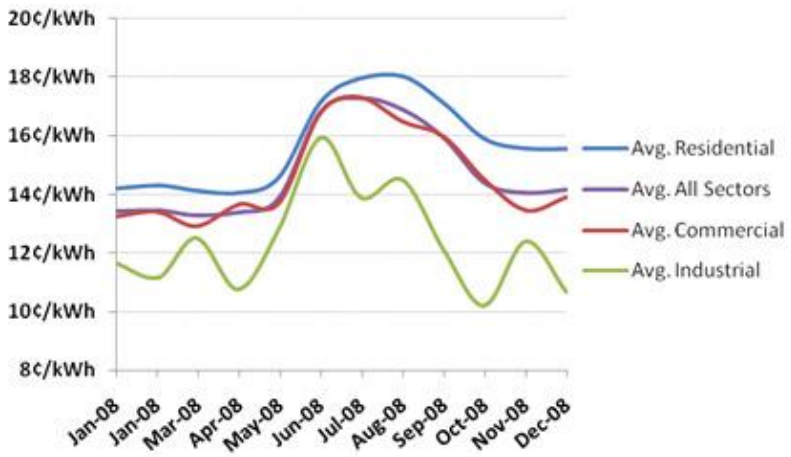

Figure 3-10. New Jersey electricity rates by sector, according to the EIA.

Given the estimates generated via PVWatts, these factors (including better weather in the summer) can be combined to give a good indication of what module tilt angle will provide the maximum economic value to the owner. Again, this is for a location in NJ at a latitude of ca. 40°. Figure 3-11 reveals that the optimum angle in terms of economic benefit will be 30°, generating $196.6 for a 1kW system. The single stipulation that should be mentioned here is that these estimates do not include the value of the generation in terms of SRECs, only the retail costs of electricity. Taking the addition of the government subsidies into account, the tilt angle coinciding with maximum energy generation will be of even higher value.

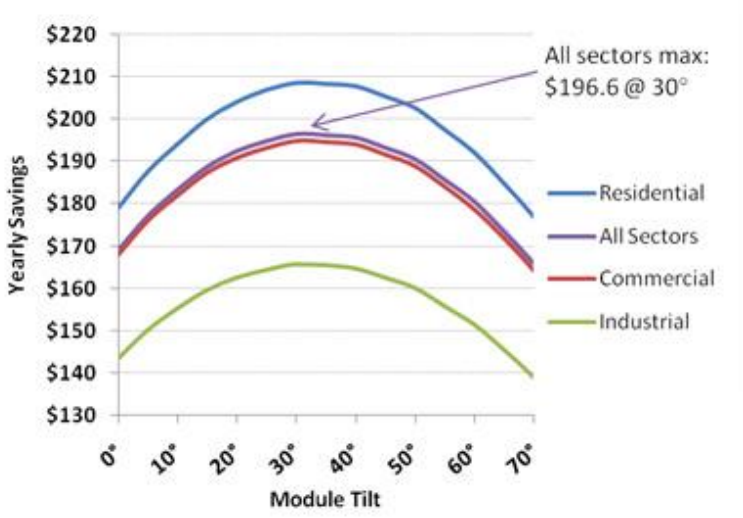

Figure 3-11. Yearly savings versus module tilt

Now that the optimal tilt angle has been selected, one would think that it should be relatively simple to design an optimal PV system around it. This turns out to be a bit more complicated and challenging when considering a flat roof, as spatial limitations for the location of such a system may change the outcome significantly. When there is a limited amount of roof or mounting space available it may be impossible to match the needed demand due to the long inter-row spacing requirements of a large (30°-35°) tilt angle. Since the tilt determines the spacing, the utilization of the available area goes down significantly the higher the tilt angle. Inversely, as the tilt angle goes down so does the spacing required to keep the modules from shading each other. This is illustrated in Figure 3-12, using a sample PV module in landscape mode (of 61”x41” dimensions), facing southward, with a liberal shading multiplier (the amount of spacing necessary per unit module height) of 2.5.

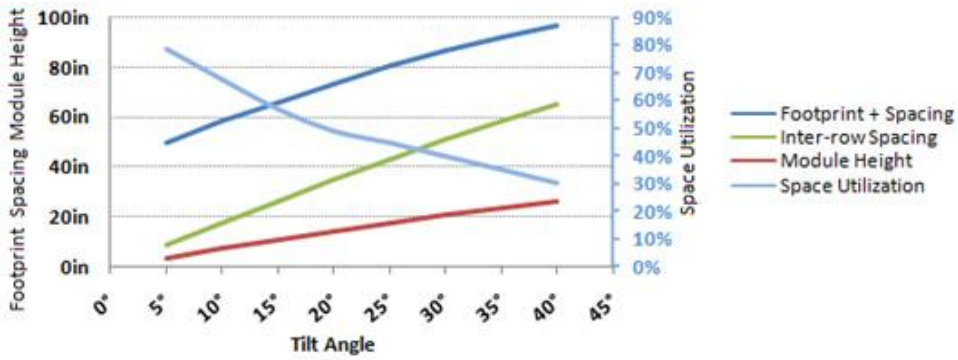

Figure 3-12. Spatial differences per tilt angle, versus percentage utilization of available area

As a designer lowers the tilt angle of the arrays the modules in the array will no longer operate at their maximum output but the total installed capacity of the PV system increases significantly. This creates an optimization challenge for determining economic value; how much should the system capacity increase and how much can we let output per PV module decrease? What is the most effective use of PV for the customer? While it is true that maximum system capacity can be obtained when the PV modules are laid flat on the roof, their energy generation per watt is reduced significantly (see Figure 3-14), not to mention that losses increase due to snow cover and dirt which accumulate more readily on a horizontal collector. Preliminary inter-row module spacing is determined by a multiplier of 2.5 times the height of the tilted module in these examples. This multiplier ensures that modules will not be shaded for more than 2% of the time sunlight is available regardless of the module tilt angle, though, as shown in further sections of this thesis, it may be excessive. The height, footprint and spacing are easily calculated by the following formulas and are illustrated in Figure 3-13.

(5) $$footprint = Module\ width * \cos(\alpha)$$

(6) $$height = Module\ width * \sin(\alpha)$$

(7) $$spacing = height * 2.5$$

Where α is the module tilt.

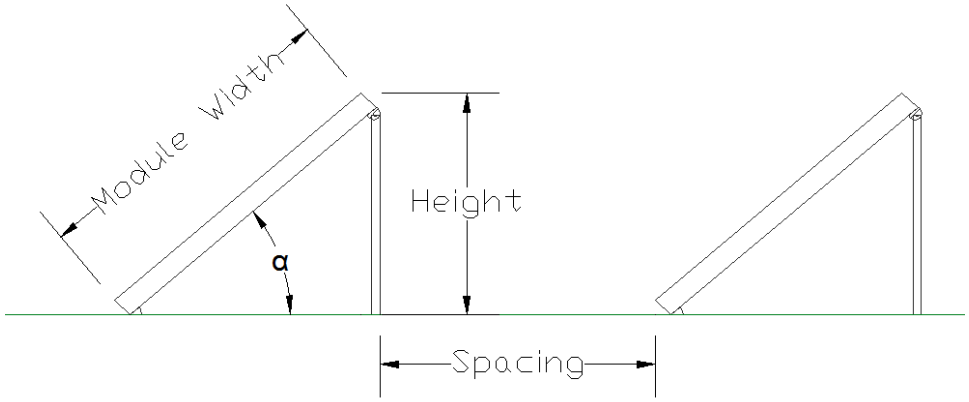

Figure 3-13. Illustrating the variables in (1)-(3)

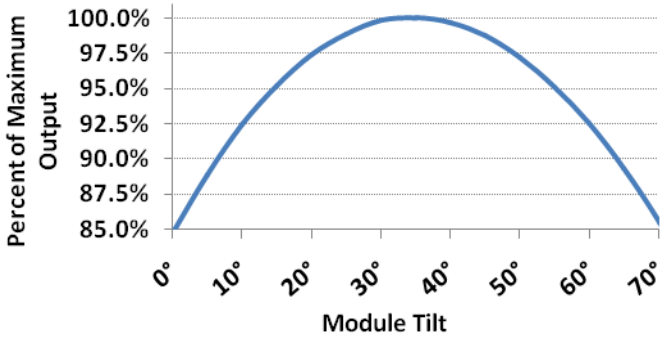

Figure 3-14. Percent of maximum output per module tilt

There is a variety of ways one could answer the previous questions; By modeling the total energy being generated in order to match a local demand, shortest payback period, maximum SREC generation, the initial investment, or even the ultimate price per kWh produced. The last answer seems to be the most useful, as it incorporates almost all the important factors mentioned thus far. It is also the most difficult, as there are a range of variables that need to be accounted for in order to paint an accurate picture of the costs

involved. With the availability of the various data already mentioned and provided in this thesis, most of these variables are taken care of (kWh per kW at every tilt angle, monthly average energy costs for NJ, expected SREC prices, space utilization and capacity, etc.) with only the need to address the few remaining. For one, it is important to set boundaries for the costs of the various aspects of a PV system – especially module & racking costs – when maximizing the effective value of a system.

3.4.c. Estimating System & Electricity Costs based on tilt

Note: It is possible for the author to approximate many of the costs associated with the installation of a PV system in large part due to his significant interaction with individuals in the renewable sector, involvement with industrial affiliates, consulting, literature and conferences the author has attended. These prices are not representative of any individual or company, but are representative of a sector average. With prices for modules having dropped to below $3/W from their previous levels of ~$4/W, they represent about half of the cost of a PV system. Roof mounted racking can be expected to cost around 38¢/W, balance of system (BoS, generally including all necessary equipment and hardware minus modules and interconnecting gear) equipment ca. $1/W and labor approximately matching BoS costs. This brings total costs for a roof-mounted PV array to just over $5/Watt.

Some estimates and stipulations apply in the following example: SREC prices are expected to sell at 70% of SACPs until 2016 and are then eliminated, module efficiency remains constant for 25 years, inflation is not accounted for, energy prices remain at 2009 levels and it is assumed that no benefits due to economies of scale are available. All of these assumptions create a very conservative outlook for PV, which in reality is expected

to be much stronger (energy prices are steadily increasing, SRECs may be around after 2016, etc.). This will give a worst case scenario for PV that errs on the side of being an underestimation.

Let us examine a theoretical system on a 100'x100' flat roof, with no obstructions (HVAC equipment, et al.) the entire surface of which is to be utilized by a PV system. Since we know the footprint of the modules, as well as their tilt angle and respective spacing, we can calculate the roof utilization, capacity, and output for each system at each tilt angle. Of course, one would be able to fit a larger number of modules on the roof by utilizing a low tilt angle. This would increase the total wattage of the system (increasing the costs) yet also increase the final electricity cost, since output is directly tied to module tilt. Figure 3-15 provide a good indication of how module tilt affects the system costs upon which Figure 3-16 is based.

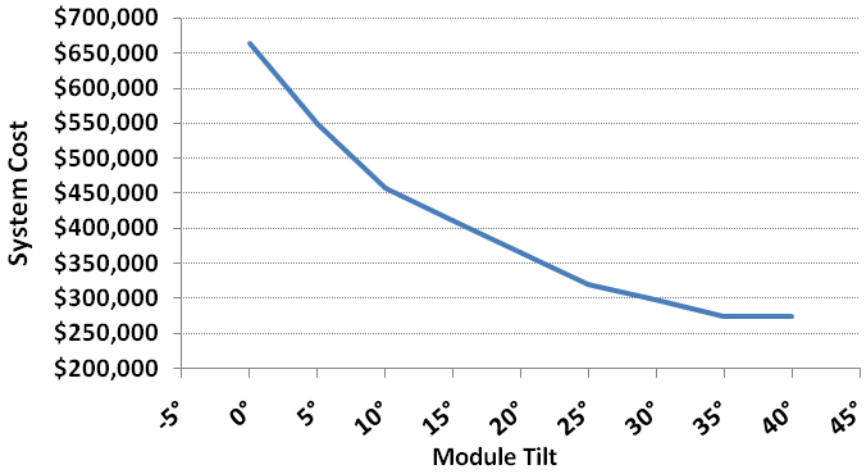

Figure 3-15. System cost vs. module tilt.

With 224W modules (used in this illustrative example), at the prices and conditions listed above, the estimated cost of each kWh of electricity generated can be calculated via Eq. (8) below. The equation incorporates all the costs of the system and all

the earnings expected from SRECs over the lifetime of a system. When dividing the net cost by the number of kilowatt-hours generated throughout the lifespan of the system, we can calculate the cost per kWh.

(8) $$\frac{(\$_{Modules} + \$_{Racking} + \$_{BoS} + \$_{Labor} - years_{SRECs} * \$_{SRECs}) * System\ Capacity * 100¢/\$}{kWh/year * LifeSpan} = ¢/\text{kWh}$$

Solving this equation by providing the necessary input values reveals a powerful trend; electricity costs associated with the output of the PV system decrease on the order of 3¢/kWh merely by ensuring proper module tilt. A system with modules laid flat on the roof is revealed to be very value inefficient, especially in comparison to low tilt angles in the 15° range that reduce capacity only slightly but reduce PV electricity costs by almost three cents per kilowatt–hour. If estimated SREC prices are included, any system will generate electricity below 7¢/kWh. *(As mentioned previously this estimate only included SRECs for 7 years, as the continuation of the REC program relies on a legislative vote to be held 2016.)*

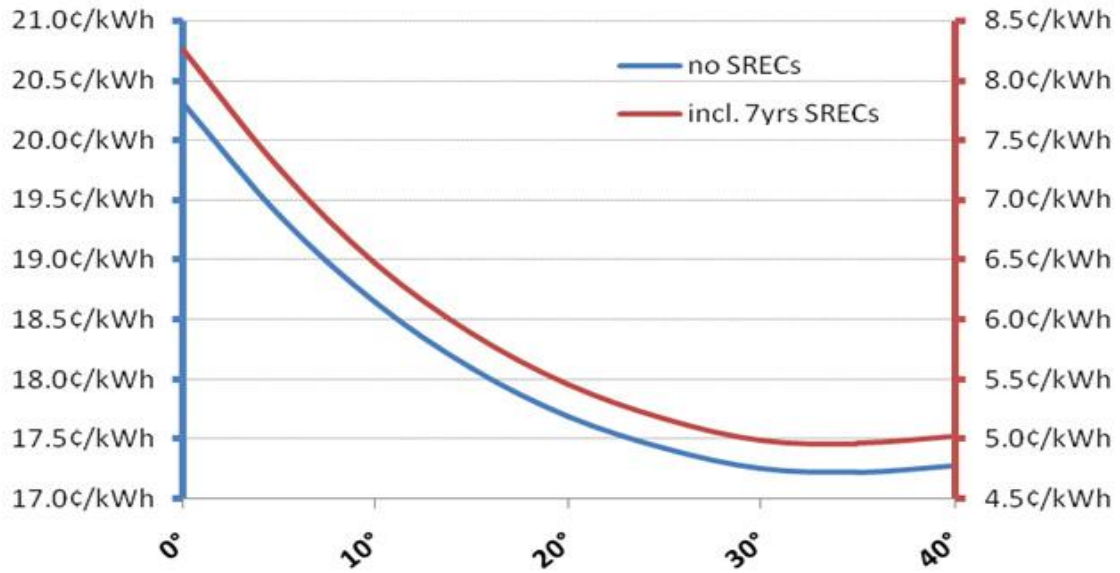

Figure 3-16. Estimated electricity costs per module tilt angle, with a 25 year system life, built in 2009

Figure 3-16 illustrates clearly that the best overall value can be gained by installing modules at around 32°, moving away from this optimal angle makes the lifetime net worth of the system progressively worse.

3.5. Effect of Module Shading

One serious issue that has often been under-addressed in photovoltaic system design is the detrimental effect shading has on the output of a PV module. Since most modules are merely a collection of 70 or more PV cells strung together in series, partial shading on one of these can cause the output of the entire module, along with the string it belongs to, to be limited by the production of that single shaded cell. This phenomenon occurs due to the fact that each cell is essentially a diode which only allows current to pass through if it is in a state of forward bias. This can, of course, only occur if the p-type side is positive with respect to the n-type side, which will only occur if a voltage is

generated by the cell via solar irradiance. If this does not occur, the cell acts as a diode in reverse bias mode and will block any current flow until it reaches its breakdown voltage. If this happens the cell may be damaged, or at the very least it will act as a load that will dissipate a large part of the electricity it is subjected to. This effect can be modeled quite well with help of circuit simulators such as OrCAD's Capture (formerly PSpice) with a simplified model of a PV cell or module. [69]

It has already been established that a PV cell acts essentially like a diode that can supply a current based on the amount of insolation it receives, which equates to a voltage controlled current source. A current source in parallel with a diode gives the basic model for a PV cell, to which only a pair of series and parallel connected resistors need to be added in order to account for various inefficiencies. *For examples given throughout this thesis, Rp=100 Ohms, Rs=0.001 Ohm unless otherwise noted.*

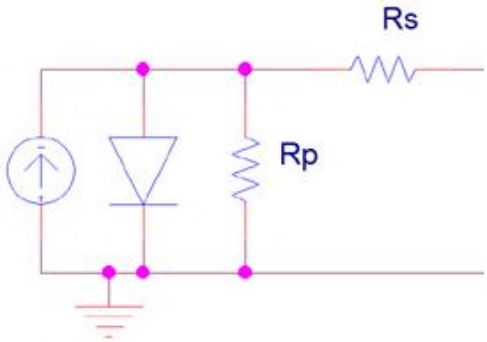

Figure 3-17. Basic model of a PV cell

Several of these cells can be strung together in order to simulate the operation of an entire module, illustrated in a model of a Photowatt 1650 in Appendix D. The effects of single or multi-cell shading can then be approximately quite easily by varying the amount of current each individual current source provides. The maximum current output correlates very nicely with the amount of insolation on a cell, meaning that current drops

proportionally to the amount of shading on a cell. This makes adjusting the current source a relatively accurate means of approximating the behavior of the cell under shading. As seen in Figure 3-18 the maximum output power will occur right before a steep drop in current, which can be attributed to the parallel diode having reached its turn on voltage, thereby letting current flow through freely. For this theoretical cell the maximum output current is 5.1A, with a nominal output power of 2.5W. As the cell is shaded to a higher percentage of its surface area, the current is affected in a proportional manner which in turn alters the output power of the cell comparatively. The output of an entire module consisting of cells only in series, without bypass diodes, will look identical with the exception that the voltage at which it operates will be significantly higher. Of course, most modules today come with bypass diodes that can help reduce losses caused by shading. Some divide the string of cells into two, thereby cutting the module capacity in half if significant shading occurs anywhere on either half, whereas others have multiple bypass diodes that allow for smaller compartmentalization of various strings of cells within the module. Bypass diodes work, as their name indicates, by completely bypassing strings of cells within a module when they are performing worse than the rest. This essentially eliminates the under-performing

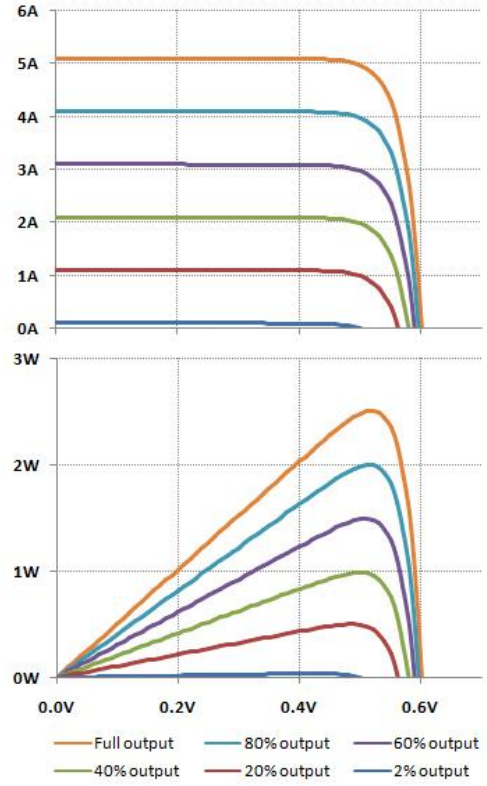

Figure 3-18. The effect on power and current of the theoretical PV cell, with adjustments of current source output.

cells and prevents them from limiting the others in the group. Two configurations to exemplify the operation of a bypass diode are given below, one diagram which incorporates the use of bypass diodes (Figure 3 20), the second being merely a string of nine cells in series.

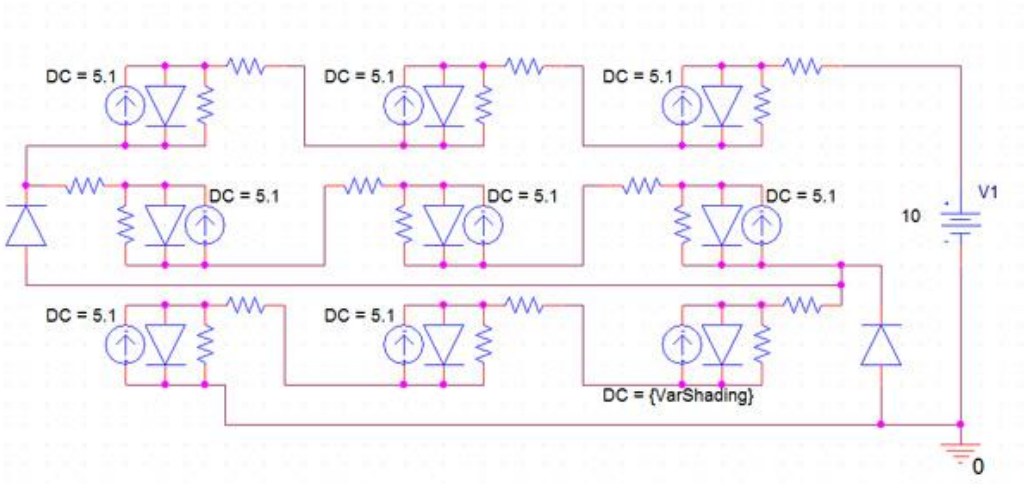

Figure 3-19. Simple 9-cell module with two bypass diodes.

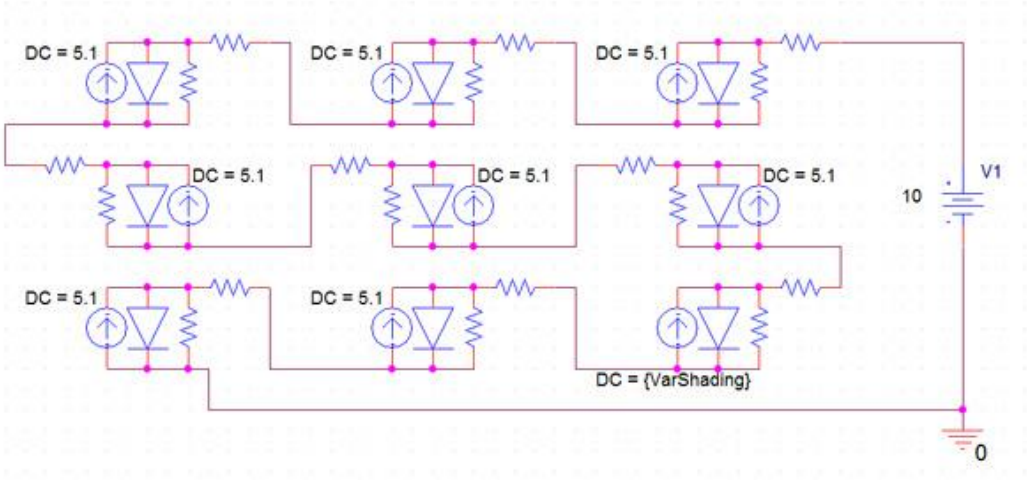

Figure 3-20. 9-cell module with no bypass diodes.

In Figure 3-19 one cell in the bottom row is subjected to a changing current, which represents the stages of shading it may go through. Just one of the three cells in that row being shaded immediately eliminates the entire row from supplying power to the

module. This means that the maximum power point may actually be at a voltage dependent on the number of modules in un-shaded rows. Figure 3-21 and Figure 3-22 make note of this effect, the former being for the 9-cell module with bypass diodes and the latter without.

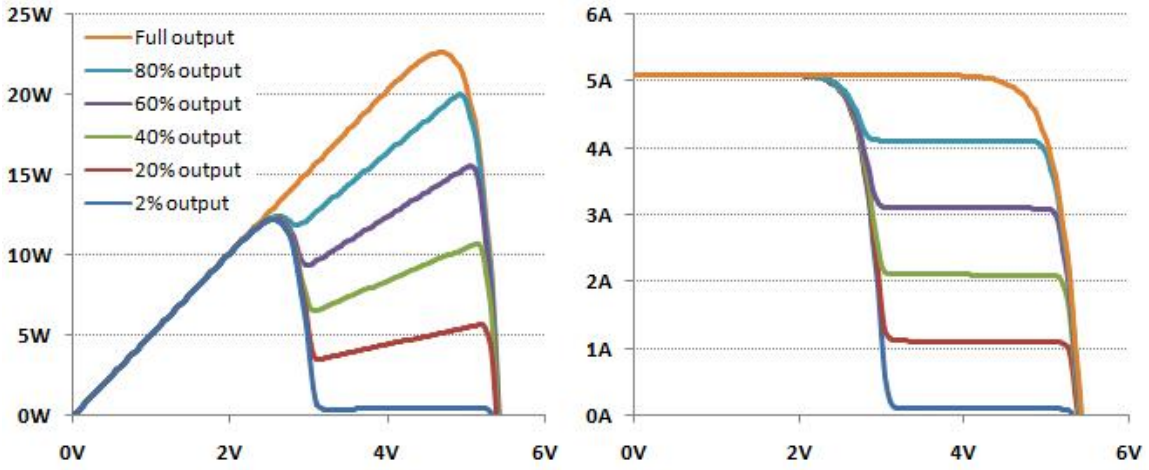

Figure 3-21. 9-cell module with bypass diodes, where one cells output is varied.

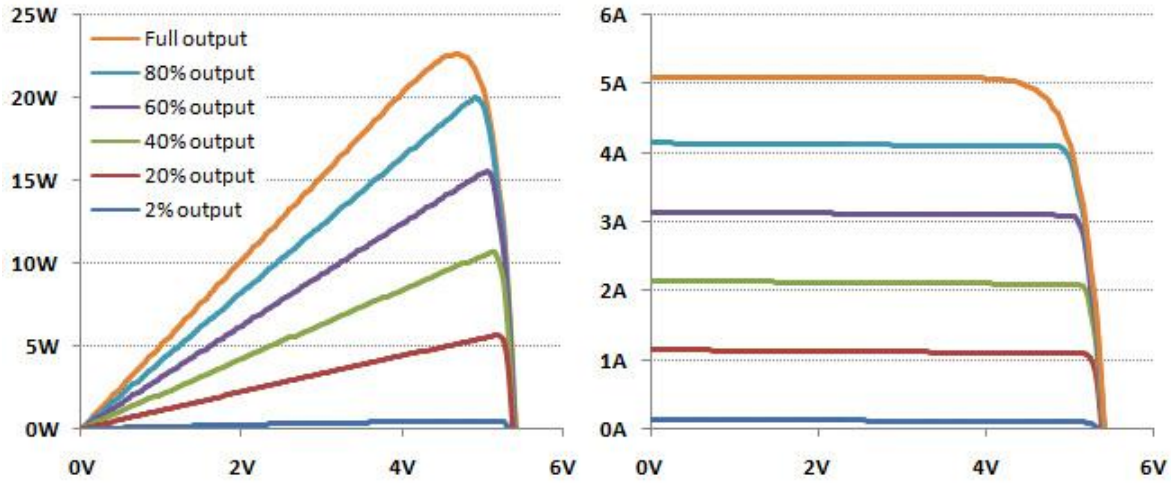

Figure 3-22. 9-cell module without bypass diodes, where one cells output is varied.

As can be seen in the following figures, bypass diodes placed in two row intervals can limit the losses incurred by shading said row to the capacity of those rows themselves. If these diodes were not present the entire module would continue to be

limited to the current output of the cells or rows being shaded and potentially cause serious issues.

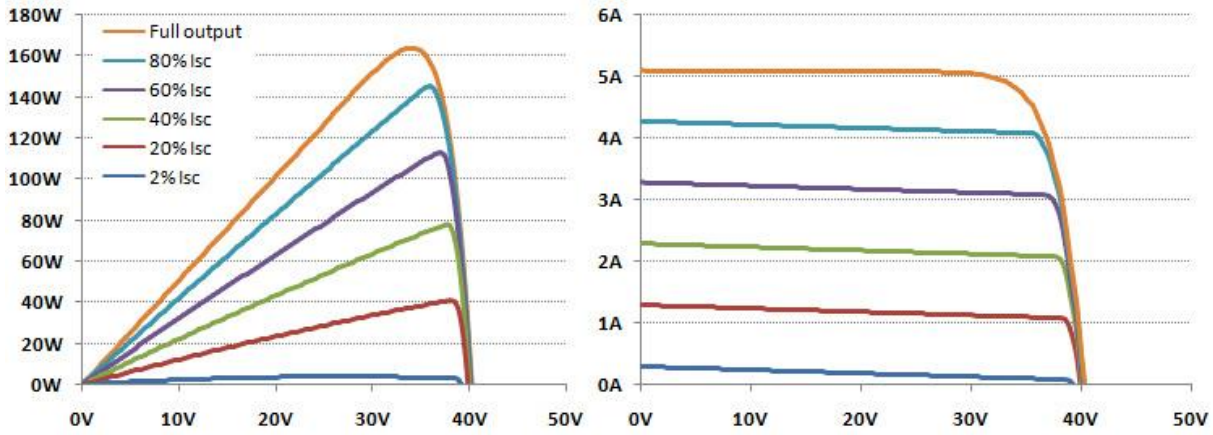

Figure 3-23. Modeled PW1650 output, no bypass diode.

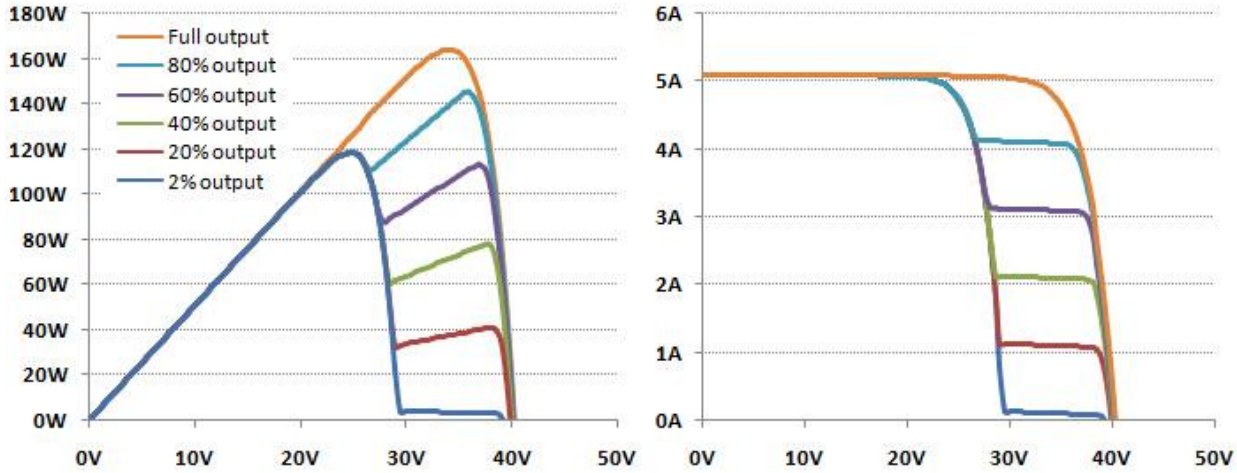

Figure 3-24. Simulated PW1650 output with bypass diodes installed every two rows

The inclusion of bypass diodes means that the maximum losses the module will be subject to will never exceed more than the percentage affected by the shading (plus small losses due to the diodes themselves). Table 3-4 gives the numerical breakdown for the PSPICE model of the 165W module used in the above figures.

Table 3-4. Maximum theoretical power and percentage for various shading simulations

	No Bypass Diode		Bypass Diode	
	Max. Power	% Nominal	Max. Power	% Nominal
2% output	3.9W	2%	118.4W	72%
20% output	41.0W	25%	118.5W	72%
40% output	77.8W	47%	118.5W	72%
60% output	113.3W	69%	118.6W	72%
80% output	145.2W	88%	145.2W	88%
Full output	165W			

In order to validate the theoretical tests completed in PSPICE, a system was designed that utilizes an electronic load to sweep through a range of resistances at set intervals. At each of the points, measurements for voltage and current were completed and recorded automatically with help of a MATLAB program. The initial program created for this purpose has since been improved upon by a clinic team at the Center for Sustainable Design (CSD), for which a publication has been accepted for presentation. [40] A PSPICE version of the test module was created, its outputs in two situations shown in Figure 3-23 & Figure 3-24, in order to compare the theoretical outputs with what was found empirically. The test module was a Photowatt 1650, a 165W module with a Voc of 40.3V, Vmp of 34.4V, Isc of 5.1A and Imp of 4.8A. Several tests were run over the last year with this module for varying insolation levels. The graphs provided here were compiled with data during a time of year where insolation did not reach the high levels necessary to ensure optimal module operation, however the outputs still correlate very nicely on a percentage basis with those of the module modeled in PSPICE.

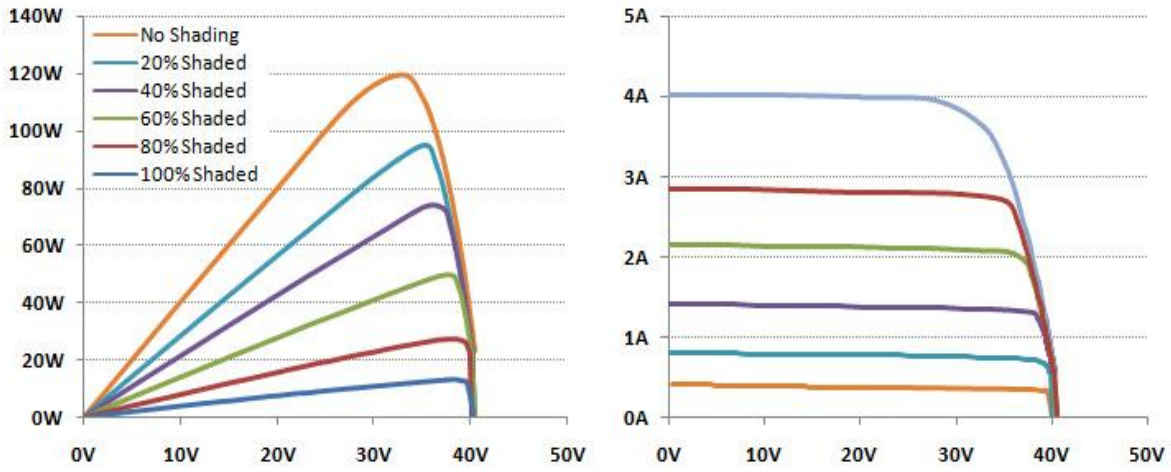

Figure 3-25. Real PW1650 output when subjected to varying levels of shading.

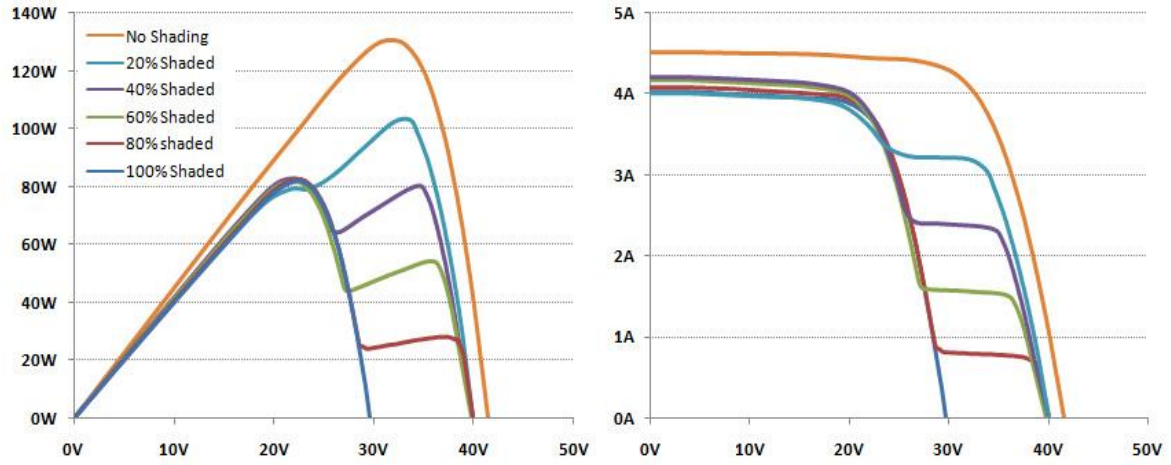

Figure 3-26. Real PW1650 output at various shading levels, with bypass diode installed.

Table 3-5 gives the outputs in terms of their percentage of the maximum output recorded that day. Only a single row was shaded in the process, yet two rows were eliminated due to the dual-row bypass setup of the module. Several runs were completed for each of the two setups, and averaged in order to smooth out small inconsistencies in the data. Though insolation changes caused the maximum output of the module to change during each of the runs, the percentages still correlate quite well with those predicted with the PSPICE model.

Table 3-5. Actual module performance under various shading tests

	No Bypass Diode		Bypass Diode	
	Max. Power	**% Maximum**	**Max. Power**	**% Maximum**
100% Shaded	13.0W	11%	81.8W	63%
80% Shaded	27.2W	23%	82.8W	63%
60% Shaded	49.6W	41%	82.1W	63%
40% Shaded	73.5W	62%	82.8W	63%
20% Shaded	94.9W	79%	103.1W	79%
No Shading	119.4W	100%	130.7W	100%

As shown, circuit simulators can be quite useful in predicting the output of PV modules in various situations. With the help of PSPICE the effect of individual cell and row shading can be approximated quite accurately, as verified by the empirical measurements by the test setup. Even though there were additions to the ideal model of a PV cell to create the effect of a "lossy" system, it is not perfect. Some effects of shading were not able to be tested, however, as they require a more detailed simulation of the materials of which PV cells are composed.

3.6. Reverse Biased Cells

The drop in output correlates strongly with the percentage of cells being eliminated, making the various manufacturer's placement of bypass diodes an important consideration during the design phase of a system. However, power loss due to shading may not be the most important reason to place bypass diodes throughout a module. A much more serious issue comes into play when modules are partially shaded without the presence of bypass diodes, causing individual cells to become reverse biased. Prolonged shading situations can cause irreversible hot-spot damage, where current becomes highly concentrated at a small number of points throughout the cell. Focal point heating can

cause local temperatures to rise to be in excess of the standard critical temperature of encapsulants of 150°C. This may lead to the deterioration of the insulation properties necessary to prevent hazardous situations, which include cell to frame shorting. [32][33] All modules that the author has seen thus far were outfitted with bypass diodes, ensuring that they are safe to use and will not be damaged by partial shading. Often only a single bypass diode was utilized to eliminate the safety hazards associated with reverse biased cells, which may not be enough to thwart heavy losses during times of partial shading. As mentioned previously, in various situations the amount of partial shading on multiple cells can cut production by a factor tightly linked with percentage of the cells affected by the shading. For large scale systems where limited inter-row spacing is utilized throughout the array this could be the cause for serious production losses that could have easily been avoided.

Chapter 4. Solar Path & Shading

4.1. Introduction

As discussed in the previous chapter, disregarding module installation parameters or inter-row shading when designing a PV system will be detrimental to the overall effectiveness of the system. For this reason, it is important to space the modules at appropriate intervals in order to maximize the system's output and, with that, its value. It has already been discussed how optimal spatial utilization increases a system's value, but those numbers rely heavily on the inter-row spacing necessary per tilt angle. Many racking manufacturers have their own spacing intervals that they recommend depending on the region in the world the system is to be located in, but depend mostly on what the manufacturer believes to be an acceptable amount of losses throughout the year. No amount of spacing will ever ensure that modules remain un-shaded throughout the entire day due to the sun's rising and setting at the horizon. For this reason it is important to take into consideration during which hours of the day what amount of energy is produced in order to determine where shading may be acceptable. This can also vary with the type of modules used, as bypass diode configurations and technology differences affect the operation of a module under shading. Discounting these for the moment and focusing on the amount of shading simplifies the situation quite a bit.

4.2. Calculating Solar & System Parameters

Since the sun is the controlling factor when determining the length of the shade created by a module, it is important to know its position in the sky based on the local

latitude, day of year and hour of day. Figure 3-6 has already shown that there are only three angles that are of interest when determining the position of the sun in the sky. First, the azimuth angle Φs gives the angle between an imaginary horizontal line in the direction of the sun and south, second the elevation angle β which gives the angle between this imaginary horizontal line and a line pointing directly at the sun, and finally the solar declination δ which is dependent solely on the day of the year and represents the earth's tilt with respect to the sun.

$$\delta = 23.45 * \sin\left[\frac{360}{365} * (n - 81)\right] \quad (9)$$

Where *n is the desired day of the year.*

The angle of 23.45° represents the maximum angle (+/-) that the sun reaches with respect to the earth's equator, 81 is the day of the spring equinox (March 21).

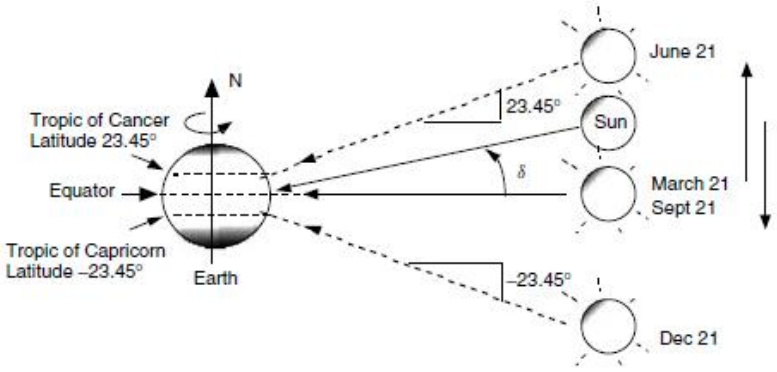

Figure 4-1. Solar Declination throughout the year [53]

The solar declination calculated with (9) is only accurate for solar noon of that day, as it actually changes slightly throughout the day. However, the change is quite insignificant as inter-day shifts are a maximum of ~.4° per day, and can be ignored within the boundaries of this analysis. Since the earth completes a single revolution per day, each hour can be attributed to a 15° change in the sun's angular location in the sky (360°/24hrs) which has been termed the solar hour angle. Solar noon, the point in time at

which the sun is at its maximum, is set to 0° meaning that ±180° represents the point at which the sun is at its minimum. Any positive solar hour angle therefore represents the amount of time passed since solar noon, and any negative the amount of time still necessary for the sun to reach solar noon. A more accurate method of calculating the solar hour angle which includes a correction for the equation of time (the actual measure of time not based on the sun) is given in (11) below.

(10) $$H = 15 * t - 12.5 + [EQT(day) + 4 * (L - TZ * 15)]/60$$

Where *H is the solar hour angle,*
t is the hour of the day,
EQT is generated with (11),
L is the latitude and
TZ is the time zone(- for W of GMT)

(11) $$EQT = 0.00007 + 0.001868 * \cos(D) - 0.032077 * \sin(D) - 0.014615 * \cos(2 * D) - 0.040849 * \sin(2 * D) * (229.18)$$

Where *D is the day angle, given by (12).*

(12) $$D = 2\pi * (n - 1)/365$$

Equipped with the solar declination of the day, the local latitude and the desired solar hour angle, it is now possible to calculate the solar elevation angle with (13) below.

(13) $$\beta = \sin^{-1}[\cos(L)\cos(\delta)\cos(H) + \sin(L)\sin(\delta)]$$

Where *β is the solar elevation angle.*

Finally the solar azimuth can be calculated with help of (14):

(14) $$\Phi s = \sin^{-1}[\frac{\cos(\delta)\sin(H)}{\cos(\beta)}]$$

Where *Φs is the solar azimuth,*

δ the solar declination,
H the solar hour angle and
β is the solar elevation angle.

Equations (9)-(14) provide all the information necessary to determine the shade path of any desired object illuminated by the sun throughout the day. The sun's elevation angle is the most important variable when calculating the length of a shadow being cast by an object, see Figure 4-2. If the height of an object is known, in this case a PV module, (15) can be used to calculate the length of the shadow given the solar elevation angle.

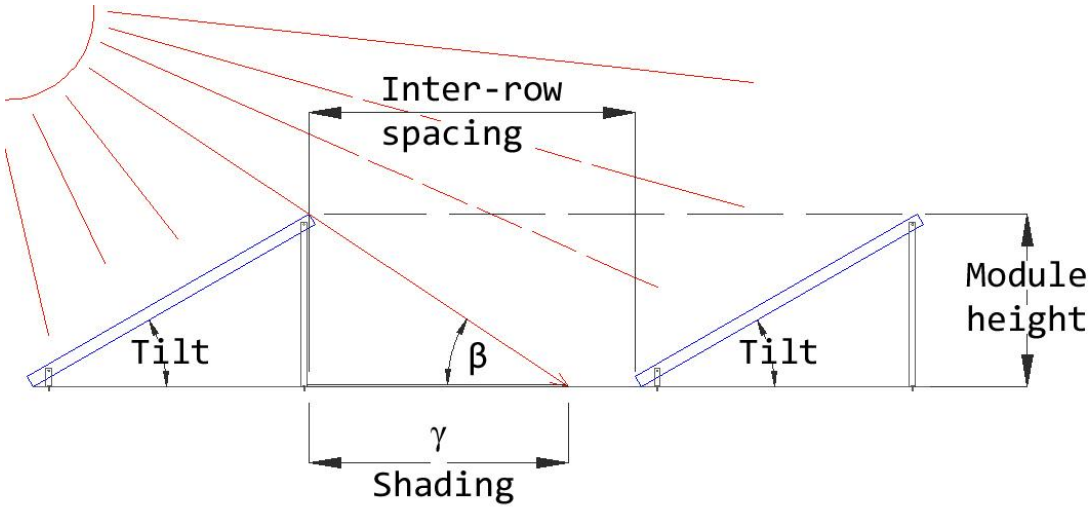

Figure 4-2. Solar angle, module tilt and shading length

$$\gamma = \frac{Module\ \ height}{\tan(\beta)} \quad (15)$$

Where *γ is the length of the shade created by the module*

However, it is not the only thing one needs to consider when determining the inter-row spacing, since the direction of the shadow will also be a key factor. As the sun comes up and goes down at relatively extreme angles (~±60°) with respect to the modules facing southward, it will cast a very long shadow in the opposing direction. Due to the

path this shadow takes, it will oftentimes not shade the following row, as only its length parallel to south (or module row orientation) is important. This effect is illustrated in Figure 4-3 where the sun striking a module with a 22" height, at an elevation angle of 11.7° in February 13th, at 4pm, at latitude 41 creates a very long shadow, but since its azimuth is -59° it is still not shading the next row of modules with the provided spacing.

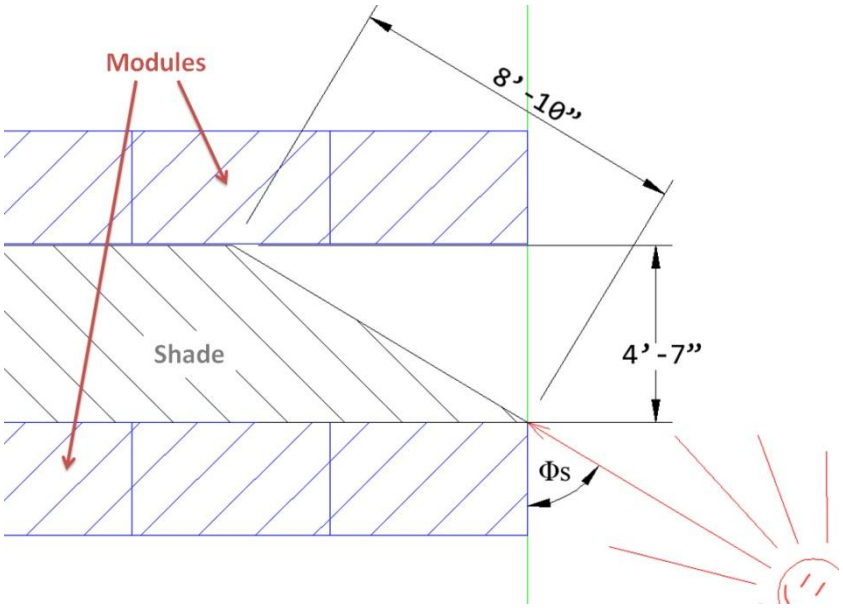

Figure 4-3. Solar azimuth and shading

Given (15), the length parallel to the modules can be calculated via (16).

$$\lambda = \gamma * \cos(\Phi s) \quad (16)$$

This can also be modified to include the module azimuth (Figure 4-4):

$$\lambda = \gamma * \cos(\Phi s - \Phi m) \quad (17)$$

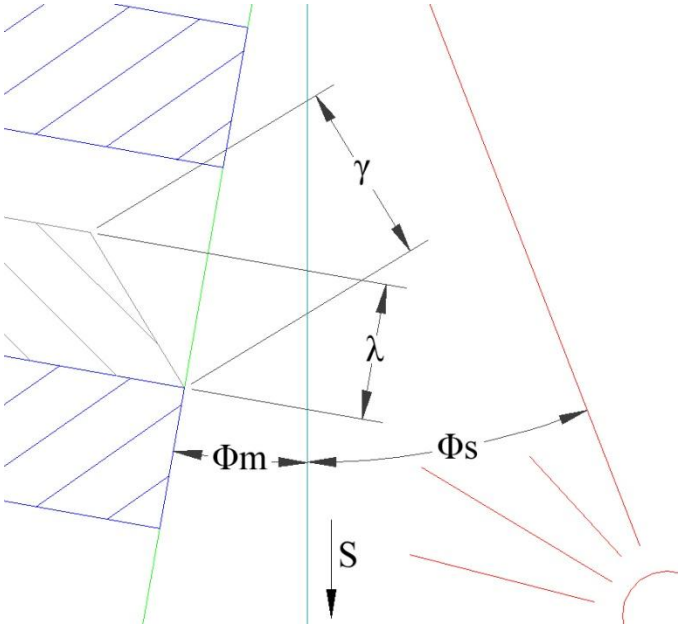

Figure 4-4. Inclusion of both solar and module azimuth

These equations may be combined in order to adjust the incoming direct normal insolation on a horizontal surface to that which is incident on the module surface throughout the day:

$$\cos(\theta) = \cos(\beta) * \cos(\Phi_S - \Phi_M) * \sin(\alpha) + \sin(\beta) * \cos(\alpha) \quad (18)$$ [53]

Where θ *is the incident angle between the sun and the module.*

4.3. Estimating Insolation

Lastly and most importantly, the insolation itself needs to either be measured or calculated. One can estimate the global horizontal insolation (GHI) at any location on earth by starting with the extraterrestrial irradiance, which is fairly constant, and adjusting it based on the earth's movement around the sun, its rotation around itself and the atmospheric conditions at a point on earth. Yet, measuring and recording every

atmospheric parameter necessary to create accurate estimates is a difficult thing to do and requires a large quantity of sensors. A much simpler approach would be to take the estimated extra terrestrial direct normal irradiance (ETRN) on earth, which is relatively easy to calculate, as well as measure the GHI at any location of interest. One can then estimate the effects of the earth's atmosphere on the measured insolation and generate a simple model that extracts the direct normal irradiance (DNI), the amount of insolation coming directly from the sun without being diffused, on a horizontal surface on earth. It is then possible to modify the DNI with (18) to create an accurate estimate for the insolation incident on a module at any azimuth and tilt.

To generate the necessary ETRN values for every day of the year, Myers' [58] equation for calculating said irradiance is a useful tool (19). The value used in the equation, 1370, is what is known as the solar constant, or the power of the sun at the earth per square meter. [35]

(19) $$ETRN = 1370 * [1.00011 + .034221 * \cos(D) + .00128 * \sin(D) + .000719 * \cos(2 * D) + .000077 * \sin(2 * D)$$

Where D *is* $\frac{2 * \pi * n}{365}$
and n is the day of the year.

The recorded GHI, as well as the calculated ETRN values are sufficient to create an accurate depiction of what is happening in the atmosphere at the location of the GHI measurements. The report goes on to explain that the effective global horizontal transmittance, K_t, was chosen as the controlling variable. This value is also known as the "clearness or cloudiness index" [54].

(20) $K_t = GHI/[ETRN * \cos(z)]$

Where *z is the zenith angle, calculated via (21)*

(21) $z = 90 - \beta$

Next, air mass (AM) values need to be calculated for the suns position in the sky throughout the day (AM is an important factor in determining the transmittance of the air the insolation is traveling through). The air mass in this situation is actually the relative air mass, the multiple of the distance that the sun's rays have to travel through our atmosphere at the sun's highest point, at any given point in time.

(22) $AM = PC * [\cos(z) + .15 * (93.885 - z)^{-1.253}]^{-1}$

Where *PC is the pressure correction value calculated by (23), and AM is the air mass at the zenith angle z.*

(23) $PC = \frac{P}{1013.25}$

Where *P is the pressure at the given location.*

Based on the air mass for each hour of the day, the clear sky direct beam transmittance, Kn_c, may be approximated with (24). This value creates the relationship between the change in horizontal transmittance and air mass, which is necessary in order to estimate the atmospheric conditions at the time.

(24) $Kn_c = .866 - 0.122 * (AM) + 0.0121 * (AM)^2 - 0.000653 * (AM)^3 + 0.000014 * (AM)^4$

Author [54] believed it would be beneficial to include the correlation between the air mass and the discrete changes in transmittances with what he termed ΔKn & ΔKt,

(18). ΔKn can be computed with (25), while ΔKt was not necessary in the evaluation of DNI.

$$\Delta Kn = a + b * e^{c*AM} \tag{25}$$

The coefficients given in the above equation are to be calculated according to the following set of equations:

$$If\ Kt \leq 0.60 \begin{cases} a = 0.512 - 1.56 * Kt + 2.286 * Kt^2 - 2.222 * Kt^3 \\ b = 0.370 + 0.962 * Kt \\ c = -0.280 + 0.932 * Kt - 2.048 * Kt^2 \end{cases} \tag{26}$$

$$If\ Kt > 0.60 \begin{cases} a = -5.743 + 21.77 * Kt - 27.49 * Kt^2 + 11.56 * Kt^3 \\ b = 41.4 - 118.5 * Kt + 66.05 * Kt^2 + 31.90 * Kt^3 \\ c = -47.01 + 184.2 * Kt - 222 * Kt^2 + 73.81 * Kt^3 \end{cases}$$

And finally, in order to get the DNI we insert our results into (27)

$$DNI = ETRN * (Kn_c - \Delta Kn) \tag{27}$$

The DNI calculated with (27) can now be used in equation (18) to provide insolation numbers for any hour throughout the year. The process described here has been implemented in a very versatile MATLAB program, "insolation_calc". Using this MATLAB model it was possible to calculate the optimum inter-row spacing multiplier. A few additions had to be made, including estimated PV module outputs which could be calculated based upon data collected in chapter 3, as well as including the effects of shading on the output. Lastly, with the efficiency and surface area of a module given, the direct insolation normal to the photovoltaic module can be estimated quite well, merely by providing the global horizontal irradiance data in hourly intervals, which can be recorded with the help of various simple GHI meters.

4.4. Calculating the Shading Multiplier

While there seems to be a nearly endless number of applications for insolation_calc, one of the most important ones, in terms of its value to a designer, is the creation of a clear guide for shading multipliers. Based upon these calculations one finds that the initial rough estimate recommendation to space rows of modules at 2.5 times the height of the highest point of the forward module (used in the preliminary excel program) was actually quite a close approximation. In fact, at 30° tilt, 0° azimuth and at Latitude 39° a system with this multiplier would be ensured of receiving over 99% of the sun's available radiation throughout the year at a latitude of 40°, Figure 4-5.

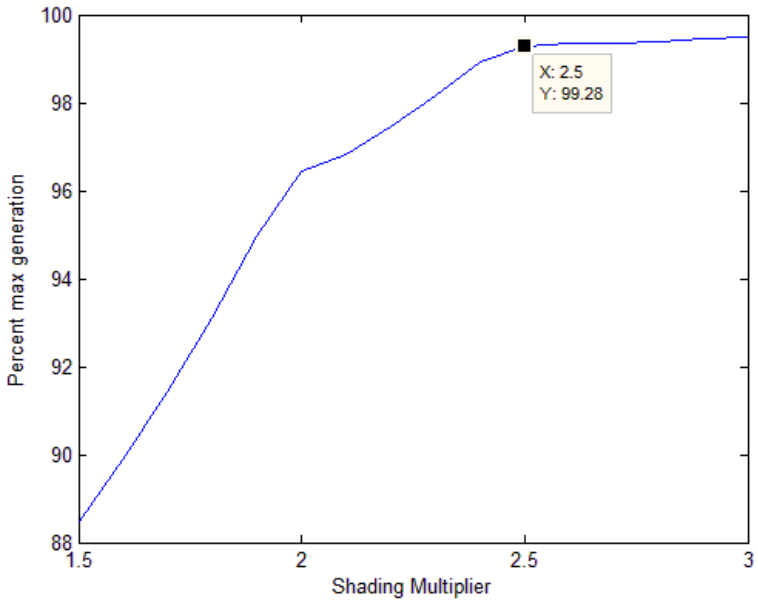

Figure 4-5. System output with various shading multipliers

Output was not regular or consistent over the entire span of tilt angles though, as shown in Figure 4-6 below, where a sweep is taken through various module tilts and the spacing multiplier set at 2. As the module tilt angle increases the multiplier must increase in order to retain the same system performance. The same remains true for changes in the

azimuth angle as well; the more oblique the system azimuth from facing south, the more losses it would experience due to shading.

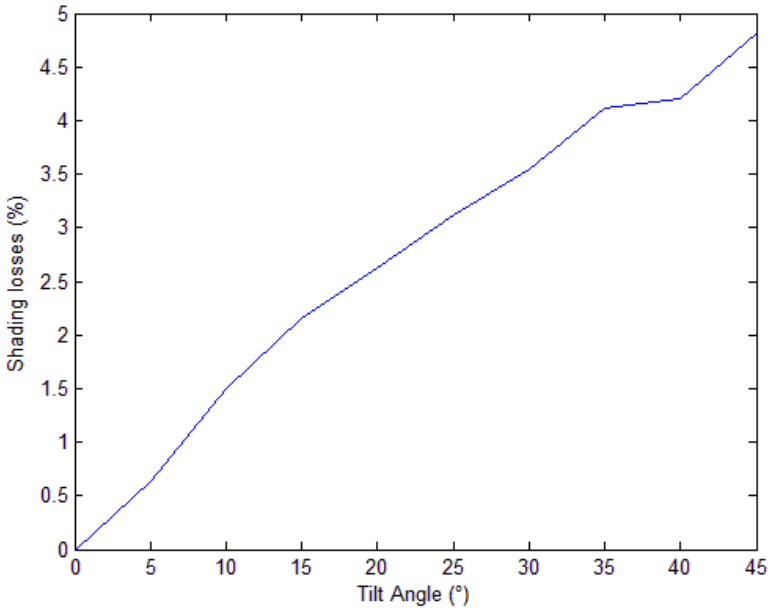

Figure 4-6. Shading losses vs. tilt angle, with a spacing multiplier of 2.

This means the row spacing multiplier should be adjusted to retain the same efficiency for every different tilt angle. Figure 4-7 illustrates that shading losses are actually more significant when a system is located off the optimal 0° azimuth, reaching close to 8% at an azimuth of 40° and spacing multiplier of two, if no adjustments to the spacing are made. When this is taken into account, a linear trend of the multipliers is created for systems at 0° azimuth, where a tilt of 10° would necessitate only a 2x multiplier, up to a 2.5x multiplier at 45° as illustrated in Figure 4-8.

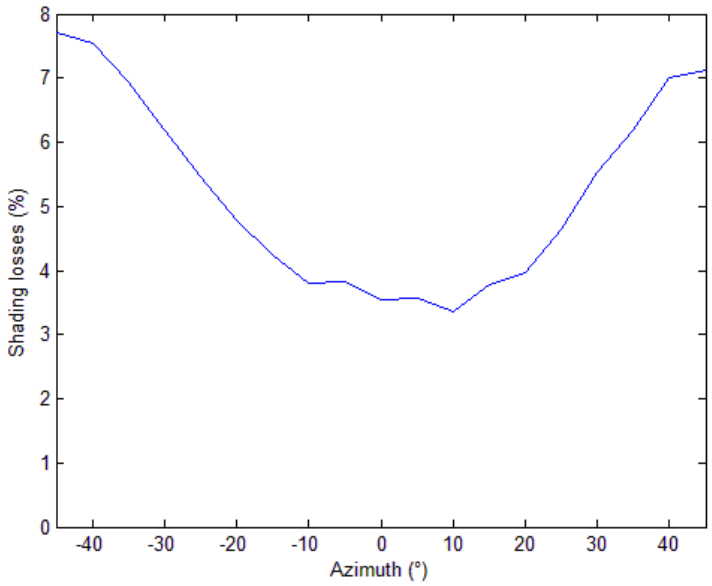

Figure 4-7. Shading losses vs. Azimuth, with Alpha of 30° a multiplier of 2.

As illustrated in these few examples, there are many different factors that must be taken into consideration when determining the optimum system layout parameters. For systems at the same latitude, facing directly south and having varying module tilts, shading multipliers need to be adjusted according to Figure 4-8 in order for the PV system to experience no more than 2% losses due to shading. As mentioned, the azimuth of the system is crucial in determining the correct spacing multiplier. Figure 4-9 illustrates the change in multiplier necessary to keep shading losses at an acceptable 2%.

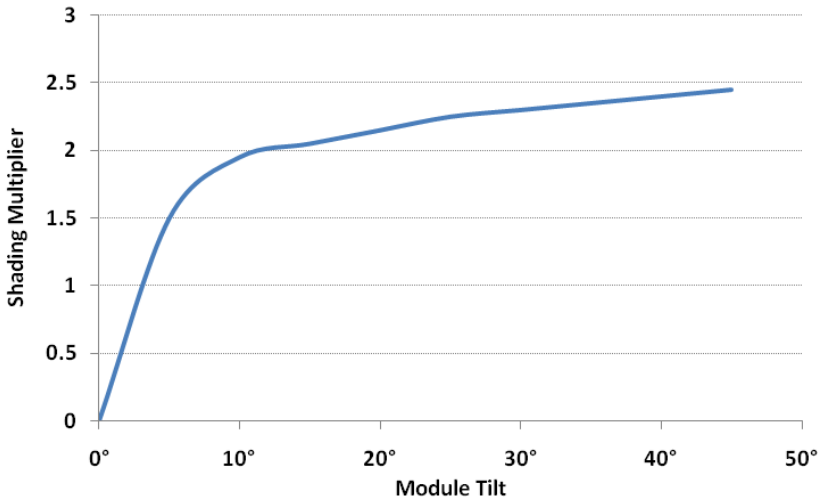

Figure 4-8. Shading multipliers with limit of 2% shading losses (Lat 40, 0º Azimuth)

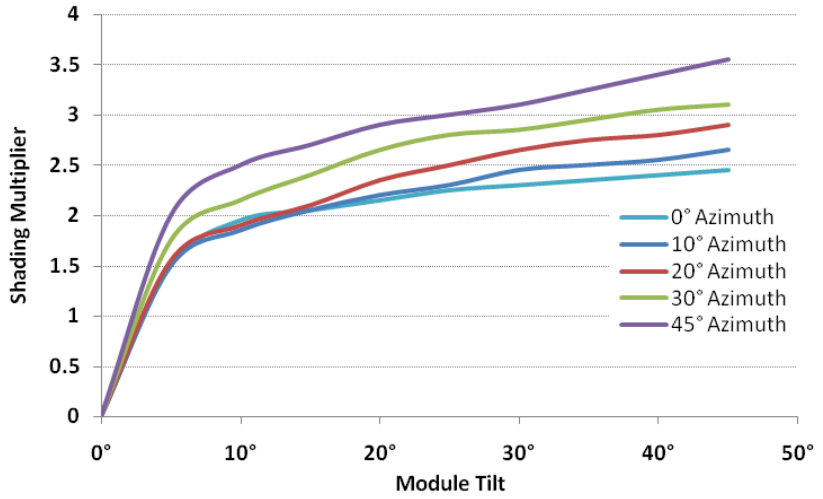

Figure 4-9. Shading multipliers with limit of 2% shading losses, multiple Azimuths.

The program, which can be found in Appendix E, was built to utilize the NREL typical meteorological year (TMY) data which can be loaded directly from the csv files present on NREL's site. Simple modifications can also be made to enable the use of this with any GHI input, with only latitude, longitude, system azimuth & tilt, spacing to test, and average local pressure in mBar given. The MATLAB implementation makes for a very powerful platform to operate various versions of this program. Some have already been highlighted herein, most will consist of different representations of the data already

generated by the base program. Some additions may be made to make for an even more accurate program that will enable a system designer to estimate system production by implementing an algorithm to compute the total diffused insolation on a module surface. Several scripts exemplifying the usage of the main program to generate various outputs of interest are also found in Appendix F.

Chapter 5. Achieving Grid Parity

5.1. Introduction

Photovoltaics have historically been characterized as unaffordable electricity generators due to exceedingly high materials and equipment prices since their invention. The steady decline in these costs raises the question of when photovoltaics will become economically feasible and competitive with other major means of generating/delivering electricity for customers. Since the costs per kWh rely primarily on the initial capital investment of a PV system, rather than on the current commodity prices of fuel as with other types of generation, the estimated output and system life expectancy create the driving costs of generation throughout the operation of a system. While maintenance factors in as well, it is not nearly as significantly as with standard generation technologies. When an approximation based on expected output and lifespan is made, it may actually undervalue the system's capability to produce electricity beyond the commonly referenced module warranty period of 25 years. Though PV modules have proven to be capable of producing energy for far longer than a quarter century, it is understandable that manufacturers would not warrant any device through the very end of its expected life. Furthermore, the extent of the degradation of module output over time is an important measure when determining how long maintaining a PV system would be worthwhile.

5.2. System "Lifetime" & Output

The total output of a system over its lifetime is one of the two most important factors in calculating the effective 'cost' of the electricity that the system produces. Many modules are warranted to retain on the order of 80% of their output performance for 25 years. Sharp, one of the top three PV module manufacturers in the world, provides a warranty providing two levels of guarantee. First, their "Limited Warranty for Materials or Workmanship" safeguards, as the name indicates, the initial consumer from any issues caused by defective workmanship or materials. This includes five years worth of coverage within which Sharp will either repair or replace defective modules at no charge to the customer. The second and more important section of the warranty is the "Limited Warranty For Power", which gives a somewhat intricate specification for allowable degradation of module output. This continues for "25 years from date of purchase by the first consumer" and covers the "first 10 years at 90% minimum rated power output and the balance of 15 years at 80% minimum rated power output." The power warranty is straight forward, guaranteeing that the modules will retain 90% of their generation effectiveness for the first ten years, even though this means that module output could drop by 10% the second year without being replaced. For the first ten years a drop of efficiency of one percent can be expected, not 10%, as degradation around 1% has been observed in several studies. [55][102][70]

In an email exchange with Bill Sekulic, the Master Research Technician at NREL in Golden, Colorado [67], he mentioned that PV life expectancy is

> "kind of the holy grail, if you will, of PV reliability testing. We do not have a clear, concrete answer for every technology produced today. For

example, mono-Si modules usually have a 20-25 year warranty, usually stating that after that period the module will retain better than 80% of its name plate rating. From the limited samples and testing we have conducted here at NREL, this appears to be the case. For thin films, there are other issues. Testing we have conducted has pointed to numerous issues with production, water ingress and other packaging issues."

He goes on to say that "no one will have an answer to this question [of expected module lifetime]. With hundreds, if not thousands of systems being installed every year, we will know in about 20-30 years. To give you an example, the automotive industry does extensive testing, [spending] millions of dollars per year to find out the MTBF (mean time before failure) for each of their components. The PV industry doesn't have that type of capital or infrastructure, not to mention testing facilities to do similar testing on each fielded module, inverter and component. This is why I refer to degradation rates and reliability [rather than MTBF]. There are ongoing studies at Sandia, DOE and NREL which are attempting to gather information about fielded PV systems and failure rates, mechanisms and reliability." [89]

What this essentially means is that it is not advisable to make estimations of a system's output beyond the warranted period. It is most realistic and conservative to use the assumption that a PV system's life ends after 25 years of service. On the production side we are able to create an accurate estimate of the system output throughout those 25 years. Going solely with the common standard exemplified by Sharp's warranty, i.e. 90% after 10 years and 80% minimum for the last 15 years, it is possible to compute the estimated total electricity a system generates throughout its life. Further, with degradation

expected to be linear, estimated output for each year may be calculated as well. Given the conservative generation scenario, where module output drops by about 1% each year for the first 10 years, and by about 0.667% over the last 15 years, we find the number of kWhs for each year, Figure 5-1.

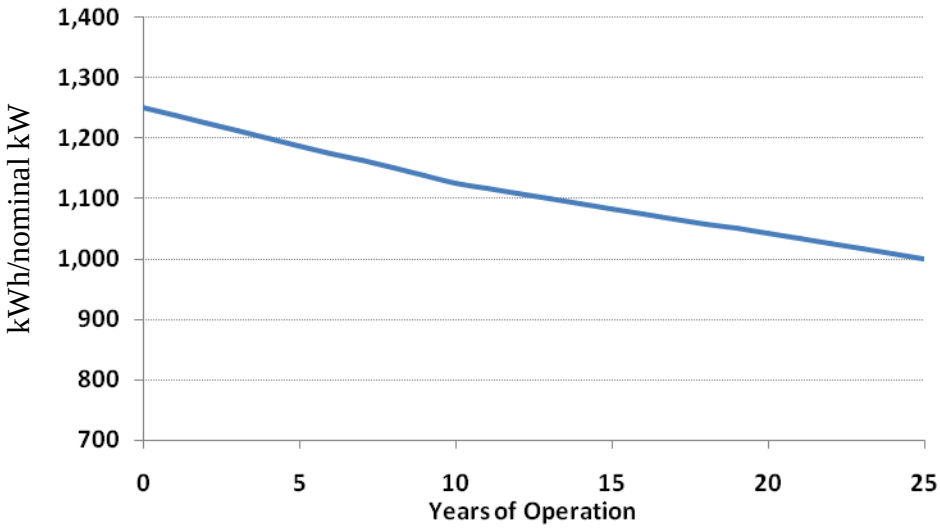

Figure 5-1. Estimated annual system output in kWh, based on the number of years in operation

For the above, which begins with a 1250kWh/kW optimal output in the first year, the total electrical energy generated by a system over its life is expected to be 27687kWh/kW. The total number of kilowatt-hours throughout a system's lifetime per kilowatt capacity, without taking into consideration degradation over time, would be 31,250kWh. Since these values correspond to the minimum and maximum values likely to be seen, the average between the two is what was used in the analysis presented below.

5.3. Electricity prices

Naturally the output of a system and its associated costs are only interesting when compared with the cost of the electricity a real consumer has to pay. Grid parity is

determined not merely by a comparison of the initial capital investment of a PV system versus other generation technologies but through a thorough analysis of the full range of costs and benefits over the system's life. One of the most important aspects of photovoltaics is the fact that they can be placed virtually anywhere, without the need for significant maintenance, fuel or associated labor. The deciding factor in determining the viability of PV therefore is the electricity costs to the end consumer on the grid, where the electricity used is offset by the generation of a local PV system. Three scenarios would lead PVs to hit grid parity; the rising cost of electricity which eventually meets and finally surpasses the costs of generating electricity via PVs, the drop in costs associated with the generation via a PV system, or a combination of the two. Naturally neither electricity prices nor the cost of PV generated electricity will stay the same over extended periods of time, the former will most likely increase over time and the latter decrease. Therefore, the outlook for electricity prices in New Jersey is an important factor for the near term viability of unsubsidized, large scale photovoltaic electricity generation.

5.3.a. Electricity Cost Forecast

In the EIA's annual energy outlook there exist estimates for future electricity prices for the entire United States. No such report exists for New Jersey alone, yet in order to create a conservative estimate the annual growth rates for all states can be used as a proxy for what may happen in New Jersey. Additionally, PJM (the RTO that serves most of New Jersey) expects an increase of ca. 1.25% in peak electrical demand every year until 2024. This means that electricity prices could only stay at current levels if the current generation scheme could be expanded at the same economic rates. The PJM value is reinforced by the NJ Energy Master Plan (EMP) which states expected electrical

growth will be 1.5% annually in a business as usual forecast. [80][64] However, this estimate seems inconsistent since the current percentage breakdown by generation type, shown in Figure 1-13, is to change quite significantly. The Modeling Report for the New Jersey Energy Master Plan [84] gives two scenarios for future generation additions in NJ. The business as usual scenario states that a total of 5,007MW of new generation will come online by 2020 of which 3,607MW is Combined Cycle, 500MW is Natural Gas and 900MW is Wind and Biomass. The alternate scenario consisting solely of 3,200MW of Wind and 900MW of Biomass, the combination of which will not be able to support electricity prices as low as new nuclear or coal generation without subsidies or tax credits. The NJ EMP lists four "factors that will combine to push wholesale energy and capacity costs higher unless policies are enacted to counteract them":

- Growth in the supply of electricity is not keeping up with growth in demand.
- More of the State's power plants are fueled by natural gas.
- Capacity prices now contribute substantially to increasing electricity bills.
- Substantial increases in fuel prices.

Since almost all new capacity additions in the last decade in New Jersey have been natural gas (Figure 5-2), prices will continue to rise as that percentage of total generation increases. This increase in reliance on natural gas will also cause major electrical generation cost fluctuations due to the highly volatile nature of natural gas prices. The doublings seen historically in the price of natural gas has already caused electricity bills to rise significantly for the end user, increasing the percentage of electricity generated by gas can only have an even greater effect. The economic downturn did bring natural gas

prices down a level not seen in almost a decade due to major reductions in demand. This, in addition to the recent developments involving the Marcellus shale and its potential for gas recovery, may keep natural gas prices lower than the last peak in costs.

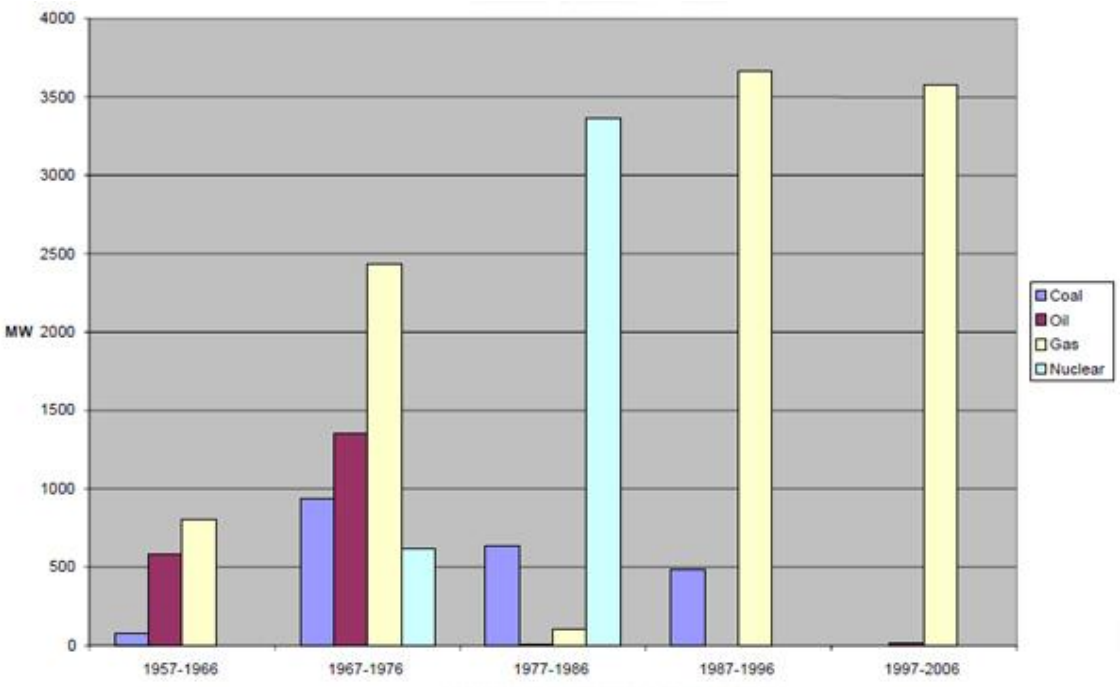

Figure 5-2. EMP - Electricity generation capacity additions in NJ

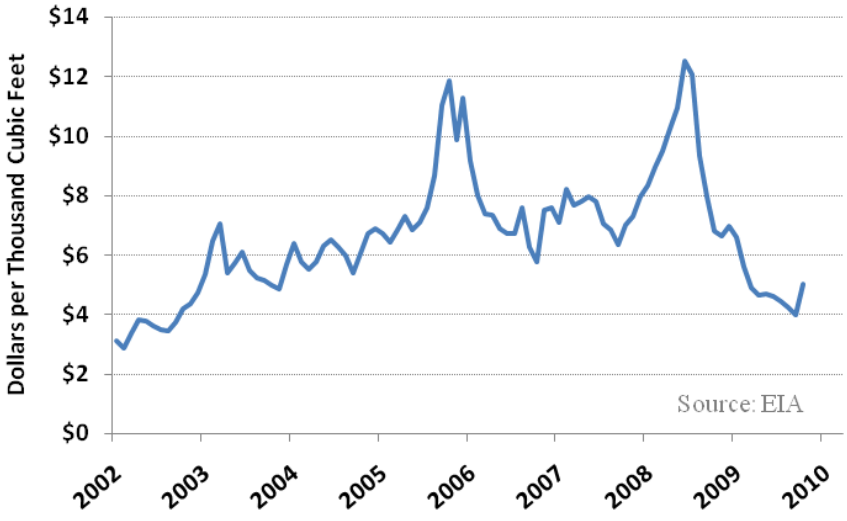

Figure 5-3. EIA historical natural gas prices, used for electric generation.

The EMP paints a very clear picture of things to come by showing the current breakdown of capacity versus electricity cost, shown in Figure 5-4. While oil peaking plants remain the most expensive in the group with upwards of 17¢/kWh, smaller combustion turbines utilizing natural gas as fuel generate electricity at 15¢/kWh.

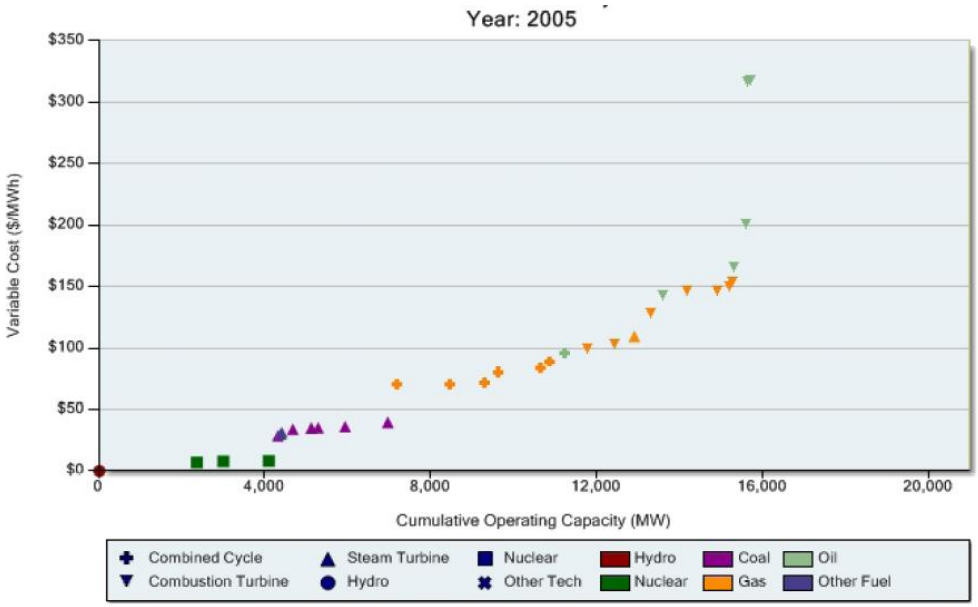

Figure 5-4. EMP - Power Supply & Technology cost for New Jersey

The higher the percentage of the total capacity coming from such expensive fuels, the higher electricity prices will be. The EIA has created forecasts for all sectors in the US, including what is dubbed the middle Atlantic region, encompassing Pennsylvania, New Jersey and New York. While electricity rates in New York are slightly higher than those in New Jersey, Pennsylvania's are much lower, which causes the overall average to be on the order of 4-5¢ lower than what is expected in New Jersey. On average, the EIA estimates that the region's rates follow the trend given in Figure 5-5.

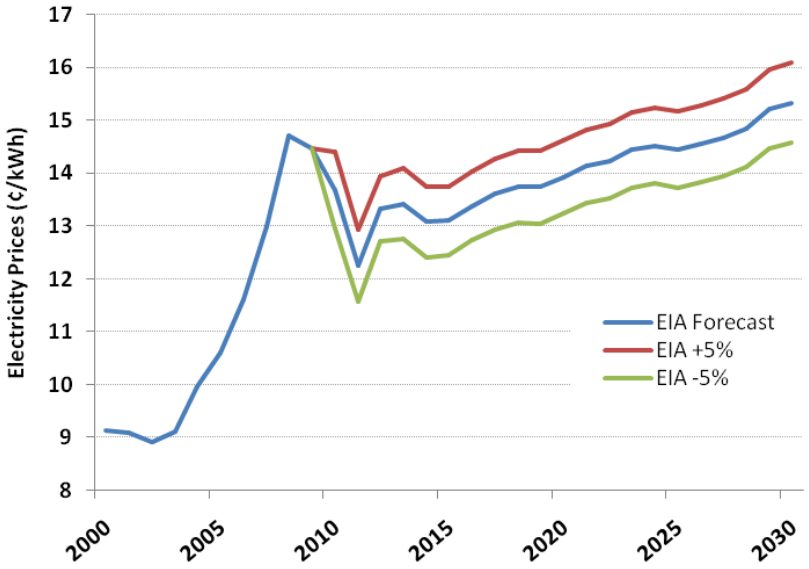

Figure 5-5. EIA electricity rate forecast for Middle Atlantic region

Since no state specific forecasts exist, the changes projected for the mid Atlantic region are used as an approximation of what may happen in New Jersey over the coming years. To create a range of possible values, ±5% were added, and compared to EIA's national forecast. The results showed that there were only minor differences in the two forecast models beyond 2017, as can illustrated Figure 5-6.

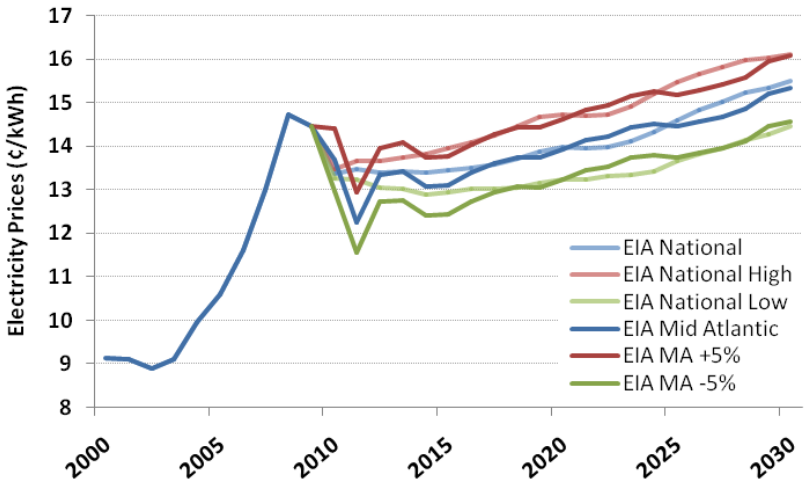

Figure 5-6. Two forecast models for NJ electricity prices, one based on the Mid Atlantic (MA) region forecast, the second on the EIA national model.

5.4. Locational Marginal Pricing

Figure 5-4 highlights a very important phenomenon that has a strong impact on the electricity rates that PV will be compared with. The most expensive peaking plants operate only during those times of day when the demand is the highest, during which they set the price for all energy generation during that period of time. This means that as peak demand is at its maximum, electricity prices will be far higher than what a simple average would provide. One important feature of PV generation in New Jersey is that their output coincides very well with the period during which electricity prices are at their peak.

5.4.a. PV and Electricity Cost Concurrence

This correlation is easily shown by plotting the hourly locational marginal pricing (LMP) throughout a day alongside the output of a PV system (such as one at the SJTP), illustrated in Figure 5-7. What this demonstrates is that *average* electricity prices, which

include sunless hours where PV does not generate electricity, are poor predictors of the actual valuation of the economic worth of PV generation.

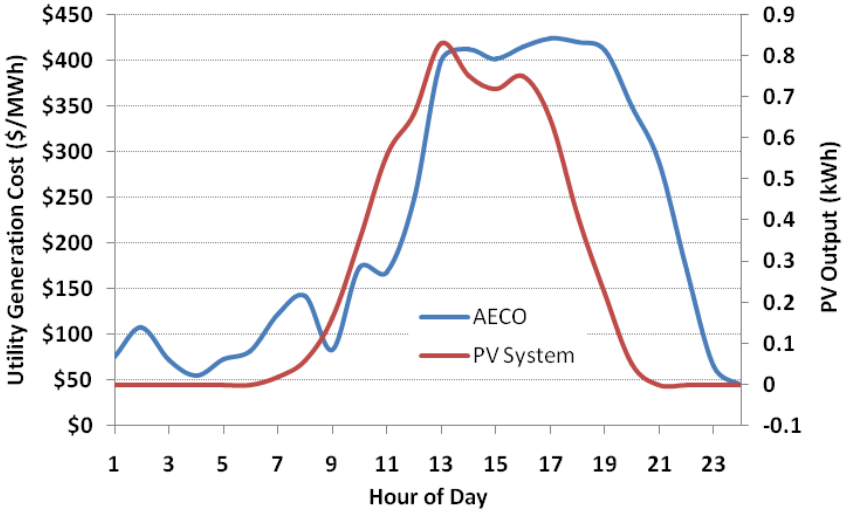

Figure 5-7. AECO LMP prices throughout July 21 2008, compared to the output of a 1kW amorphous system.

In order to get a proper estimate of the total worth of the electricity generated by a PV system, these hourly values of generation should be taken into account. The difference between an electricity bill based on average utility rates and one based on real time, dynamic, or other time-based pricing would be quite substantial. For example, average electricity generation costs (not including transmission, distribution and various other charges) in the summer of 2008 were 7.85¢/kWh for PJM and 10.44¢/kWh for AECO, this section demonstrates that there are significant differences between these average numbers upon which utility rates are established and hourly estimates which take into consideration when a PV system generates its electricity. The data provided by PJM makes correlating actual LMP generation costs with the measured output of a local New Jersey based PV system relatively easy since the price for generation is given for each hour of the day. This data is available for any month of interest going as far back as 1998.

The comparison discussed in this section was generated by taking actual hourly outputs of two small PV systems on the roof of the SJTP and multiplying their combined totals with the appropriate costs of the LMP data. Due to the massive quantity of data points to be analyzed a Matlab program was written to compile and calculate the results, Appendix J. Equation (28) calculates generated value at a certain hour, (29) computes the weighted average price of all electricity generated by a system for one year, (30) gives the offset value. [85]

$$CE(i) = E_{PV}(i) \times LMP_{UTIL}(i) \tag{28}$$

Where E_{PV} *is the PV generated energy,*
LMP the marginal cost of the utility UTIL,
i is the hour in question and
CE is the value of energy generated at that hour.

$$\overline{CPV_{UTIL}} = \frac{\sum_{i=1}^{8760}[CE(i)]}{\sum E_{PV}} \tag{29}$$

Where *CPV is the energy cost during PV operation.*

$$O_{UTIL} = \overline{CPV_{UTIL}} - \overline{LMP_{UTIL}} \tag{30}$$

Where *O is the average offset for an entire year.*

These simple operations revealed that during times in which the PV system was operating, average electricity costs were on the order of 2.21¢/kWh and 3.37¢/kWh higher in the PJM and AECO grids respectively in 2008. Ostensibly due to the very temperate weather and potentially the economic downturn of 2009, the immense peak demand never materialized to the extent of previous years, leaving electricity prices more stable. Slight differences between the offset and average generation costs were still prevalent, yet never reached higher than 1.2¢/kWh for AECO and 0.93¢/kWh for PJM.

Average offsets were quite small for PJM at 0.46¢/kWh, but rather significant at 0.83¢/kWh for AECO. Average weighted offsets for both years combined were 1.29¢/kWh for PJM and 1.85¢/kWh for AECO. Provided that demand charges follow, and PV systems continue to offset demand charges in accordance with trends observed over the last two years, it is estimated that electricity charges will be cut by an additional 25% of marginal prices within PJM and 30% in AECO. In 2008 those percentages were 31.7% and 37.5% for PJM and AECO respectively, with the very mild 2009 summer causing these to drop to 'only' 12.7% and 23% above average. [85] The compiled excel tables containing the data used in these graphs can be found in Appendix G.

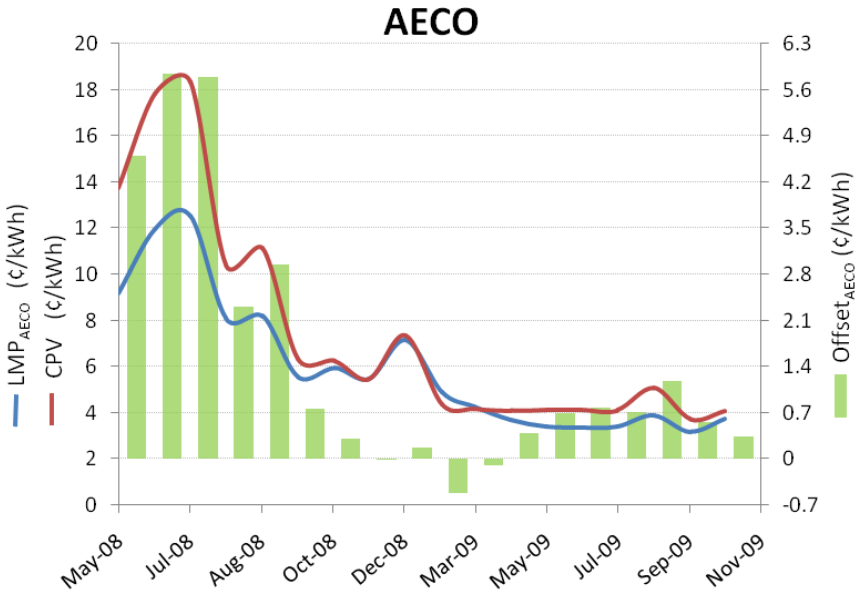

Figure 5-8. Average monthly electricity costs for AECO

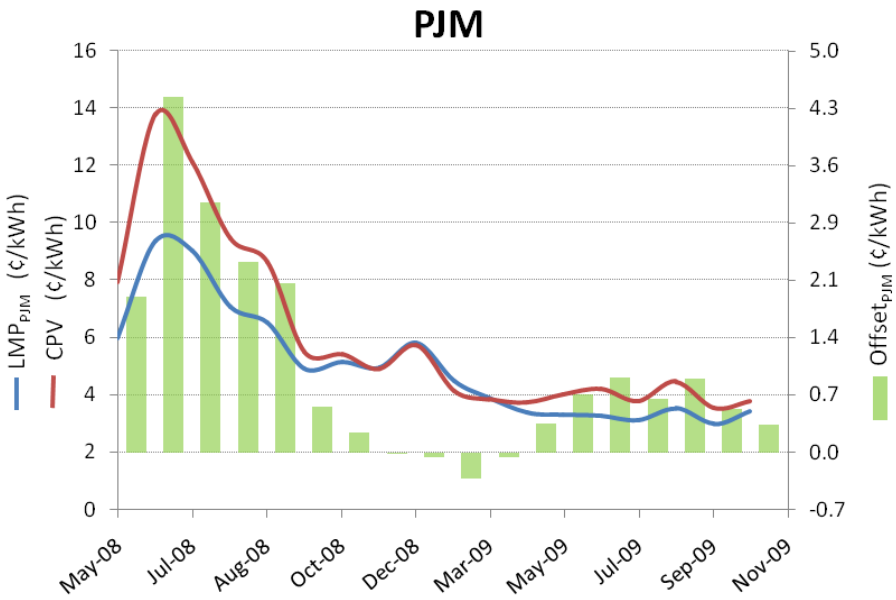

Figure 5-9. Average monthly electricity costs for PJM

Table 5-1. Calculated PV Generated electricity cost offset, for AECO and PJM, for years 2008 & 2009

	2008	2009	Total
PJM Offset:	2.21¢	0.46¢	1.23¢
AECO Offset:	3.37¢	0.83¢	1.88¢

5.4.b. Delivery Costs

Customers currently pay for their distribution, transmission and various other utility charges as major components of their electricity price. Since a net-metered PV system actually offsets local usage, transmission and distribution charges (henceforth to be described only as 'delivery') represent additional value. Unfortunately PJM does not maintain an hourly database of average delivery costs for each utility, as this would prove to be a nearly impossible task since rates for transmission and local distribution company costs for utilities vary heavily by region, time of day and usage. For this reason, the author has compiled a table of electric delivery rates to present values that are currently

paid by residential customers in the region of southern New Jersey. Figure 5-10 gives the total delivery costs for each month of the year from January ’08 through October ’09.

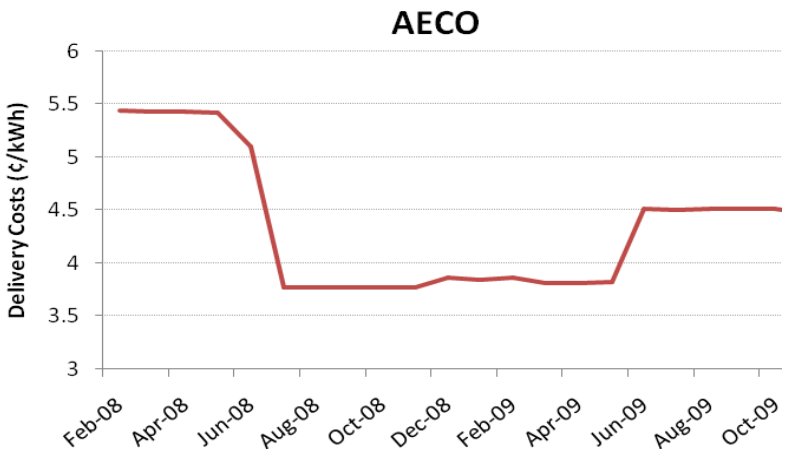

Figure 5-10. Actual residential delivery costs for AECO

It is important to note that delivery costs vary in the same way generation costs do, where the maximum output of a PV system again coincides strongly with the highest prices to be paid for delivery, making the values mentioned above extremely conservative. Not enough data was available to determine if delivery costs showed peak pricing similar to that of LMP, but it is expected to be highly dependent on peak demand as well. If delivery due to congestion follow the same pricing trend that generation costs have seen, offsets of ca. another one cent per kWh are plausible for the summer months. These were, however, not assumed to occur in this analysis. [85]

5.4.c. The Real Cost of PV Electricity

To date average unsubsidized PV system installation costs were found to be as low as $5.38 per watt, while regional, large commercial size (>100kW) PV turnkey suppliers are able to provide complete packages for $4.7 per watt [78]. These PV system prices actually bring overall costs per kWh generated by a PV system to 18.2¢ and 15.9¢ respectively. The addition of federal and state financial incentives will only cause these systems to accrue greater financial benefits for their owner due to significantly shorter payback periods. In New Jersey, where SRECs have recently traded at the $500-600/MWh level, newly built PV systems not only offset local electric use at little to no cost, but generate a large profit for their investor.

Though state and federal subsidies will not be available at such levels for extended periods of time, the incentives they provide have already driven the market to reduce prices significantly over the last few years. These low costs for systems, in conjunction to the savings incurred through the operation in a marginal market similar to that in New Jersey, already bring PV generated electricity across the threshold to grid parity in regions where electricity costs are at levels similar to those within AECO.

Table 5-2 provides a breakdown of electricity prices for PV systems purchased outright at costs already observed today, EIA estimates for electricity prices and those with the calculated offset applied. For 2008, average priced systems become viable at AECO levels, with the most competitively priced systems already being more than 2¢/kWh more cost effective.

Table 5-2. Comparison of Electricity Costs for PV System and EIA Estimate with Offsets applied [1]

	PV System		EIA Electricity Cost Estimates		
	$4.7/W	$5.38/W	EIA	EIA + PJM Offset	EIA + AECO Offset
2008	15.9¢	18.2¢	14.72¢	16.93¢	18.09¢
2009			14.46¢	14.92¢	15.29¢
Both Years			14.59¢	15.88¢	16.85¢

The EMP mentions the implementation of real time pricing in their efforts to achieve "GOAL 2" which hopes to "Reduce peak demand for electricity by 5,700 MW by 2020." [64] Real time electricity pricing would be one of the strongest incentives for consumers to reduce peak demand, while at the same time acting as a strong boost for photovoltaics. Since the offset described herein is affected in large part by costs during peak demand, the rising peak demand prices can only cause this offset to increase. This makes the estimates provided here very conservative.

5.5. Module and System prices

With a good approximation on the number of kilowatt-hours a system will produce, the only other factor in determining the costs of the electricity it generates will be the cost of the system itself and its maintenance. Historical numbers for PV module and system prices have been compiled in commercial reports completed by a large number of consulting companies which are sold for upwards of several thousands of dollars. However, the analysis below uses publicly available data and accepted methods for analyzing a growing, new commercial market.

5.5.a. Module Prices

A few key reports are released to the public by government funded institutions, such as the Lawrence Berkley National Laboratory (LB) report "Tracking the Sun." [92] The Prometheus Institute (PI) [81] and Photon Consulting [76] reports (though exclusively for-pay companies), provide some valuable information in public releases of their reports' executive summaries. Solarbuzz [92] provides a module price index on their website, though these only correspond to retail prices, which is very helpful when observing trends but not very useful in calculating actual costs to installers. Their "lowest prices" found in the retail world do however provide a good estimate of what the average sized solar provider will pay. Finally, the author's involvement with local large scale PV projects, consulting experience with various solar providers in the US and research into specific companies (such as First Solar, which provides a breakdown of costs and sales in its quarterly reports) give a strong basis for the assumptions made on the pricing of modules and other equipment in this thesis. The PI's trend for module prices, Figure 5-11, provide a clear indication of the dropping costs of PV modules from 1993 to 2002. The feature highlighted in red shows a steady increase in prices before 2007, where demand outstripped supply and pushed prices higher. As more manufacturers entered the market, prices again declined in 2008, at the end of which the worldwide economic slump and large increases in supply caused prices to drop more significantly. Mid-way through 2009, poly-crystalline modules were available for $2.5/W and less, which was a significant departure from the average price of around $3.5/W over the previous 10 years.

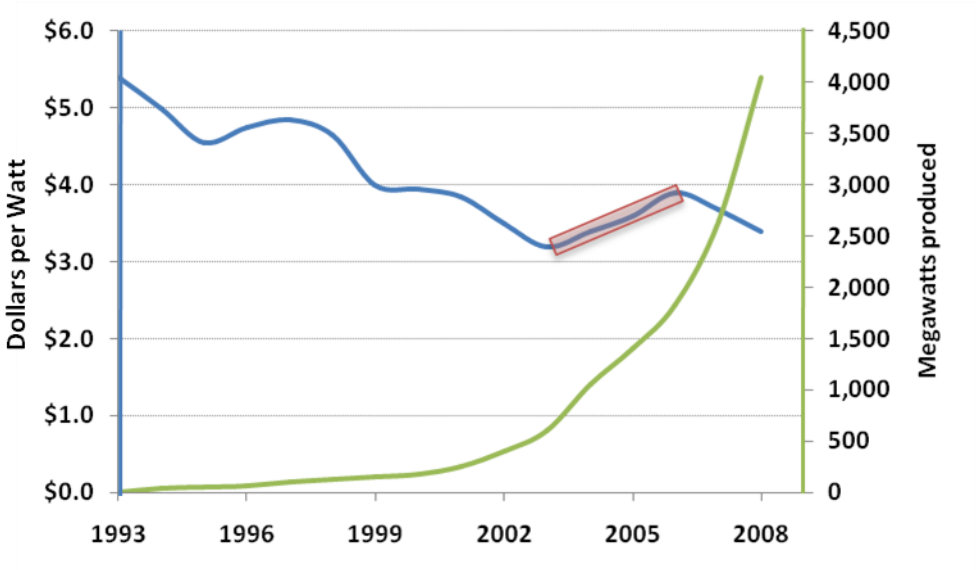

Figure 5-11. PV module prices & capacity produced as per [29]

When compared to the Lawrence Berkley numbers for total system cost, it can be seen that the two do not correlate very well and the module price increase from 2003-on highlighted on the PI curve (in Figure 5-11) does not seem to have caused an increase in system costs. This could mean that equipment & BOS costs dropped significantly during that time or that installers did not pass increases in module costs on to their customers.

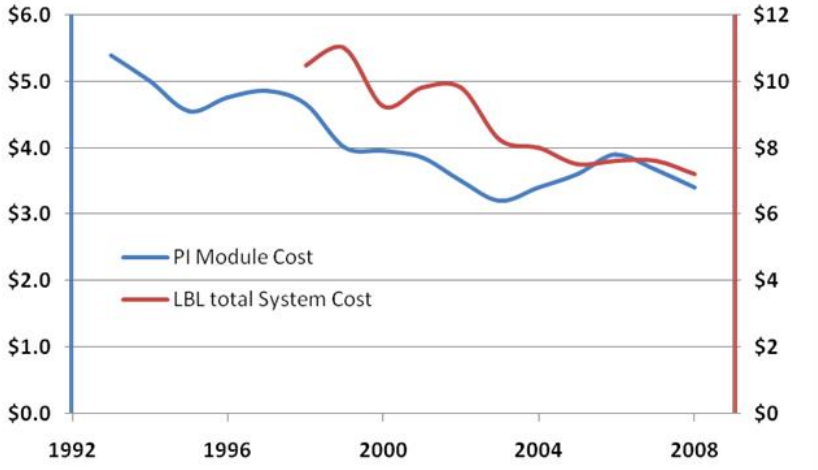

Figure 5-12. Module and System costs via Prometheus Institute and Lawrence Berkley reports

Module prices for 2009 have dropped dramatically with respect to what both LBL and PI reported through 2008. Modules can now be procured for far less than $2.5/Watt, even the lowest US retail (single modules) cost only $1.98/W for poly-crystalline modules according to SolarBuzz. [92] Large scale turnkey systems in New Jersey cost a maximum of $5/W, and the most inexpensive systems can be had for $4.5/W or less. The estimates for system cost that the author is familiar with do not correlate well with what LBL has published for NJ in their 2009 estimates, which have estimated costs of $7.2/W for the first half and $6.8/W for the second half of 2009 for systems over 100kW in capacity. However, Photon Consulting's Solar Annual 2009 seems to more consistent with the author's experience. The Photon numbers for 2009, though representing the global market, are just below $5.4/W and in significant contrast to their 2008 report which proclaimed: "*With so much volume coming, the central question for the sector remains: When will prices crash? Our answer: No time soon.*" [77] It is clear that every prediction made thus far for PV has fallen short, with no indication that any of the consultancy services ever fully appreciated the rapid growth of the sector.

Numbers given for the U.S. in these reports could be higher for several different reasons; First, since most consumers are still unaware of the level of competition on the market today, along with incentives that are sometimes confusing, many of the systems may have been built for prices that are not competitive. Second, some providers may not pass reductions in module costs along to the customer to hedge a possible increase. Third, there is a possibility that most systems are built by relatively new developers that have not yet established their business and achieved economies of scale that would present themselves in the form of lower costs. Lastly, possibly one of the most interesting and

important impacts of these numbers is a trend the author has observed numerous times with large scale projects. Though there are several large full-service developers/integrators in New Jersey who are perfectly capable of promoting themselves and handling everything from system design all the way through to actual installations, several firms have arisen that are primarily acting as 'middle-men'. These companies do little more than relaying information back and forth between the end consumer and a sub-contractor that provides for the actual installation, for which they charge sums upward of 10% on top of what the actual costs of the systems are. This causes the customer to pay more for a PV system than they really need to, yet many consumers prefer using these entities, in keeping PV (and other renewable) prices high.

5.5.b. Cost Reduction Predictions Via an Experience Curve

A more logical approach than estimates solely utilizing historical year over year reduction percentages for future predictions would be an analysis of the correlation between increases in worldwide PV module manufacturing capacity and average module prices. As cumulative production of PV modules steadily increases, one can expect the industry to learn and advance technologically. This would mean their processes become more efficient and effective, driving their manufacturing costs down. These cost reductions will ultimately be passed along to the consumer, causing prices to decrease at a similar rate. This assumes that demand will not vastly outstrip supply where module manufacturers, while cutting production costs, could charge customers market based prices. This phenomenon has been documented for over a century and been applied to the growth of various different technologies, ranging from semiconductors to sattelites. Aptly

named an ‘experience curve’ or ‘learning curve’, it enables predictions of reductions in cost with each doubling of the number of manufactured items (in our case PV modules). While differences in supply and demand alter the points along this curve, the effective "experience" gained by the industry can be estimated by a power function such as in (31) below.

(31) $$C_x = C_0 * x^{\alpha}$$

Where C_x *is the module cost per watt with*
x being the cumulative module production,
C_0 *being the cost of the very first module per watt (estimated) and*
α *being the experience index.*

The experience index can be calculated via (32):

(32) $$\alpha = \frac{log\frac{C_1}{C_2}}{log\frac{P_1}{P_2}}$$

Where C_1 *and* C_2 *are the costs at two corresponding cumulative production values* P_1 *and* P_2.

The experience index will correspond to the slope of the experience curve on a log-log graph and is related to the learning rate, which is the ratio of the costs per doubling of cumulative capacity (or production). The learning rate may be calculated with (33):

(33) $$LR = 2^{\alpha}$$

By analyzing all the historical data available from the EIA's Annual Energy Review, NREL's photovoltaic overview and Greentech Media's reports it was possible to match module prices with the cumulative capacity at any given year, which allowed for

the creation of the experience curve in Figure 5-13. The resulting data can be found in Appendix H [13][68][29]

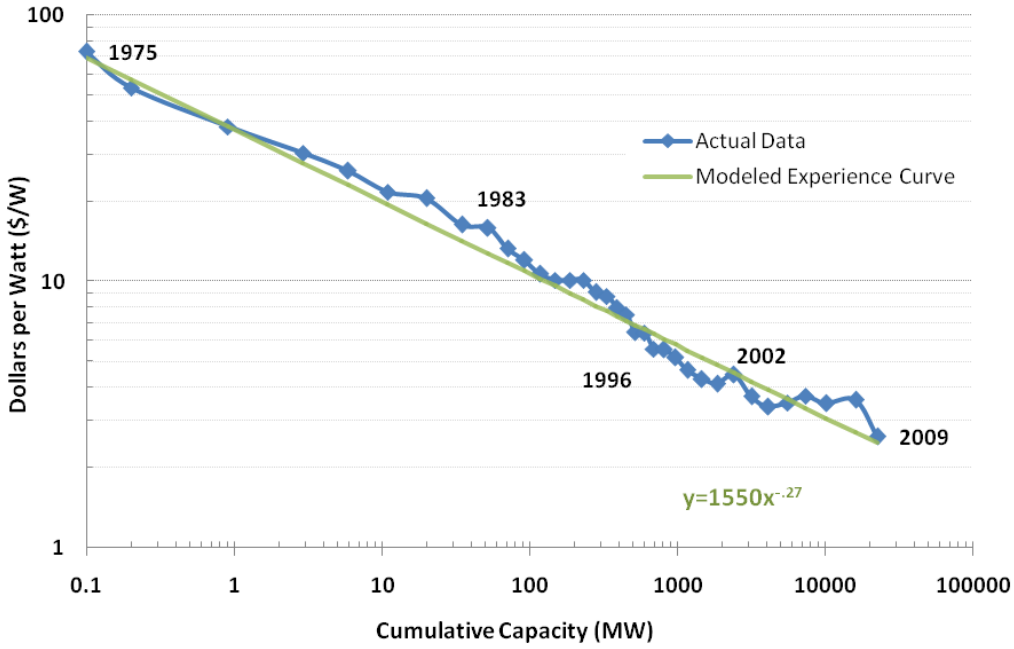

Figure 5-13. PV Module cost per watt versus worldwide capacity

The years noted on the graph (1975-1983, 1983-1996, 1996-2002, 2002-2009) also indicate periods which the author has selected for future closer analysis. The periods were picked based on their apparent yearly growth which differed substantially from one another since the creation of the first commercial, rather than laboratory grade, PV modules. These periods and their yearly capacity increases are illustrated in Figure 5-14, along with compound annual growth rates (CAGR) observed for each period. These historic growth rates can be used to estimate plausible capacity increases in the future and were incorporated into a model that utilized the estimated approximate experience curve mentioned previously. SolarBuzz recently released the latest report on worldwide PV installations, noting that for 2009 it had reached 7.3GW. [93] Though this represents only installations and not total production, it is assumed that this represents close to the total

production of that year. It is remarkable that PV capacity increased at all during the global economic troubles, let alone by 20%. For all data referred to in this chapter, please see Appendix I.

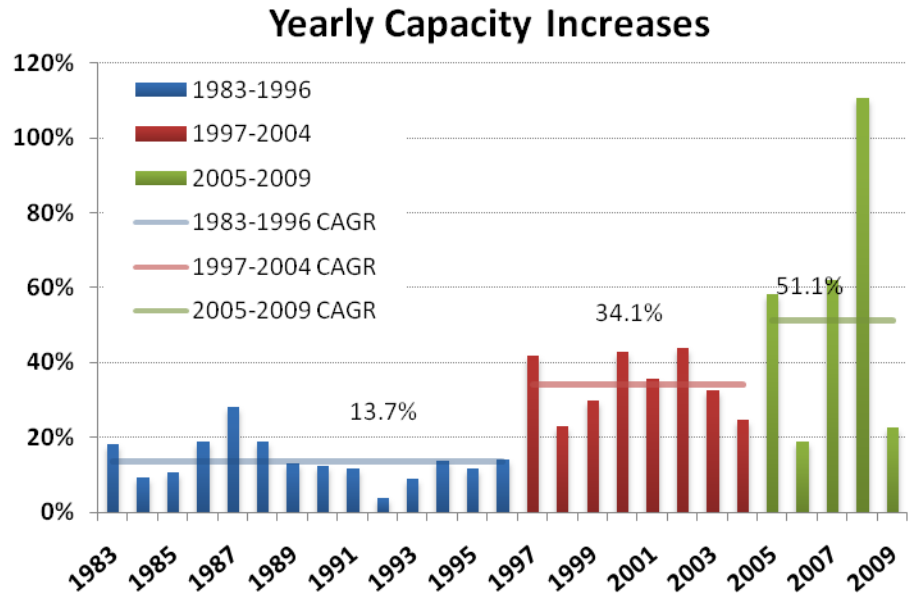

Figure 5-14. Yearly change in worldwide capacity per year, along with CAGR for each period

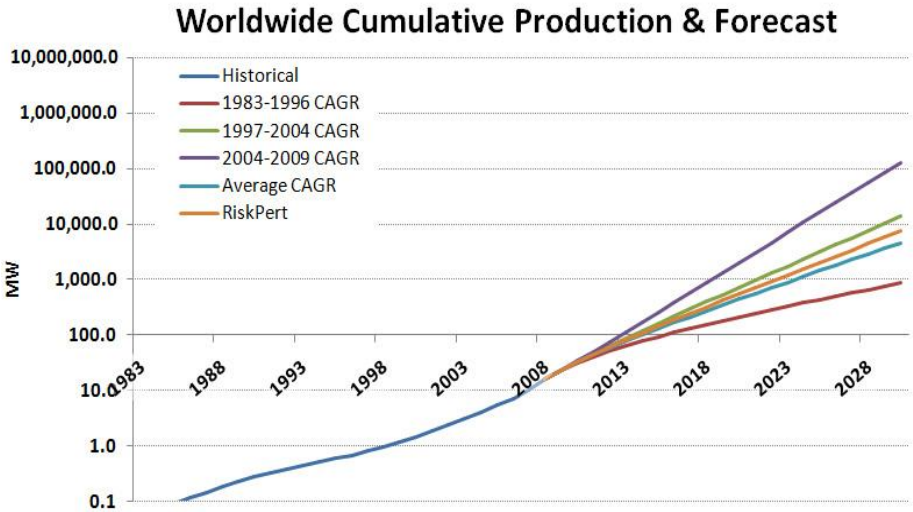

Figure 5-15. Cumulative production and forecast utilizing historical CAGRs. Average CAGR for the years 1983-2009 was 26.15%

As mentioned, these CAGRs were utilized to predict a range for growth until 2030, given in Figure 5-15. Since these are cumulative production values, it is possible to

use the experience curve to estimate module prices per watt. Though the cumulative production rates vary greatly, costs per watt stay within a relatively narrow range. Figure 5-16 provides historical values and the forecast numbers for 2010 onward for PV modules, Figure 5-17 shows a close-up for the forecast.

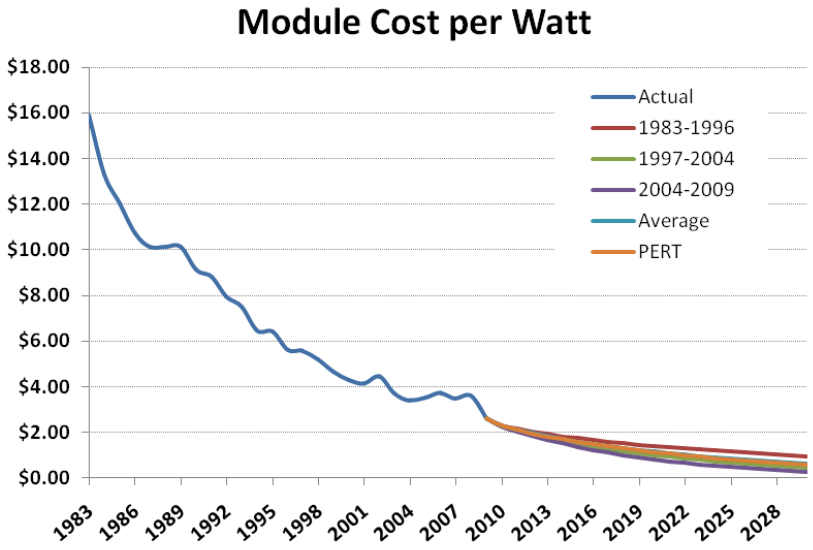

Figure 5-16. Historical and estimated PV module costs per watt. (1983-2030)

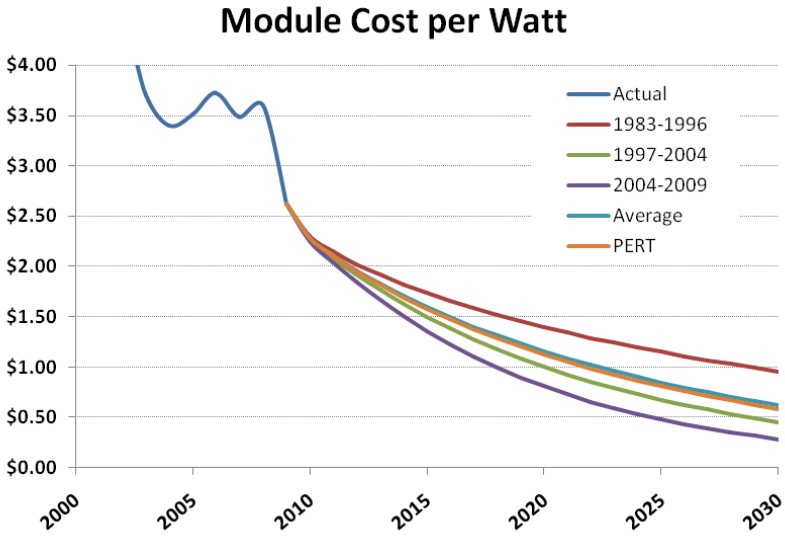

Figure 5-17. Historical and estimated PV module costs per watt. (2000-2030)

Since historical BOS costs were not available, they were approximated until 1998 with the help of a LBL report and known historical module costs. [49] BOS costs throughout this time have decreased on average by about 3% per year. Due to the fact that a large percentage of the BOS costs are directly tied to commodity prices (copper and aluminum for wiring, steel for racking, etc.) of well developed industries, these are unlikely candidates for big future savings. It is likely that hardware such as Transformers, switch gear, fusing, conduit, cables and wiring are very close to being as inexpensive as they are today, since utilities represent such a large customer base. The only real advantage on the horizon may be achieved with new inverter and harvesting technologies that may cause reductions in the equipment and materials necessary for a system. Labor, unless racking and module manufacturers develop a standardized method of mounting for all types of modules, such as the "clip-in" type emerging on the thin film front, will also likely stay relatively stable at current prices. Though significant downward pressure will be placed on BOS costs in the future due to their ever increasing percentage of the total system cost, too little information was available to the author at the time of this writing to give educated future estimates. For this reason, BOS costs are taken to decrease by 3% per annum.

Using the historical system costs from LBL, the experience curve and the BOS estimate, Figure 5-18 was developed which shows the estimated total system cost per watt. With the system output mentioned in the first section of this chapter, it is now possible to give an approximate for the cost of the electricity generated by a PV system which has been purchased outright without any government incentives, SRECs, tax

breaks etc. Figure 5-19 is a graph of PV's future, giving the cost of PV electricity throughout the lifetime of a system built in that year, at prevailing system costs.

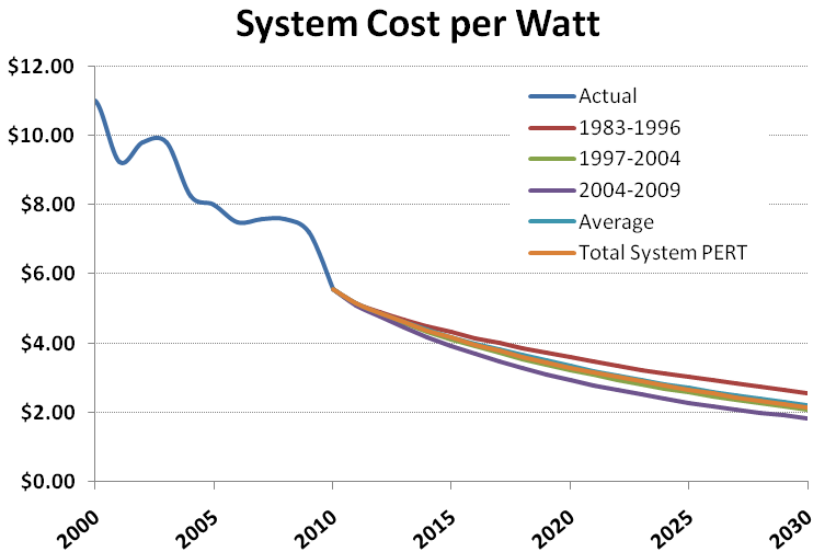

Figure 5-18. Projection of PV System costs per watt

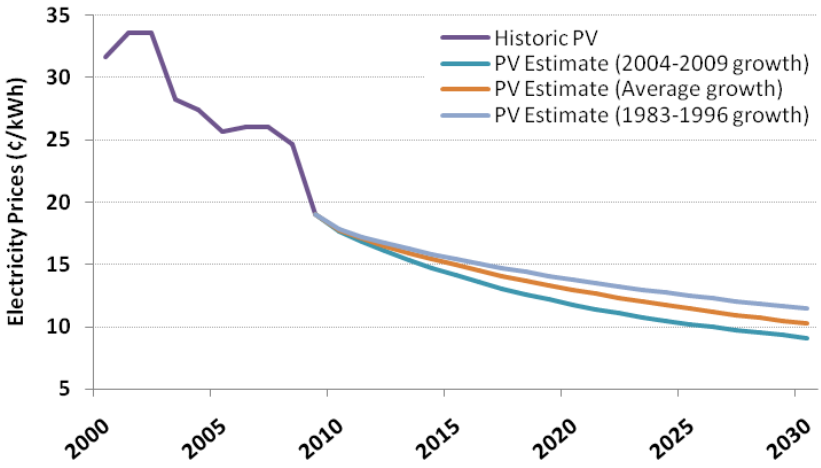

Figure 5-19. Electricity cost per kWh for past, current and future PV systems

5.6. Grid Parity for PV in New Jersey

Superimposing the forecasts for PV electricity cost on that for average non-industrial electricity rates in New Jersey provides a range within which PV systems (purchased outright, no cost of capital) will reach grid parity, as seen in Figure 5-20. With the relatively slight changes in electricity prices over the years, PV system prices remain the deciding factor, bringing grid parity closer with each reduction in total system cost. The following analyses presents a wide range of possibilities and explores the effects that incentives, engineering optimizations, etc. have on the time it will take for grid-tied PV to reach grid parity in New Jersey.

5.6.a. PV System Direct Purchase – (No Financing, No Incentives)

Starting with the actual PV system cost, and the forecast EIA electricity costs, the model revealed that the unadjusted cost of PV generated electricity could reach grid parity as early as 2013 with the best case scenario. Since system and utility electricity costs are not a known value but rather a range of possible values, grid parity would also be reached within the range of plausible outcomes. In this analysis, the best and worst case scenarios created a six year span within which PV generated electricity is expected to reach grid parity in New Jersey namely between 2013 and 2018. Even the worst case scenario is considerably closer than the "mid-century" quotes by some energy pundits. [99]

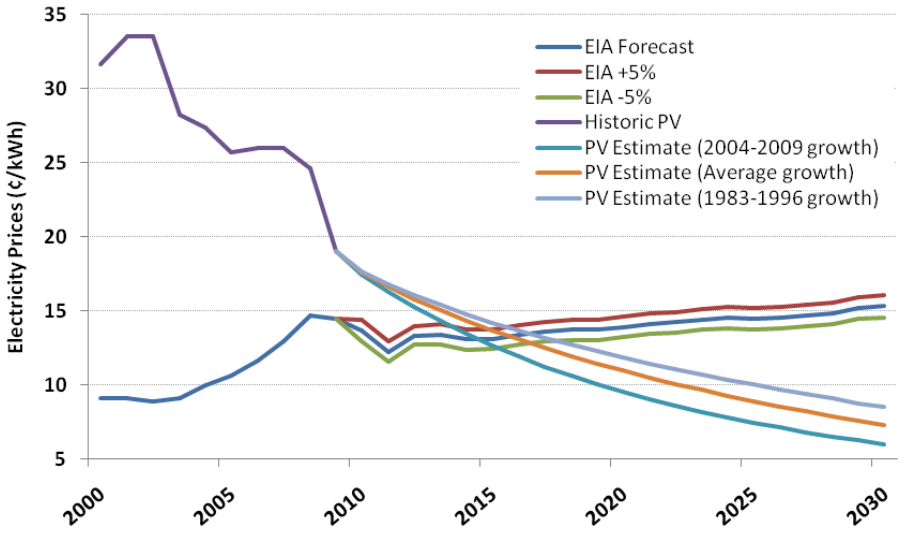

Figure 5-20. Forecast PV electricity generation costs compared to forecast NJ electricity rates.

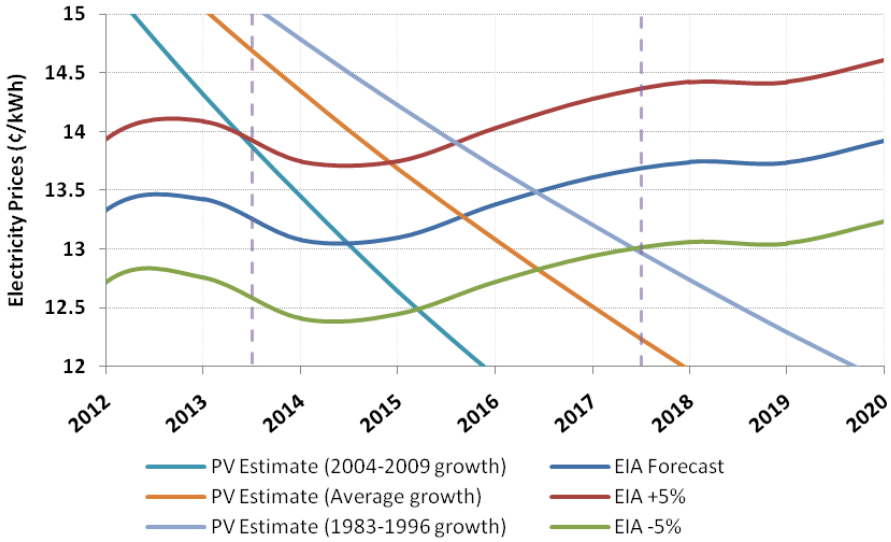

Figure 5-21. Close-up of the critical region, best and worst case scenarios are marked by purple dotted lines.

Even without any government or market incentives, reaching grid parity at the average scenario would be quite a few years ahead of many expectations. Since the previous estimate does not take into consideration any of the incentives such as SRECs, the Federal Investment Tax Credit (ITC), system optimization, or the real time pricing

benefits of electricity prices when PV actually generates, it serves as the most conservative and pessimistic model. Ignoring these features would ignore some of the most important aspects of the present market conditions for photovoltaics, features which were implemented for the sole reason of advancing the technology. In the next sections, the impact of various combinations of these proposals and incentives on PVs' movement to grid parity and is described.

5.6.b. Direct Purchase with Engineering Optimizations

First, the engineering optimizations discussed in Chapter 3 are not only crucial but often very inexpensive or free. While the analyses presented throughout this thesis take for granted that optimal system parameters were used for the azimuth, tilt angle and inter-row spacing, none have thus far incorporated the DC optimizations developed by the Author to increase efficiency, nor included the savings to be had from going with the type of loop-feed setup mentioned earlier. Figure 5-22 shows that PV generated electricity cost from a PV system purchased directly without incentives, built to the standards described in this thesis at an appropriate utility voltage, will reach grid parity between 2012 and 2016. It is remarkable that some very basic and creative design changes can shave two years time off this critical grid parity cross over period. This includes the savings from the elimination of the switchgear, various DC wiring optimizations and the reduction in losses due to the eliminated isolation transformer. When combined, these changes can reduce PV generated electricity prices by 1¢ or more per kWh.

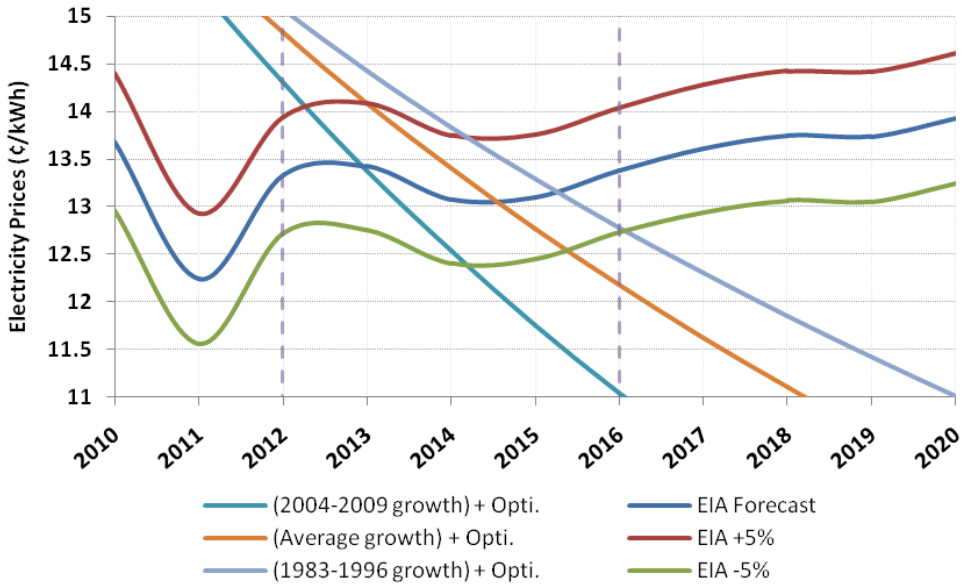

Figure 5-22. PV Electricity Prices with Engineering Optimizations implemented.

5.6.c. Direct Purchase, with Real-time Electricity Pricing

Next, the inclusion of the offset pricing mentioned in the LMP section of this thesis will be considered. If real time pricing does become a reality in New Jersey as it has been proposed in the EMP, this offset will prove to be a very real and valuable addition to the value of PV generated electricity. The few cents difference per kilowatt-hour could become a boost pushing grid parity nearer by 2-3 years. Of course the numbers used in the analysis were chosen conservatively, not taking into consideration that the EIA growth for electricity prices will likely be outstripped by the growth in peak demand. The higher peak demand prices are, the higher the real time price offset will be for PV systems. With these conservative assumptions the model predicts grid parity being achieved in the 2011-2015 time period.

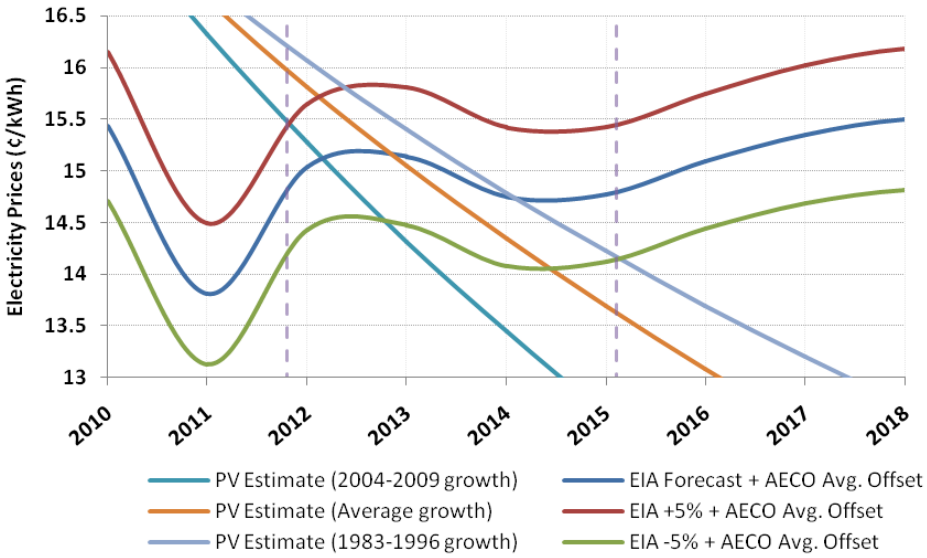

Figure 5-23. Electricity prices during PV operation, EIA estimates having been adjusted by the average AECO offset calculated for 2008 and 2009.

5.6.d. Direct Purchase with Government Incentives

The largest financial incentives available to PV system owners in New Jersey are the lucrative SRECs, as well as the ITC. While the ITC is an easily calculable tax credit that can be subtracted from initial price of a newly installed system, SRECs are somewhat more complicated. Since they are earned on a year by year basis, actual system output needs to be calculated for each year, which must include the change in output over time for a PV system discussed previously in Section 5.1. Both the SACP bill and the ITC are set to expire in energy year 2016 (ending July 2017), the vote on the continuance in 2016 for NJ SACPs will determine if they will exist from that point on, though it is expected that they will persist with a lower ceiling. The decision for the continuance of the ITC will be determined by the President of the United States in 2016, though even a reduction to 10% will ensure PV electricity costs below grid electricity prices beyond that year (Figure 5-25). For now and at least the next few years, these two incentives will be

the most significant financial game changers as their inclusion into the analysis model reveals. A year after the ITC was put into effect, PV electricity generated in New Jersey became much cheaper than the cost of that purchased directly from the electric utility.

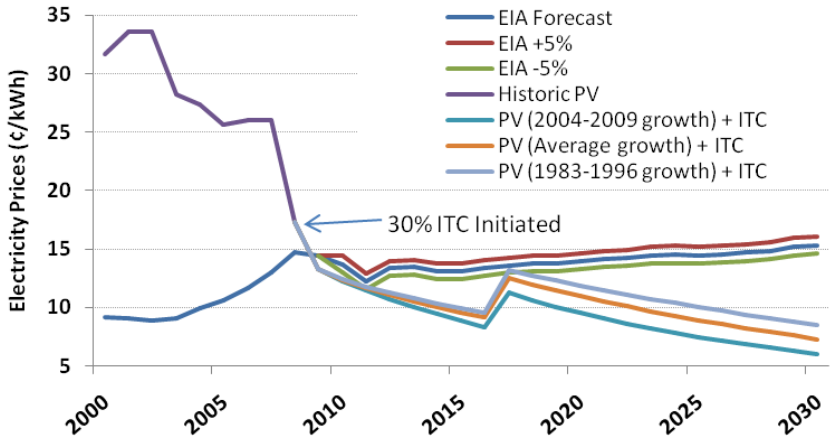

Figure 5-24. PV Electricity cost with Federal Investment Tax Credit active until 2016

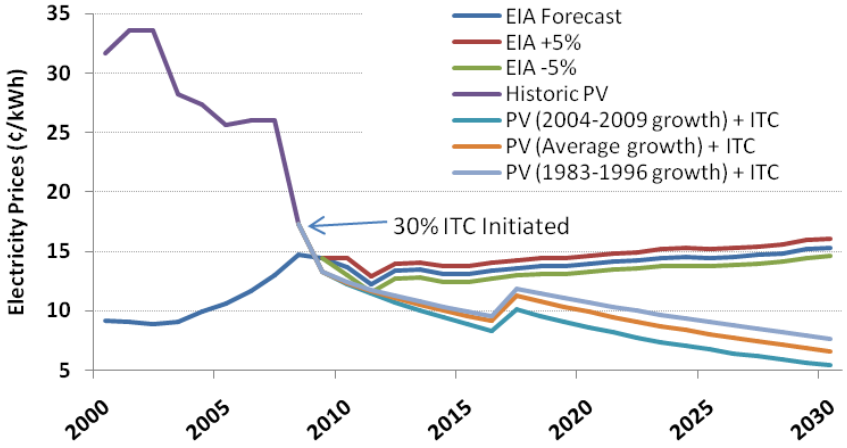

Figure 5-25. PV Electricity cost with ITC decreased to 10% after 2016.

The same finding remains true for the implementation of the SACP and the associated SRECs that system owners are able to collect revenue from, Figure 5-27. With the average SREC price expected to track SACPs at conservatively 70% of their value, PV electricity will be far less expensive than that purchased from the grid until 2016. Included in the projections given in Figure 5-27 are SACPs until 2020 with ceilings set at

only 10% of those of the years prior to 2016. These incentives continue to play a major role in spurring more demand which will put downward pressure on future prices, while also making PV a viable means of generating electricity. The combination of the two actually manages to create a negative cost for any PV system installed before 2011 and ensures that PV electricity costs remain below grid parity for all future years, Figure 5-28. SRECs listed in the Figure 5-27and Figure 5-28 only include SRECs starting with year 2007, when the New Jersey Board of Public Utilities eliminated the installation rebate program, and significantly increased the SACP levels. Though SRECs were available starting in 2004, the average value rose to only $250 by the end of energy year 2007. Since the abandoned rebate and SREC program is not included in this thesis, only the new SREC only program is taken into consideration in this analysis.

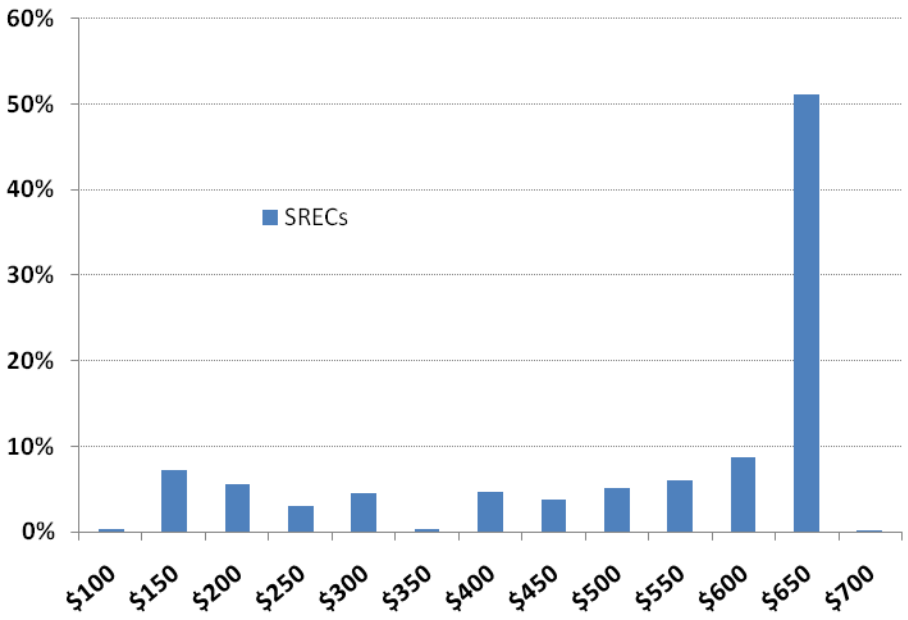

Figure 5-26. SREC price distribution for 2009.

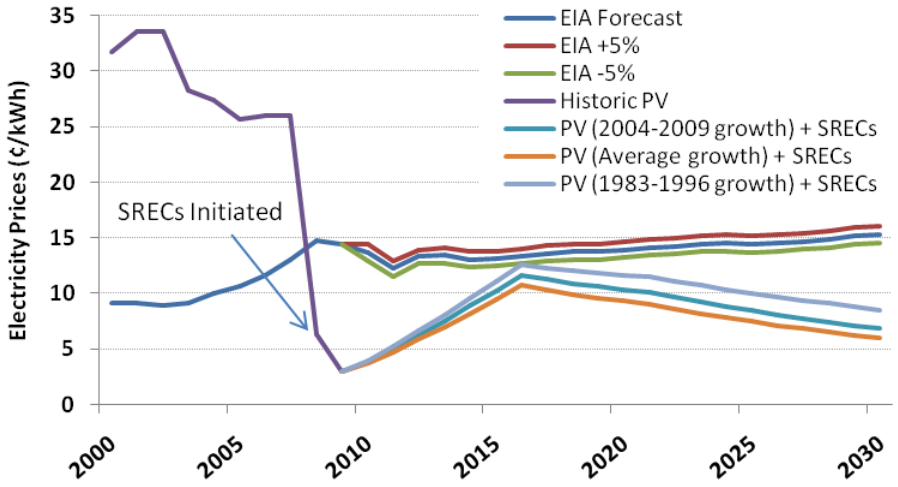

Figure 5-27. Price of PV electricity with SREC revenues applied

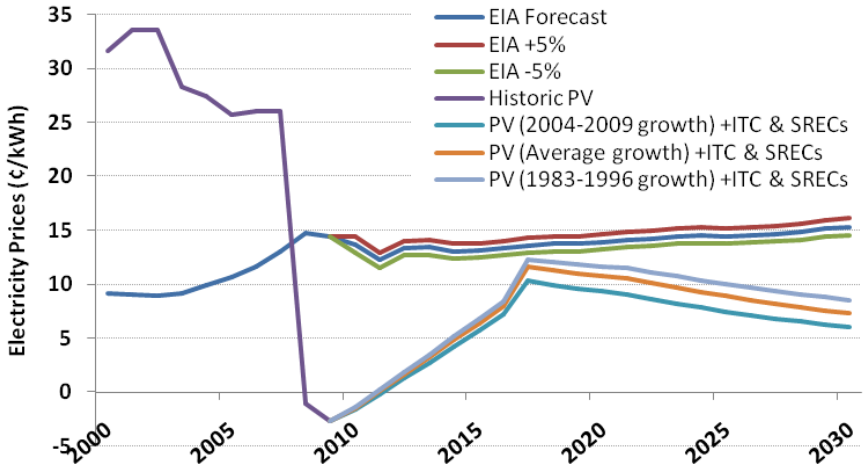

Figure 5-28. PV Electricity costs with ITC and SREC revenues accounted for

5.6.e. Direct Purchase with Incentives, Engineering Optimizations and Real-time Pricing

Lastly, the inclusion of all savings to be found from the DC wiring optimization, LSPV equipment elimination and optimal system design, proper module installation and orientation, current SREC plans and the ITC. The combination of these bring PV electricity to a maximum of 11.43¢/kWh, well below what average retail costs of electricity are in New Jersey today. The effect of the monetary incentives on the price of

PV electricity is quite significant, which for systems built before 2010 manage to bring actual electricity costs negative, essentially earning more money than what the electricity cost. This is not to be confused with saving the difference between PV electricity and that from the utility, for it is an actual return on the total initial capital investment. More benefits are also available to commercial entities which have not yet been included in the model (e.g. accelerated depreciation), painting an ever clearer picture that PV has a healthy economic future in New Jersey.

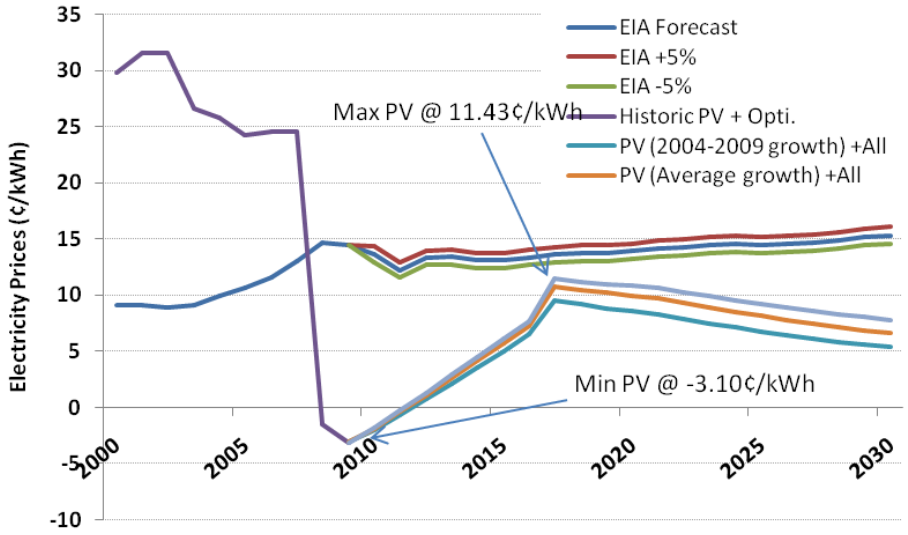

Figure 5-29. Forecast of PV electricity prices, including all financial benefits discussed in thus far with the exception of real-time pricing.

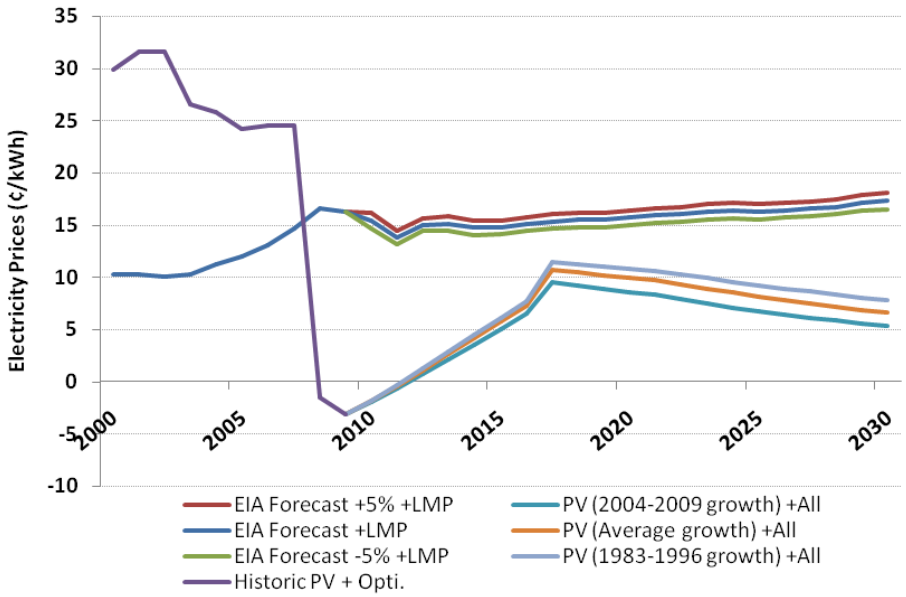

Figure 5-30. Forecast given in Figure 5-29 compared with real-time pricing.

5.7. Cost of Capital, Depreciation & Taxes

Of course, only very few entities actually have the means to purchase a multi-million dollar system without some sort of financing. In some cases it may actually be more prudent to invest an amount less than the total cost of the system even if enough capital is available. Financing is rarely free, so the cost of any loan on the system must be taken into consideration when calculating the effective cost of the electricity being generated by a PV system. Additionally, the benefits of the depreciation of such a system have been left out of the model, these will be included in this section as part of a more in-depth financial analysis.

A few assumptions are made in this analysis that should be noted. First, it is assumed that the entity which is to own the system and thus benefit from the ITC,

depreciation and other tax benefits, has a large enough tax liability to take advantage of the positive benefits at the year they become available. This is less important for the ITC in most cases, since the government will actually cut a check at the end of the fiscal year for any amount above the taxes owed by the owner, but very important for this simple analysis of the depreciation benefits. Second, it is assumed that the total maintenance, fees, insurance and other operational expenses are four percent of the total cost for the first year and one percent thereafter. The interest rate is anticipated to be seven percent and it is expected that a loan is taken for six years on 50% of the cost of the system. Additionally, the modeled system is 1MW in size and cost $5/W everything inclusive. Lastly, no inverter or other equipment replacements are made throughout the lifetime of the system.

5.7.a. Operating Income

Since a system will actually provide a revenue stream over the course of its life, it is important to get a firm grasp on the total income and expenditures generated each year. This will represent the basic foundation of the worth of the system and make it possible to estimate, among other things, the taxes to be paid and the final cash flow at each year throughout the expected life of the system. Income for this system will be composed of solely the revenue generated by the sale (or in net-metering cases the offset) of electricity, as well as the sales of SRECs. Operating income is the total revenue each year minus the overhead costs, such as maintenance and insurance (in the case presented, 4% of the cost of the system the first year and 1% thereafter ($200,000 and $50,000 respectively). Based on previous SREC & module output estimates, this example system

will generate $668,250 in SRECs and ~$180,000 in electricity offsets in the first year, totaling ~$848,250 in taxable revenues.

5.7.b. Depreciation

Depreciation is a rather simple concept; objects which we buy depreciate in value over time and it is thus legal for companies to apply these apparent losses against their annual income. The federal government has set limitations as to how one can depreciate which types of goods, and has culminated in a guideline called the Modified Accelerated Cost Recovery System (MACRS). [100] Large portions of the materials used to build a solar system are considered to be five year property, meaning that their costs can be depreciated over the course of five years after the first year of operation (thus, six years in total), see Table 5-3. Though there are many different classifications under MACRS, only the five year and 25 year sections are of interest in this analysis. 25 year depreciation rates are a standard 4% per year.

Table 5-3. MACRS 5yr depreciation rates

Year	Depr. %
1	20.00%
2	32.00%
3	19.20%
4	11.52%
5	11.52%
6	5.76%
Total:	100%

Since an object's depreciation over time can be seen as loss incurred by the owner, it can only offset taxable operating income rather than the tax liability itself. And this makes intuitive sense, since the government is not responsible for any losses an entity incurs in its effort to produce a good or provide a service. Consequently,

depreciable assets hold a great amount of value for any company that has large tax liabilities and very little for those which are exempt from, or pay very little taxes.

However, the situation can be more complicated; depreciable assets are assets which can be traded or sold. This means that a company unable to make use of the depreciation of an object may simply sell them to another who can, and then "lease" the object from the second. What this means is that the installation of a solar system can be partially funded by selling the right to depreciate the equipment in the future. Though this happens at a slight discount, schemes such as these provide a benefit to both parties involved and help provide capital for the system in the first place.

The most important part in an analysis which is to include depreciation as part of the financial model will be the correct assignment of the depreciation basis. This basis is essentially the total value of the depreciable assets which may benefit the owner from a tax standpoint. Initially this should approximately equal the total value of the system (disregarding engineering fees, etc.), though the inclusion of the ITC changes this slightly. Since the federal government provides a tax credit for the purchase of a system, it does not allow one to depreciate the total cost of the system without taking the tax credit into consideration. It states that 50% of the received ITC shall be deducted from the depreciation basis. [28] Assuming that a 1MW system will cost $5 per Watt, the total system cost would be $5M and the 30% ITC would be $1.5M, leaving the depreciation basis at $4.25M. However, since we assume 20% of all assets will not be ranked in the PV category, the total five year depreciation property basis comes to $3.4M (with an ITC of $1.2M {$5M x 80% x 30%}). The second half of the ITC which could not be part of the depreciation must be included in the financial analysis as a loss for internal

accounting purposes. With the percentage values given in Table 5-3, we know that in the first year $680,000 will be depreciated for the five year and $40,000 for the 25 year portions. Total depreciation for the first year thus comes to $720,000.

5.7.c. Taxes

With the operating income and depreciation calculated, the interest of the loan taken on 50% of the value of the system must also be incorporated. Given a six year, 8% loan, the first year's interest payment will come to $200,000. After tallying up the total operating income ($848,250), the total depreciation ($720,000), maintenance ($200,000) and the interest payment ($200,000), the earnings before tax for the first year of this system would be ~$272,000. Assuming a 45% tax rate for this imaginary company, this would come to a total income tax credit of $122,400. Since the depreciation benefits are strongly front-loaded these tax credits (rather; losses to income) are present only in the first three years. After this time, total operating income overtakes the apparent losses accrued due to depreciation and interest, spelling positive earnings and thus the addition of an income tax liability. For the first year, the total tax credits assumed by the company would amount to $1.32 Million (ITC: $1.2M, Income tax: $122k), after the third year total tax liability created by the operation of the PV system will be ca $76k. And if

5.7.d. Internal Accounting

In order to get a firm grasp on what the costs or benefits of this system are to the company owning it, it is necessary to calculate the annual and cumulative cash flow. Cash flow is the measure of total intakes or expenditures associated with the ownership. Adding these yearly cash flows up over time gives the total cost or earnings of the system over the elapsed time. Therefore, annual cash flow numbers include the total tax liability,

depreciation (both tax and non-tax deductible), income and principle payment (the interest having been included in the taxes) incurred over that year by the ownership of this system. The cost of the electricity generated by a PV system can be calculated on an annual basis (using annual cash flow) or throughout the lifetime of the system (using cumulative cash flow). Following the same methods used thus far in this thesis, only the cumulative cash flow is of interest, since this will enable the estimate of the electricity costs associated with the ownership of a system throughout its lifetime. For the example given herein, cumulative cash flow lay at $1.58M at the end of the expected 25 year and the internal rate of return would come to 9.9%. This IRR changes significantly with a change in the portion of the system to be financed, ostensibly this is due to the fact that the interest of the loan reduces the taxable earnings which, with a tax rate of 45%, would be a sizable negative factor on the calculated cash flow.

While the IRR may not be what most financial investors would consider a worthwhile investment, the lopsided cost recovery presents very interesting investment possibilities. Depending on the percentage financed, the incentives, etc., the initial investment in a PV system can be recovered within five to eight years. This makes it possible for a single investor to fund an installation, recover the entirety of his money in a few years, and then reinvest in another. If this were to be done several times, it would enable an individual or business to receive returns from multiple systems with the same initial investment. Figure 5-31 shows the cash-flow per year for the previously mentioned system. The break-even point occurs around years seven and eight.

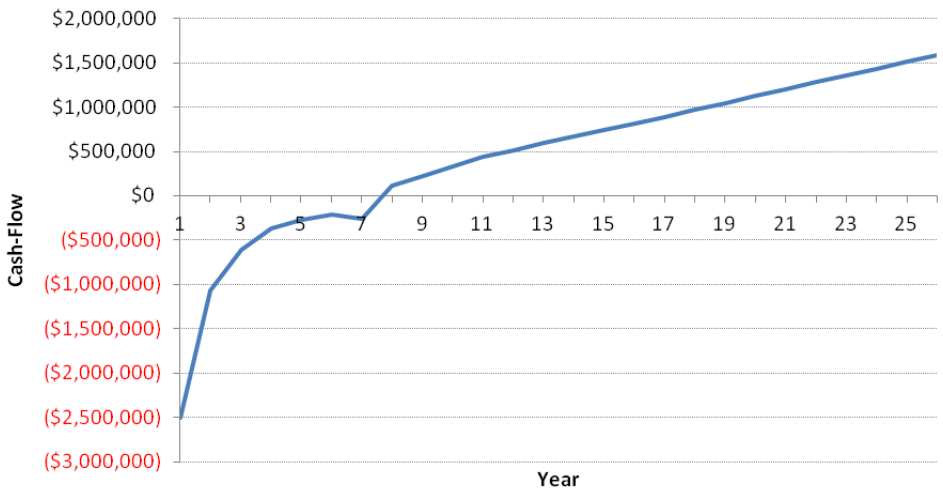

Figure 5-31. Cash-Flow for each year throughout the lifetime of a PV system.

What is most interesting in this analysis is the effect that taxes, depreciation and financing have on the overall cost of electricity coming from the plant. All that is necessary to get a levelized cost of the electricity generated on a per-kWh basis is the removal of the expected income (or savings) of the electricity generated by the system, and dividing this sum by the cumulative cash flow at the 25th year. With the benefits of the depreciation and the lucrative nature of the SRECs, the costs of the electricity are found to be a low 2.1¢/kWh, the removal of the SREC revenues bring the costs up to a still reasonable10.84¢/kWh. If the benefits of the ITC are removed, the addition of the depreciation still manage to bring the levelized cost of electricity to only 12.71¢/kWh. Far removed from the oft repeated 20+¢/kWh numbers, these costs show how in-depth tax analyses that incorporate available tax benefits oftentimes left by the wayside in the depiction of PV financials, paint a much brighter picture for company owned PV systems. [99] Data for the above example can be found in Appendix K.

Chapter 6. Summary, Conclusions, and Recommendations

6.1. Summary

This thesis has reviewed a number of the key issues regarding PV technology and large scale PV arrays, specifically in New Jersey due to the inclusion of SRECs and local electricity prices. While electricity costs and subsidies may vary greatly from state to state, the general overview of the technology, performance analyses, design optimizations, system cost outlook, financial modeling and various other points discussed herein are applicable anywhere in the US and around the world. Presented are the basic design parameters that should always be followed in the construction of a PV system, regardless of its size. It is shown that the effectiveness of a system depends not only on the efficiency of the components used, but also greatly on the engineering design. The adherence to specific guidelines, be they in existence through the federal or state governments, standards committees or are merely good engineering practice, is a vital part of ensuring that photovoltaics operate as efficiently (thus cost effectively) as is possible. The selection of technology proper for the local environment, alongside design optimizations such as those discussed herein will necessarily play a role in future installations as the need to cut costs becomes ever more important. Subsidies and incentives will not and cannot remain the sole reasons for PV affordability, making it increasingly important to be able to estimate what PV electricity costs will be in the future. The advancement of PV technology spurred on by incredible growth is surprising, especially given the cynicism of various reports and articles that have all but predicted that PV will take another 40 years or more to reach grid parity. [99]

Inexpensive thin-film modules are found to cut system costs by 40¢/W or more and generate up to 20% more energy per watt in torrid regions. Additional savings may be had in the reduction of labor necessary for installations, as well as in the performance throughout the lifetime of the modules.

The effects that shading, varying tilt angles and changes in orientation have on system output are explored and incorporated into an overall guide for proper design. The creation of an open-source tool which can estimate the generation of a system, given various inputs, provides an immense number of possibilities. For example, a clear guideline for shading multipliers has sprung from this research, to be utilized in the selection of necessary spacing for modules at any tilt angle.

Proper engineering design ensures energy losses of no more than 1% in the wiring of a system, and can also cut costs on the AC side by over 20%. Intelligently oriented and tilted modules cut electricity costs by 15-40%.

The approximation of electricity costs for PV systems makes a fair comparison with utility prices possible, and allows for the inclusion of the true average cost of electricity during PV operation. The enhancement of this research with the prediction of future prices sets the stage for various scenarios created to forecast the point of grid parity for PV. Excluding worst case scenarios, the model forecasts this to occur between 2015 and 2019 without any incentives, 2013 and 2017 with optimized engineering, and to have already occurred in 2008 in NJ with government incentives. An in depth handbook for financial analysis is also provided, which should give anyone the tools necessary to estimate payback times, out of pocket costs, and more.

6.2. Conclusions and Recommendations

6.2.a. Crystalline and Thin-film

The comparison of a-Si and c-Si modules provided a wealth of data and insight into the operation of the differing technologies. Where ample space is available, thin film modules most definitely present a greater value than their high-efficiency brethren. This may be advantageous in areas of the world, such as the US, where space has not yet become an over-valued commodity throughout all regions. Coupled with amorphous' strong adherence to nameplate ratings where output does not suffer significantly at elevated temperatures, these types of modules will undoubtedly find strong support in locations with plentiful sun once truly large-scale PV farms become a part of our infrastructure. This is especially true in areas where modules can be expected to reach temperatures above 45°C consistently, in locations such as these, data show, amorphous modules will generate 10-20% more electricity than crystalline modules. This would cut

electricity costs by similar amounts. System cost reductions due to various physical advantages can be had through innovations that include modules as part of racking structures and the ease of installation of thin, light-weight yet rigid packages. While their greatest advantage still lies in the ultimate cost of the modules per watt, some crystalline module manufacturers (especially from China) are closing in on thin-film prices. However, today amorphous silicon and other thin-film variants are still significantly less expensive, to the point where system costs can be reduced by up to 40¢/W.

The data presented in Chapter 2 of this thesis could be enhanced with additional testing of various other technologies. While being grouped into a single category, a-Si, CIGS, CdTe, etc. will all likely have their own advantages and disadvantages which should be highlighted and explored further. The collection of module performance and operation data could be compiled into a database holding both different manufacturers and types, and would provide an invaluable tool for engineers involved in the development of PV systems.

6.2.b. Engineering and Design Optimizations

Often overlooked are the design aspects for PV systems of all sizes. Current electrical standards do not incorporate any requirements for efficiency, only safety. This means that the overall efficiency of a system relies solely on the designer's whims, which may or may not be concerned with providing the highest value to the ultimate owner. Following the efficiency standards given in chapter 3 will ensure systems produce far higher kilowatt-hours per rated kilowatt capacity than tools such as PVWatts estimate. Eliminating unnecessary equipment and innovative engineering design can create savings

on the AC side of over 20%, and guarantee modules operate as effectively as they can. Utilizing proper orientation for the location of the system, as well as module spacing and tilt optimizations, electricity costs can be ensured to be as low as possible. Modules tilted at 30° (in southern NJ) produce over 40% more electricity than those laid flat on a roof or ground, and over 15% more than those tilted at only 10°. As a testament to these claims, Chris Baralus', a design engineer for RAI Inc., mentions the fact that the systems which make full use of these design optimizations produce electricity well above the estimates of their competitors. "With the design optimizations given by the RU team such as low voltage drop tolerance, and expansion of those optimizations developed internally such as including ventilation of the components where possible, the systems we have installed produce electricity well above standard estimates and those of our competitors. The quality in design has become a trademark and selling point for the company, helping to earn the reputation of being the top PV developer in the region." [2] Ensuring that proper care is taken in the design process can also save large scale systems' owners hundreds of thousands of dollars over the course of the lifetime of a system. Optimizations on the engineering side create savings that help reduce ultimate electricity costs by 1¢ or more per kWh.

However, as technologies change so will system design, meaning that low level optimizations will be more difficult to find. Equipment manufacturers are now making headway in creating highly integrated systems with efficient harvesting being part of an overall package. As more sophisticated solutions are brought onto the market efficiencies will continue to rise while costs will come down. For developers it will become ever more important to utilize the newest innovations to be competitive in the market.

6.2.c. Solar and Shading Modeling

A comprehensive MATLAB tool, based on the contents of Chapter 4, which calculates solar paths, insolation levels, the effects of shading on module output and more, is encompassed in a program capable of being modified to suit the needs of anyone designing PV systems or completing research in the field. All major software available on the market today are strictly for-pay and most certainly not inexpensive. Hopes are that the release of this code will help create many tools for solar design which may benefit any interested student or professional. One example of the applications is the guide for inter-row spacing provided in Chapter 4. It provides a clear chart of the spacing multiplier, depending on module tilt and system azimuth, to ensure losses are no more than 2% due to inter-row shading.

To perfect the program and enable it to accurately calculate total system output without any historical data, one would need to include a more detailed model for the effects of diffused lighting on module output, since the current algorithm only takes into account the effects of direct sunlight incident on the module plane. This version of the program may already be utilized in conjunction with typical meteorological year (TMY) data, available from NREL, to provide accurate estimates for almost all regions in the US. Possibilities for future research with this tool are nearly endless, and as simple as calling a function within MATLAB.

6.2.d. Grid Parity

With proper financing and the ability to take advantage of tax deductions used for decades by businesses in all sectors, PV has managed to reach beyond grid parity when net-metered. Subsidies such as SRECs and tax incentives such as the ITC will undoubtedly be phased out, ceasing to exist at the point in time when PV systems will no longer be cost neutral, but healthy investments with enticing returns. For now, the availability of these programs has been crucial in driving the market and spurring competition to compact the span of time until PV becomes wholly self-perpetuating. The projections provided in this thesis attempt to give plausible prediction of future large scale PV prices in a wide enough range to include a number of unforeseen events. Yet, given that every prediction by consultancy firms and analysts for the growth of PV have fallen short of reality time and time again, the worst case scenarios created by the model will be omitted from the following summary. The span of times, anticipated through the research in this thesis in Chapter 5, at which the average large scale PV system will reach grid parity can be approximated with some confidence. First, PV systems acquired in direct purchases, or without any subsidies or optimizations, are expected to reach this point in time between 2013 and 2018, meaning New Jersey is already remarkably close to crossing this important threshold. PV systems utilizing the kind of proper engineering outlined in Chapter 4 can be expected to reach grid parity between 2012 and 2016, highlighting the fact that good design can strongly affect financial feasibility. Finally a variety of options for the inclusion of government incentives were modeled, such as the inclusion of the 30% ITC, available until 2016, which brought prices down to below grid parity only a year after its inception in 2008. The availability of SRECs, which are also

up for renewal come 2016, had the greatest effect on PV electricity prices and brought these to only 3¢/kWh in 2009 and 2010 or more than 10¢/kWh lower than that available from the utility. The combination of these two lucrative incentives actually created a slightly negative cost for the electricity costs in 2009 and 2010, and kept PV below the point of grid parity for all years after their approval. Lastly, the inclusion of both incentives available and the suggestions in this thesis held the price of electricity for the average large scale PV system at a minimum of 4¢/kWh below the cost from the utility, reaching a maximum of only 11.43¢/kWh (in 2018) and a minimum of -3.10¢/kWh in 2009. The point to take away from these results is that if these incentives stay in place it will guarantee the self perpetuation of large scale PV systems throughout our time.

There are only two additions that come to mind for the enhancement of this model. The first being the inclusion of the value of system depreciation which can have a strong impact in favor of PV, the second being the overall increase in electricity costs due to "reserve" generation costs. Once intermittent renewables such as PV become a large part of the supply portfolio in New Jersey, there will necessarily have to be a certain amount of reliable generation at the ready, to be utilized during times of low renewable output. Since these generators will often lay dormant yet have to be very reliable and be able to be called upon within minutes, their costs will be higher than standard generation in today's world. With the exception of the possibility that large scale electricity storage (such as widespread use of electric vehicles) will become financially feasible, these reserves could alter the costs of PV significantly.

References

[1] Anthony, M.. "Cadmium Telluride Casts Shadow on First Solar." *Seeking Alpha*. N.p., n.d. Web. 10 Jan. 2009. <http://seekingalpha.com/article/55392-cadmium-telluride-casts-shadow-on-first-solar>

[2] Baralus, Chris. Personal interview. 18 Aug. 2010.

[3] Bookrags. "A. E. Becquerel Summary" *BookRags.com*. N.p., n.d. Web. 23 Mar. 2009. <http://www.bookrags.com/wiki/A._E._Becquerel>.

[4] Burnham, Laurie, and Thomas B. Johansson. *Renewable energy: sources for fuels and electricity*. Washington, D.C.: Island Press, 1993. Print.

[5] Carlson, Carlson and Wronski, Applied Physics Letter 28 (1976)

[6] Conergy AG. "Conergy AG - Renewable Energy" N.p., n.d. Web. 7 Mar. 2009. <http://www.conergy.com>.

[7] Deffeyes, Kenneth S. *Hubbert's peak* . Princeton (N.J.): Princeton University Press, 2008. Print.

[8] Discovery. "Coal Supply May Be Vastly Overestimated." *Discovery Channel*. N.p., n.d. Web. 11 May 2009. <http://dsc.discovery.com/news/2009/05/11/peak-coal-energy.html>.

[9] EERE. "Doping Silicon for Photovoltaics" *eere.energy.gov*, Web. 10 Apr. 2009. <http://www1.eere.energy.gov/solar/doping_silicon.html>

[10] EERE. "Overview of Silicon for Photovoltaics" *eere.energy.gov,* Web. 10 Apr. 2009. <http://www1.eere.energy.gov/solar/silicon.html>

[11] EERE. "EERE State Activities and Partnerships: States with Renewable Portfolio Standards." *eere.energy.gov*. N.p., n.d. Web. 5 May 2009. <apps1.eere.energy.gov/states/maps/renewable_portfolio_states.cfm>.

[12] EIA. "U.S. Energy Information Administration - EIA." *Independent Statistics and Analysis*. N.p., n.d. Web. 9 Apr. 2009. <http://www.eia.gov>.

[13] EIA. "Annual Energy Review (2008)", *U.S. EIA. N.p., n.d.* Web 16 Aug. 2009. <http://www.eia.doe.gov/emeu/aer/renew.html>.

[14] EIA. "This Week In Petroleum Crude Oil Section." *U.S. EIA*. N.p., n.d. Web. 9 Apr. 2009. <http://www.eia.doe.gov/oog/info/twip/twip_crude.html>.

[15] EIA. "State Electric Profiles." *U.S. EIA*. N.p., n.d. Web. 14 Aug. 2009. <http://www.eia.doe.gov/cneaf/electricity/st_profiles/new_jersey.html>.

[16] EIA. "Electric Power Monthly." *U.S. EIA*. N.p., n.d. Web. 14 Aug. 2009. <http://www.eia.doe.gov/cneaf/electricity/epm/table1_1.html>.

[17] EIA. "International Energy Outlook 2009" *U.S. EIA*. N.p., May 2009, Web. 27 May 2009. < http://www.eia.doe.gov/oiaf/ieo/pdf/0484(2009).pdf>.

[18] EIA. "Current and Historical Monthly Retail Sales, Revenues and Average Revenue per Kilowatt-hour by State and by Sector (Form EIA-826)" *U.S. EIA*. N.p., May 2009 <http://www.eia.doe.gov/cneaf/electricity/epm/table5_6_b.html>

[19] Energy Watch Group. "Coal: Resources and Future Production." *Energy Watch Group*. N.p., 10 July 2007. Web. 15 Mar. 2009. <www.energywatchgroup.org/fileadmin/global/pdf/EWG_Report_Coal_10-07-2007ms.pdf>.

[20] EPIA. "Global Market Outlook for PV until 2013." *EPIA*. N.p., 9 Mar. 2009. Web. 15 Nov. 2009. <www.epia.org/fileadmin/EPIA_docs/publications/epia/Global_Market_Outlook_Until_2013.pdf>.

[21] Epuron. "EPURON." *EPURON*. N.p., n.d. Web. 24 Aug. 2009. <http://www.epuron.de>.

[22] ERS. "New Jersey Fact Sheet: NJ agriculture." *USDA Economic Research Service* N.p., n.d. Web. 25 Oct. 2009. <http://www.ers.usda.gov/statefacts/NJ.htm>.

[23] Evans, A., et. al. 2008. "Assessment of sustainability indicators for renewable energy technologies." Renewable and Sustainable Energy Reviews. Volume 13, Issue 5, June 2009, Pages 1082-1088

[24] Estrom, Tommy. "Sattelite History." *Vanguard 1*. N.p., n.d. Web. 26 Jan. 2010. <http://home.swipnet.se/~w-52936/index20.htm>.

[25] Exelon. "Exelon Corporation." *Exelon Corporation*. N.p., n.d. Web. 22 Nov. 2010. <http://www.exeloncorp.com>.

[26] FirstSolar. "Corporate Overview Q4 2009." *First Solar*. N.p., n.d. Web. 15 Nov. 2009. <http://investor.firstsolar.com/phoenix.zhtml?c=201491&p=irol-calendarPast>.

[27] FirstSolar "Product Overview - Datasheet" *FirstSolar,* N.p., n.d. Web. 10 Oct. 2009. <http://www.firstsolar.com/pdf/PD_5_401_02_NA.pdf>

[28] Getsolar. "Federal Incentives for Commercial Solar." *Getsolar.com*. N.p., n.d. Web. 10 Oct. 2009. <http://www.getsolar.com/commercial_federal-incentives-for-commercial-solar.php>.

[29] Greentech Media "PV Technology, Production and Cost, 2009 Forecast: the Anatomy of a Shakeout" *Exec. Summary, Greentechmedia & the Prometheus Institute.* 7 Mar 2009

[30] Guardian.co.uk. " Solar energy 'revolution' brings green power closer." *guardian.co.uk*. N.p., 29 Dec. 2007. Web. 17 May 2009. <http://www.guardian.co.uk/environment/2007/dec/29/solarpower.renewableenergy>.

[31] Gupta, A. Gupta, I. Matulionis, J. Drayton and A. Compaan, “Effect of CdTe thickness reduction in high efficiency CdS/CdTe solar cells”, Mat. Res. Soc. Symp. Proc., Vol. 668 (2001)

[32] Herrmann W., M. Adrian, W. Wiesner, “Operational Behavior of Commercial Solar Cells under Reverse Biased Conditions” 2nd WCPEC, Vienna 1998 pp. 2357-2359

[33] Herrmann, W.Herrmann, W.Wiesner, W. Vaassen, “Hot Spot Investigations on PV Modules – New Concepts for a Test Standard and Consequences for Module Design with respect to Bypass Diodes”, Photovoltaic Specialists Conference, 1997., Conference Record of the Twenty-Sixth IEEE, Oct 1997

[34] IAEA "Analysis of Uranium Supply to 2050", www-pub.iaea.org, 2001

[35] IPS, "The Solar Constant" *Australian IPS Radio and Space Services* 23 Apr. 2009 <http://www.ips.gov.au/Category/Educational/The%20Sun%20and%20Solar%20Activity/General%20Info/Solar_Constant.pdf>

[36] Jansson, P.M. "Solar and PV Basics" Advanced Power Systems. Rowan University. Glassboro, NJ, 26 March 2007.

[37] Jansson, P.M., Schwabe, U.K.W. and A. Hak, “Large-Scale Photovoltaic System Design: Learning Sustainability through Engineering Clinics”, Proceedings of the 2008 Annual ASEE Conference, Pittsburgh, PA June 22 – 25, 2008

[38] Jansson, P.M. and Schwabe, U.K.W., "Performance Measurement of Amorphous and Mono- crystalline Silicon PV Modules in the Eastern US", 2009 IEEE I2MTC Conference, Singapore, May 5-7, 2009

[39] Jansson, P.M., Schwabe, U.K.W. and A. Hak, “Medium Voltage Switchgear, Transformer and Interconnection Specification in an ECE Clinic”, Proceedings of the 2008 Annual ASEE Conference, Pittsburgh, PA 23 Jun., 2008

[40] Jansson, P.M., Schwabe, U.K.W., "Photodiode Sensor Array Design for Photovoltaic System Inter-Row Spacing Optimization", IEEE SAS Symposium, Limerick, Ireland,23 Feb., 2010

[41] Kaneka. "Kaneka Corporation." *Kaneka Corporation*. N.p., n.d. Web. 5 June 2009. <http://www.kaneka.com>.

[42] Kaneka. "Why Amorphous?." *Kaneka Silicon PV*. N.p., n.d. Web. 6 May 2009. <http://www.pv.kaneka.co.jp/why/index.html>.

[43] Kaneka. "GSA-60 Datasheet" *Kaneka Co.*Web. 7 Jun. 2009. < http://www.sistemifotovoltaici.com/pdf/kaneka%2060%20uk.pdf>

[44] Kolodziej, A.Kolodziej, “Staebler-Wronski effect in amorphous silicon and its alloys”, Opto-Electronics Review 12, 2004

[45] Kray, D. Kray and Keith McIntosh, “Analysis of ultrathin High-efficiency silicon solar cells”, Physica Status Solidi A. Online, 2009

[46] Kumazawa, S. Kumazawa, S. Shibutani, T. Nishio, T. Aramoto, H. Higuchi, T. Arita, A. Hanafusa, K. Omura, M. Murozono, H. Takakura, “15.1% Highly efficient thin film CdS/ CdTe solar cell”, Elsevier Science, 1997

[47] Kurtz, Efficiency Comparisons - S.Kurtz, “Opportunities and Challenges for Development of a Mature Concentrating Photovltaic Power Industry”, NREL Technical Report Feb 2009

[48] Lawrence Berkeley National Laboratory. "Lawrence Berkeley National Laboratory." *Lawrence Berkeley National Laboratory*. 2009. <http://www.lbl.gov>.

[49] Lawrence Berkeley National Laboratory. "Tracking the Sun, The Installed Cost of Photovoltaics in the US from 1997-2007" *Lawrence Berkeley National Laboratory*. Feb. 2009 < http://eetd.lbl.gov/ea/ems/reports/lbnl-1516e.pdf>

[50] Mah, O., "Fundamentals of Photovoltaic Materials", NSPRI – Solar Academy Report, 1998

[51] Masters, From G.M. Masters, Renewable and Efficient Electric Power Systems, NJ, Wiley-Interscience, 2004: p.396.

[52] Masters, From G.M. Masters, Renewable and Efficient Electric Power Systems, NJ, Wiley-Interscience, 2004: p.394.

[53] Masters, Gilbert M., Renewable and Efficient Electric Power Systems, Hoboken NJ, Wiley-Interscience, 2004: p.397

[54] Maxwell, E. L. Maxwell, "A Quasi-Physical Model for Converting Hourly Global Horizontal to Direct Normal Insolation", SERI, Golden, Colorado 1987

[55] McMahon, T.J. of NREL, King, D. L. of Sandia, "Module 30 Year Life : What Does it Mean and Is it Predictable/Achievable?", National Center for Photovoltaics Program Review, Denver, CO, 17 Apr. 2000

[56] Mehta, S. Mehta, T. Bradford, "PV Technology, Production and Cost, 2009 Forecast: the Anatomy of a Shakeout" Exec. Summary, Greentechmedia & the Prometheus Institute, 2007

[57] MISO. "Midwest ISO." *Midwest ISO*. N.p., n.d. Web. <http://www.midwestiso.org/home>.

[58] Myers, D. Myers, "Estimating Direct Radiation from Global", Solar Spectrum Vol.13, RAD of the American Solar Energy Society, 2000

[59] NanoSolar. "Nanosolar." *Nanosolar*. N.p., n.d. Web. 22 Mar. 2009. <http://www.nanosolar.com>.

[60] NCDC. "NCDC." *National Climatic Data Center*. N.p., n.d. Web. <http://www.ncdc.noaa.gov>.

[61] NCWARN. "NC WARN Solar Report." *NC WARN*. N.p., n.d. Web. 10 Aug. 2010. < http://www.ncwarn.org/wp-content/uploads/2010/07/NCW-SolarReport_final1.pdf>.

[62] NEI, "Nuclear Energy - NJ Fact Sheet", NEI.org, Washington DC July 2009 <http://www.nei.org/filefolder/New_Jersey_Fact_Sheet.pdf>

[63] NFPA, From NEC 2008: Table 690.7, National Fire Protection Association.

[64] NJ Energy Master Plan. "Energy Master Plan." *The Official Web Site for The State of New Jersey*. N.p., n.d. Web. 1 Jan. 2009. <http://www.state.nj.us/emp/docs/pdf/081022_emp.pdf>.

[65] Noufi, CdTe/CIGS SEM Pics -R. Noufi and K. Zweibel, "High-efficiency CdTe and CIGS thin-film solar cells: Highlights and Challenges", IEEE 4th World Conference on Photovoltaic Energy Conversion, 2006

[66] Noufi, R. Noufi and K. Zweibel, "High-efficiency CdTe and CIGS thin-film solar cells: Highlights and Challenges", IEEE 4th World Conference on Photovoltaic Energy Conversion, 2006

[67] NREL. "NREL ." *National Renewable Energy Laboratory* . Web. 2010. <http://www.nrel.gov/>.

[68] NREL, "Photovoltaic energy program overview: fiscal year 1994". DoE, Washington D.C., 1995

[69] Orcad. "OrCAD." *Cadence Design Systems*. N.p., n.d. Web. 2010. <http://www.cadence.com/products/orcad/pages/default.aspx>.

[70] Oserwald, C.R. Osterwald, J. Adelstein, J.A. del Cueto, B. Kroposki, D. Trudell, and T. Moriarty, "COMPARISON OF DEGRADATION RATES OF INDIVIDUAL MODULES HELD AT MAXIMUM POWER", NREL 2006

[71] PECO. "Service Information Resources ." *PECO*. N.p., n.d. Web. Nov. 2010. <http://www.peco.com/pecobiz/contractor_and_builder_services/service_information_resources.htm>.

[72] Perkins, J. Perkins, M. Taylor, M. van Hest, C. Teplin, J. Alleman, M. Dabney, L. Gedvilas, B. Keyes, B. To, D. Readey, A. Delahoy, S. Guo and D. Ginley, "Combinatorial Optimization of Transparent Conducting Oxides (TCOS) for PV", 31st IEEE PV Specialists Conference, (2005)

[73] Perlin, John. *A History of Photovoltaics*, University of Southern California, Lectures, 2008

[74] Perlin, John. *From space to Earth: the story of solar electricity*. Ann Arbor, Mich.: Aatec Publications, 1999. Print.

[75] Phipps, G. Phipps, C. Miklajczak, T. Guckes, “INDIUM AND GALLIUM SUPPLY SUSTAINABILITY September 2007 UPDATE”, Indium Corporation (2007)

[76] Photon. "Research, Analysis & Consulting ." *PHOTON Consulting*. Web. 2009. <http://www.photonconsulting.com/>.

[77] Photon. "Solar Annual 2008." *PHOTON Consulting*. Web. 2009. <http://www.photonconsulting.com/files/sa_2008_exec_summary.pdf>

[78] Photon. "Solar Annual 2009." *PHOTON Consulting*. Web. 2009. <http://www.photonconsulting.com/files/reports/sa09_overview.pdf>

[79] PJM. "PJM - Home." *PJM*. N.p., n.d. Web. 2010. <http://www.pjm.com/>.

[80] PJM. "PJM Load Report 2009." *PJM*. N.p., n.d. Web. <www.pjm.com/~/media/documents/reports/2009-pjm-eia-411-report.ashx>.

[81] Prometheus Institute. "Prometheus Institute for Sustainable Development." *Prometheus Institute for Sustainable Development*. N.p., n.d. Web. 2009. <http://www.prometheus.org/>.

[82] PVWatts "PV Watts Parameters" *rredc.nrel.gov*. Web 2009. <http://rredc.nrel.gov/solar/codes_algs/PVWATTS/version1/>

[83] Resource Investor. "Byproducts Part I: Is There a Tellurium Rush in the Making? "*Resource Investor*. N.p., n.d. Web. 22 Nov. 2010. <http://www.resourceinvestor.com/News/2007/4/Pages/Byproducts-Part-I--Is-There-a-Tellurium-Rush-in.aspx>.

[84] Rutgers. "Energy Master Plan Electricity Modeling" *Rutgers University*. 2008. <http://rei.rutgers.edu/index.php?option=com_content&task=blogsection&id=4&Itemid=9>

[85] Schwabe, U.K.W. and Jansson, P.M., "Utility-Interconnected Photovoltaic Systems Reaching Grid Parity in New Jersey", 2010 IEEE PES General Meeting, Minneapolis, Minnesota July 25, 2010

[86] Schwabe, U.K.W. and Jansson, P.M., "Streamlining Large Scale Photovoltaic Arrays for Utility Interconnection", 2009 IEEE PowerTech Conference, Bucharest, Romania, 28 June - 2 July, 2009

[87] Schwabe, U.K.W. and Jansson, P.M., "Undergraduate Analysis of three Different Photovoltaic Module Types: A Comparison Completed for an Industrial Affiliate" 2009 Annual ASEE Conference, Austin TX, June 14 - 17, 2009

[88] Seeking Alpha. "The Tellurium Supernova Has Erupted." *Seeking Alpha*. N.p., n.d. Web. 2009. <http://seekingalpha.com/article/71942-the-tellurium-supernova-has-erupted>.

[89] Sekulic, Bill. Email interview. 12 Jan. 2009.

[90] Sharp. "Sharp Module Warranty". *Sharp*. Web. 2010. <www.sharpusa.com/SolarElectricity/~/media/Files/Solar/Solar_Warranty/sol_war_module_warranty.ashx>

[91] SMA "SMA Solar Technology" *SMA*. Web 2010 <http://www.sma-america.com>

[92] Solarbuzz "Current Retail Module Prices" *Solarbuzz*. Web 2009 <http://www.solarbuzz.com/Moduleprices.htm>

[93] Solarbuzz. "Marketbuzz 2010" *Solarbuzz.*Web. 2010 <http://www.solarbuzz.com/Marketbuzz2010-intro.htm>

[94] Southwire. "Rooftop Installations? Watch Out for Sunshine." *Southwire*. 2005. <http://www.southwire.com/support/RooftopInstallationsWatchOutForSunshine>

[95] Street, R.A. Hydrongenated Amorphous Silicon. Cambridge: Cambridge University Press, 1991

[96] SunnyPortal. "SunnyPortal." *SMA Solar Technology AG*. N.p., n.d. Web. 2009. <http://sunnyportal.com>.

[97] SunTech Power "STP170s-24-Ab-1" *SunTech Power*. Web 2010. <http://www.affordable-solar.com/admin/product_doc/Doc_STP170S-24-Ab-1%20JAN%2020081_20080325111514.pdf>

[98] SunTechnics "SunTechnics" Web 2009 <http://www.suntechnics.be/>

[99] Sweet, Bill. "Photovoltaic Grid Parity." *IEEE Spectrum Online*. N.p., n.d. Web. 20 Nov. 2009. <http://spectrum.ieee.org/energywise/energy/renewables/photovoltaic-grid-parity>.

[100] U.S. Department of the Treasury, "How to Depreciate Property." Internal Revenue Service Publication 946. Washington, DC: U.S. Government Printing Office.

[101] Ullal, H. Ullal and B. von Roedern, “Thin Film CIGS and CdTe Photovoltaic Technologies: Commercialization, Critical Issues, and Applications”, 22nd European PVSEC (2007)

[102] Vazques, M. Vazquez, I. Rey-Stolle, "Photovoltaic Module Reliability Model Based on Field Degradation Studies", Progress In Photovoltaics: Research and Applications, 2008

[103] WM, "WM" Web 2009 <http://www.wm.com/>

[104] Wronski, C.Wronski, J. Pearce, R. Koval, A. Ferlauto and R.Collins, "Progress in Amorphous Silicon Based Solar Cell Technology", RIO 02 World Climate & Energy Event (2002)

[105] Yuma Solar http://www.yuma-solar.com/pvl.htm

[106] Zweibel, K. Zweibel, "Thin Films: Past, Present, Future", Progress in Photovoltaics NREL (1995)

Appendices

APPENDIX A
12.47kV System Design and

Utility Interconnection Specifications

FOR A 2MW PHOTOVOLTAIC GROUND MOUNTED SYSTEM

AT

SEABROOOK FARMS

5 Finley Road

Seabrook, NJ 08302

Prepared for

SunTechnics Energy systems

222 W. Lancaster Avenue, Suite 200
Paoli, PA 19301

Prepared by

Integrated Systems

604 Cedar Avenue
Pitman, NJ 08071

Table Of Contents

Acknowledgements

Integrated Systems would like to acknowledge the support, assistance and review of the enclosed system designs by:

Mr. Jeffrey Ciccone, PE of Atlantic City Electric,
Mr. Jeffrey Tisa, MSECE EIT of Pepco Holdings Incorporated
and the INTEGRATED SYSTEMS engineering team including
Mr. Ulrich KW Schwabe, BSECE and
Dr. Peter Mark Jansson PP PE

for the work provided here in its application to the Seabrook Farms 2MW PV project contracted by SunTechnics Energy Systems of Paoli PA. Use on any other project without permission of INTEGRATED SYSTMES is not permitted beyond the scope of the current design contract.

We would also like to thank Russ Ehrlich at Atlantic City Electric and Blake Buxton of Systems Control for their helpful comments and suggestions.

I. Executive Summary

The following documents represent the work of INTEGRATED SYSTEMS (IS) to complete its contract with SunTechnics Energy Services of Paoli, PA with respect to their proposed 2MVA photovoltaic system to serve Seabrook Farms.

The original proposed scope of work for electrical engineering assistance for electrical design includes the specifications for the recommended transformers to raise the inverter output AC voltage (yet to be fully specified by SunTechnics – but assumed to be 208V/120V for the project) to the required utility interconnection voltage of 12.47 kV for Atlantic City Electric (the host utility service Seabrook).

IS was also requested to provide technical details suitable for procurement of the interconnection equipment (specifically the needed switchgear between the step-up transformers and the utility system.)

The design of all overhead components (poles, cross-arms, lightning protection, insulators, switches, etc.) required to complete the design was also IS' responsibility.

Added to the project scope near the end of the task was the request to procure equipment quotes for both delivery lead-times and cost. This was for the most part completed before SunTechnics requested IS discontinue these activities.

Finally, IS was contracted to review, sign and seal all electrical plans developed by SunTechnics for the project to assure they are approved by the local authorities and meet the requirements necessary for interconnection with the local utility.

II. Introduction and Project Scope

Integrated Systems was contracted by SunTechnics to provide electrical designs from the Inverter onward for a PV system at Seabrook Farms. Good engineering design standards, input from ACE engineers, and the guidelines set forth by ACE interconnection specifications to complete the scope of work.

Details Omitted

III. Medium Voltage System and Overhead Design

Simple single line diagrams are provided for both the AC side and the necessary ground connections. Pole overviews were generated to give an overview of all specified equipment and organization. Some structural details for the riser pole may be extracted from the diagrams as well as accompanying PHI / ACE power distribution standards (Appendix A)

i. System Overview

Figure 1 gives an overview of the AC side from the Inverters to the riser pole which will be connected to the existing utility poles. Four Xantrex GT500-208 inverters provide 208Y/120 to 500kVA step-up transformers. The inverters were chosen to come without an isolation transformer to increase efficiency by ca. 1%. The step-up transformers will consequently double as the isolation transformers, and must therefore provide 208Y/120 on the secondary. Three 600kcmil Cu 600V cables will provide the conductors for each phase from the inverters, routed through 4" PVC piping to the transformers. After being stepped up to the necessary 12.47kV, 200A load break elbows connect to 1/0 Al XLPE in 4" PVC conduit to provide connection to the next pad. The transformers will be configured in a loop to remove the need for any individual switchgear on each inverter pad. The final transformer that provides connection to the riser pole

will have 9kV MOV elbow arresters in addition to the 200A load break elbows, these lightning arrestors will provide the necessary lightning protection from the pole downward.

Figure 2 shows a simplified grounding one-line. Per manufacturer recommendations, each inverter shall have a separate ground rod to act as an EMI filter. This is necessary only on inverters that come without the standard isolation transformer (as with our current proposed system). Air terminals will provide the necessary static drain for each pad enclosure designed by SunTechnics to eliminate lightning hazard, and will be grounded with two ground rods spaced a minimum of 10ft apart. Separate from previously mentioned ground connections will be the grounding system required for the step-up transformers. A minimum of three ground rods spaced evenly around the pad are connected to the transformer, if the 25ohm minimum impedance cannot be met, additional rods may be driven a minimum of 5ft away from any other rods. This may be done up to a total of six grounding rods. All ground connections will be provided by 4 gauge soft-drawn copper wire and appropriate clamps.

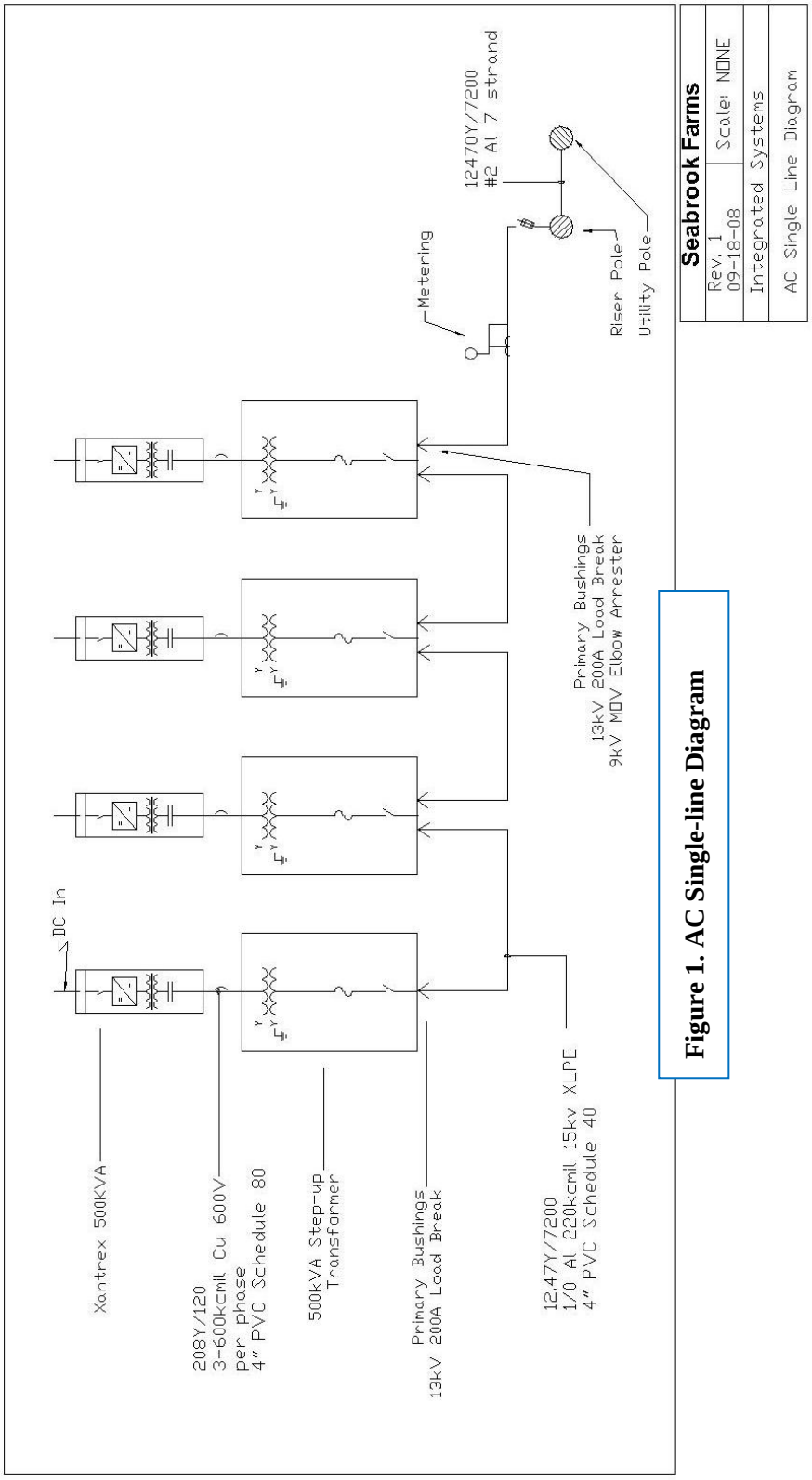

Figure 1. AC Single-line Diagram

Figure 2. Grounding Single-line

IV. Overhead Design

Figure 3 shows the existing 12.4kV overhead system that will serve as an interconnection feeder to Atlantic City Electric's distribution feeder serving Seabrook Farms.

Figure 3. Existing Customer-owned Overhead adjacent proposed site

Figures 4 & 5 are the front and side view of the proposed riser pole respectively. Coming from 5" PVC up the pole, each cable receives a 3M QT-III cold shrink termination. Each phase will then be connected via a #4 Cu wire to its respective S&C Type XS cutout, over an Ohio Brass PDV-100 and will then go up the top cross arm to be connected to the existing pole via #2 Al 7-strand overhead. All connections must be made with H-tap or other no-ox filled compression connectors that are appropriate for Al-Cu connections. This is necessary to eliminate any corrosion due to dissimilar metals. As the dead-end insulators of the overhead lines Veri*Lite PDI-15's were proposed. Cross-arms were specified to be 10ft wide in order to accommodate for common wingspans of birds, and other animals.

Figure 6 depicts the existing pole at Seabrook that the riser pole will connect to. Several poles at the proposed site were found to have the potential to hold the additional cross-arms needed to clamp onto the existing overhead. The overhead coming from the riser pole will be terminated on a new cross-arm on an existing pole with Veri*Lite PDI-15 terminations. Standard pin-type insulators may be needed to bridge the #4 copper wire, depending on the final setup. The system is then connected to the existing overhead via three #4 copper wires and compression clamps.

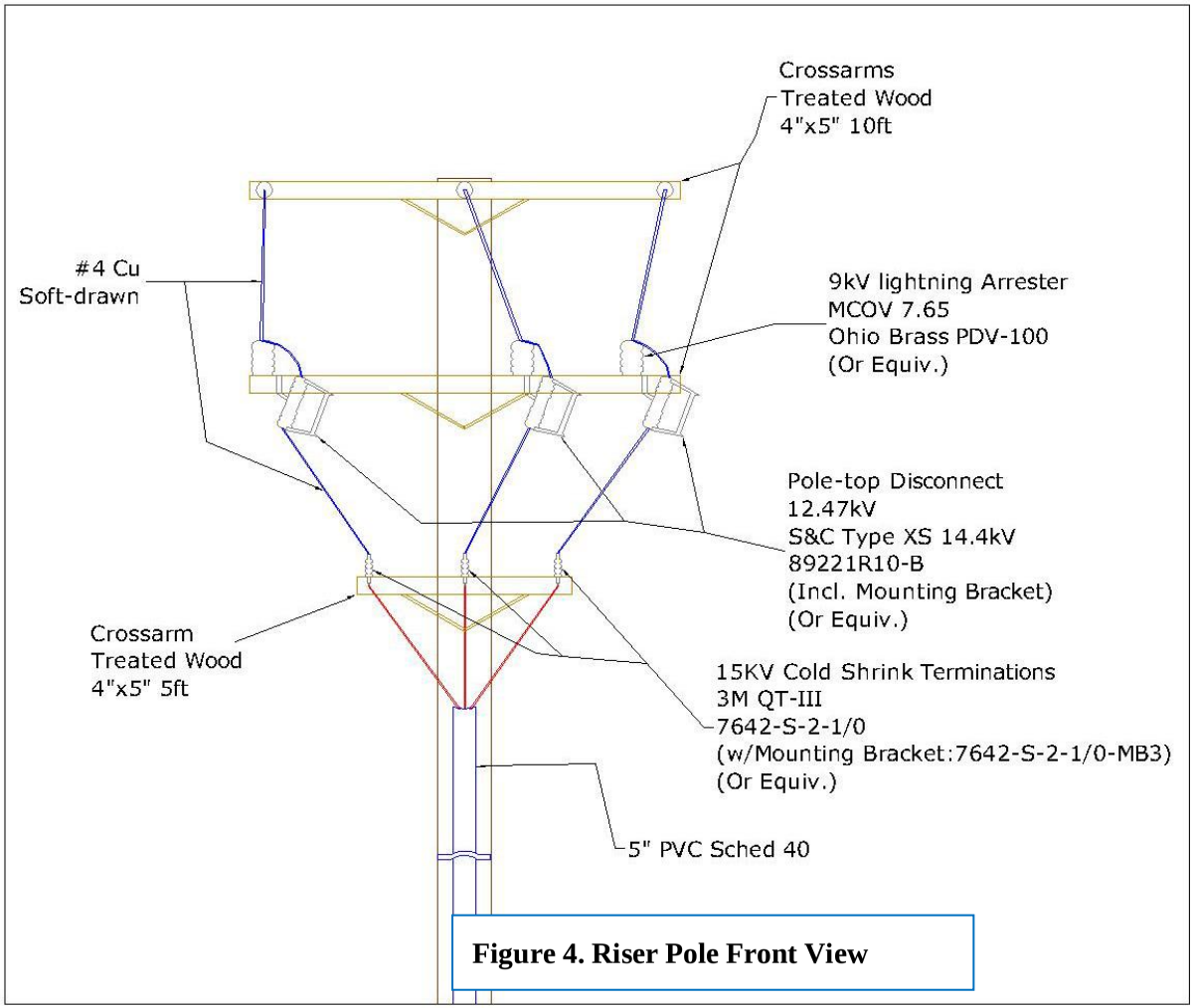

Figure 4. Riser Pole Front View

See Appendix A

for proper spacing and

guy-wire requirements

Seabrook Farms	
Rev. 1 09-18-08	Scale: NONE
Integrated Systems	
Riser Pole - Front View	

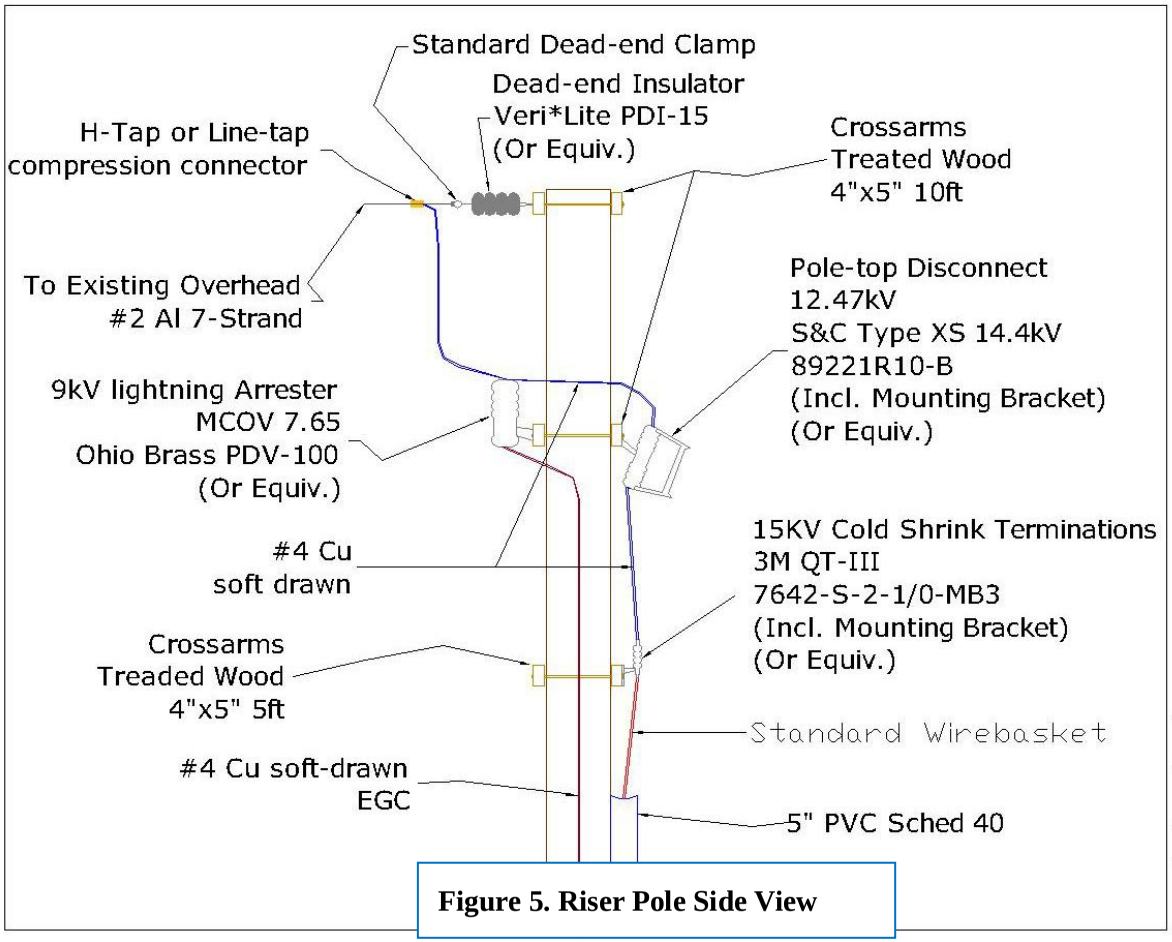

Figure 5. Riser Pole Side View

See Appendix A

for proper spacing and

guy-wire requirements

Seabrook Farms	
Rev. 1 09-18-08	Scale: NONE
Integrated Systems	
Riser Pole - Side View	

Figure 7 shows grounding necessary for the riser pole. In order to reach a maximum 25ohm impedance of the system, a minimum of three ground rods are to be installed around the pole. This small grid will be connected to the ground grid of the transformer pads.

Figure 8 is an illustration of the conduit containing the conductors going up the riser pole. A metal guard to protect and hold the 5" PVC on the pole for the first 8 feet is necessary.

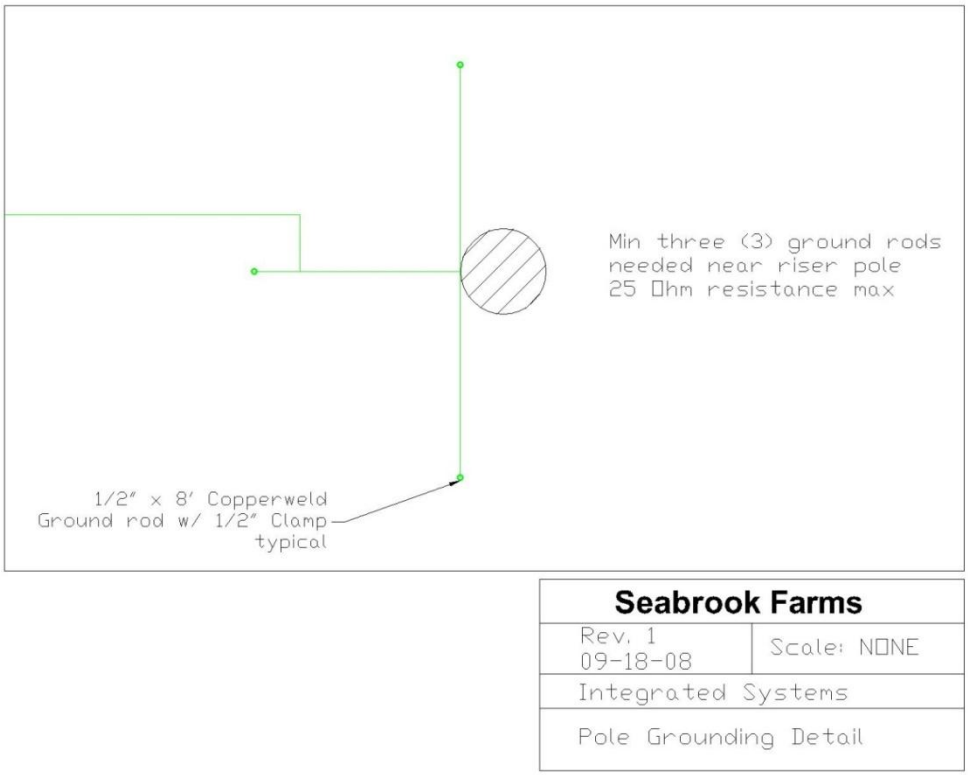

Figure 7. Pole Grounding Grid

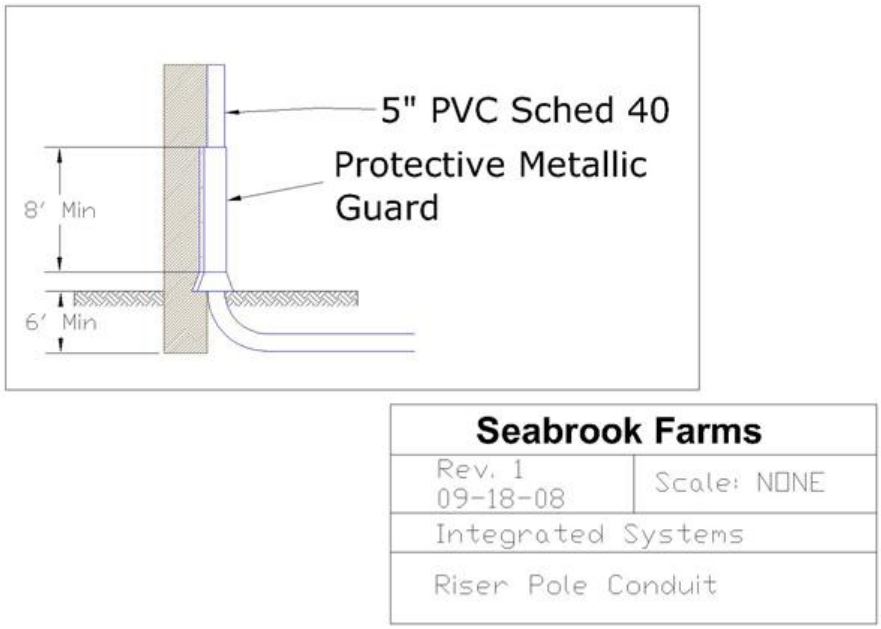

Figure 8. Riser Pole Conduit and Guard

Figure 9 shows the proposed plan of equipment location originally specified by SunTechnics at the time this work was proposed. Shown on this draft plan are the locations of the equipment it has specified in this document.

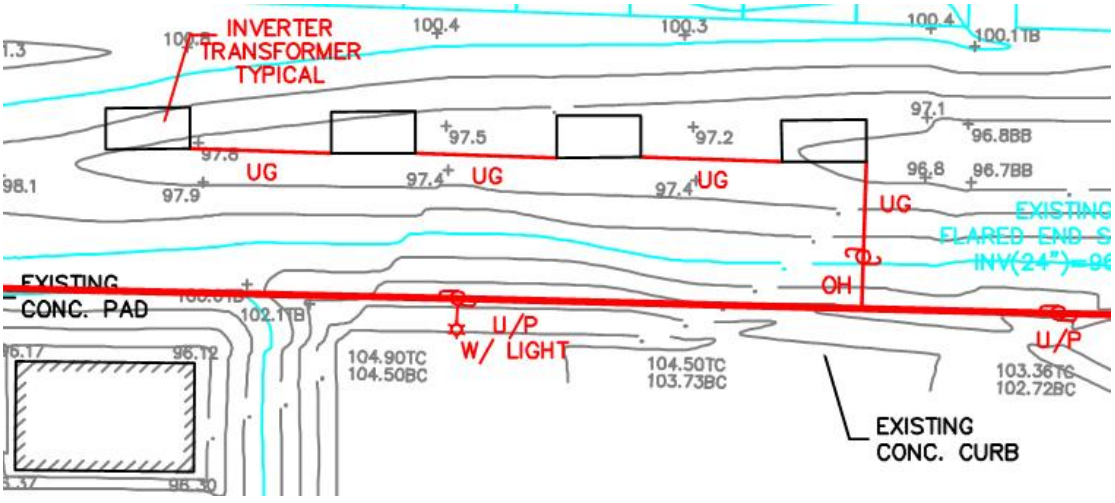

Figure 9. AC Interconnection Plan

V. Equipment Specifications

The transformer spec was generated to meet the highest efficiency standards of NEMA with a TP-1 designation. Increases in efficiency with this designation are generally around 1% compared to standard models. Premiums for this designation are by and large around $1000, making pay-back periods relatively short – especially when taking the SREC value into consideration. In order to eliminate the need to bring the entire production to a halt during maintenance of a subsystem, loop-feed configurations for the transformers were specified. This allows the hot side of a transformer to remain energized while power generation may be halted. MOV Elbow Type Arresters were used on the final transformer instead of more expensive arrester provisions.

All equipment was chosen to be readily available, high quality as well as competitively priced. 3M Terminations QT-III cold shrink terminations will be used for cable end potheads on the riser, as well as Hubbell's PDV-100 lightning arresters. Hubbell's division Ohio Brass was also chosen to provide the necessary insulators for the dead-end pole overhead. S&C fused cutouts were selected to be the main switchgear for the system, ACE interconnection specifications do not require interface transformers less than 10MVA to have protective relaying – only high side fuses.

The riser pole was specified to be a 40ft class-3 with 4"x5" treated cross-arms for the cutouts, lightning arresters and aerial terminations supports.

Much of the information necessary to make these decisions were collected from various conversations with ACE engineers.

The following list represents a Bill of Materials for procurement of appropriate types of equipment to build the design specified by IS. Some values (such as cable distance) will be dependent upon final design location of inverter, transformer pads, riser pole and selected pole interconnection.

Transformer Connectors

- Three (3)-Hubbell MOV Elbow Type Arresters
- 9kV
- 7.65 MVOC
- Catalog #: 611508
- Twenty-one (21) - Cooper Power Systems Load-break Elbows
- 200Amps
- Catalog #: LE215C06

Cable & Conduits

- (Pad involved cable lengths pending final layout)
- Inverter to Transformer
- 600kcmil Cu XHHW (or 600V equiv)
- 4" PVC Schedule 40
- Neutral pending Xantrex response
- Transformer to Pole
- 1/0 Al 220kcmil TRXLP 15kv (or #2 copper EPR 175kcmil or equiv)
- Concentric Neutral

- 4” PVC Schedule 80

Grounding

- #4 Cu solid soft drawn
- Overhead
- #2 Al 7-Strand (150ft)
- #4 Cu solid soft drawn (200ft)
- Note: When connecting Al to Cu – Al always on top.
- Use only H-tap or other no-ox filled compression connectors for Al-Cu connections

Additional Required Equipment

- Three (3) - S&C Type XS 14.4kV
- Porcelain Insulator
- 110kV BIL
- 300A
- 8½ in leakage distance
- Catalog #: 89221R10-B (With bracket)
- Four (4) – Standard pin-type 15kV
- Ceramic/Glass
- Six (6) - Hubbell Ohio Brass Veri*Lite dead-end insulators
- 4 Sheds
- 110kV BIL
- Catalog #: 4010150215
- Three (3) - Hubbell Ohio Brass PDV-100 Lightning Arresters

- 9kV
- 7.65 MCOV
- Catalog #: 217608

Three (3) – 3M QT-III cold shrink terminations

- (Or other elastimold premolded slip on terminations)
- 15kV
- 125kv BIL
- Catalog #: 7642-S-2-1/0-MB3

Eight (8) 24" Airterminals (pending SunTechnics enclosure design)

- Appropriate adaptors pending roof material
- Lightning Protection Systems
- Catalog #: 330B

(Min) Twenty-Seven (27) - Standard grounding rods

- Copperweld
- 8ft long
- Additional clamps and connectors necessary
- Perpendicular Direct-bury ground rod clamps
- Copper parallel groove-type clamps

One (1) 40ft Class 3 Utility Pole

- (Two (2) Poles if overhead metering utilized)
- 40ft
- Six (6) 4x5x10ft cross-arms
- Treated wood
- Mounting and spacing bolts
- Braces
- Two (2) 4x5x5ft cross-arms
- Treated wood
- Mounting and spacing bolts
- Braces

VI. Transformer Specification

Details Omitted

VII. Transformer Bids from Manufacturers

Details Omitted

Confidential Quotes & Prices Removed from Package

VIII. Manufacturer Specification Sheets

Appropriate excerpts from data sheets for all specified equipment are attached for ease of product selection and manufacturer catalog numbers. Some degree of product information may be extracted for each apparatus.

Disconnect Overhead—Pole-Top Style

Dimensions in inches (mm)

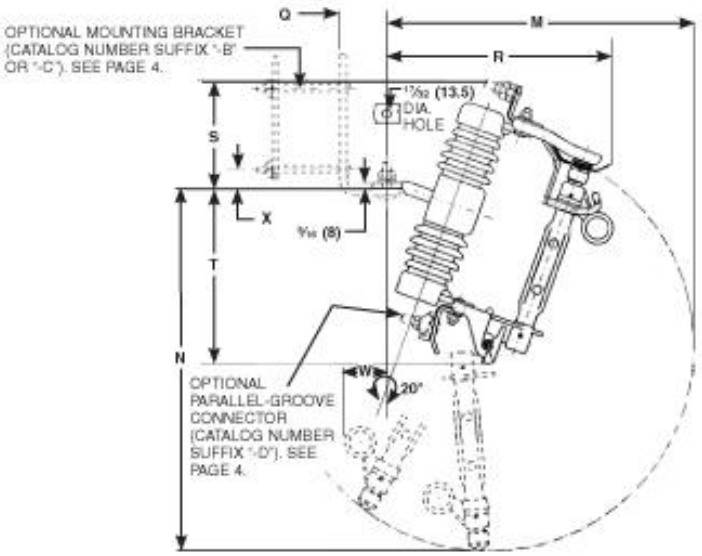

Catalog Numbers 89221R10, 89222R10, and 89223R10

Rating						Leakage Distance to Ground, Min., Inches (mm)	Catalog Number (Less Mounting Bracket and Connectors)①		Dimensions in Inches (mm)								Net Weight, Lbs. (kg)
kV			Amperes, RMS														
Nom.	Max	BIL	Cont.	Short Time			Porcelain Insulator	Polymer Insulator	M	N	Q②	R	S②	T	W	X①	
				Mom. (Asym)	15-Cycle (Sym.)												
14.4	15	110	300	16 000	10 600	8½ (216)	89221R10	—	17 (432)	20¼ (514)	2⅝ (67)	12½ (318)	6¼ (159)	9¾ (248)	2⅜ (60)	1½ (38)	13 (5.9)
14.4	15	110	300	16 000	10 600	8½ (216)	—	89221R10-P	17 (432)	20¼ (514)	2⅝ (67)	12½ (318)	6¼ (159)	9¾ (248)	2⅜ (60)	1½ (38)	8½ (3.9)
25	27	125	300	12 000	8 600	11 (279)	89222R10	—	19⅞ (505)	25¼ (641)	2⅝ (67)	13⅛ (333)	7⅞ (200)	11⅜ (289)	4¼ (108)	1½ (38)	15½ (7.0)
25	27	150	300	12 000	8 600	17 (432)	89223R10	—	22⅝ (578)	31⅜ (797)	2⅝ (67)	13⅜ (349)	9½ (241)	13 (330)	6¼ (159)	1½ (38)	18 (8.2)

① Specify mounting bracket, if desired, and connector option by adding suffix letter(s) to catalog number. For example, 89221R10-BD. See table on page 4.

② Dimension applies to cutout furnished with optional NEMA Type B Mounting Bracket (cutout Catalog Number Suffix "-C"). If cutout is furnished with optional S&C Extended Mounting Bracket (cutout Catalog Number Suffix "-B"), dimension is 5⅛ inches (132 mm).

③ Dimension applies to cutout furnished with optional parallel-groove connectors (cutout Catalog Number Suffix "-D"). If cutout is furnished with optional eye-bolt connectors (cutout Catalog Number Suffix "-M"), dimension is slightly smaller.

④ Dimension applies to cutout furnished with optional NEMA Type B Mounting Bracket (cutout Catalog Number Suffix "-C"). If cutout is furnished with optional S&C Extended Mounting Bracket (cutout Catalog Number Suffix "-B"), dimension is 1⅛ inches (29 mm).

HUBBELL POWER SYSTEMS

OHIO BRASS

PDV-100 OPTIMA

Solves Problems:

- *"Finally someone has listened to us and has a more reliable disconnector for the product."* — Utility in Louisiana
- *"We have never had a moisture failure of an Ohio Brass arrester. You guys are the only ones that know how to seal the product."* — Utility in Washington State
- *"At last someone has a 21st Century disconnector for our 21st Century arresters."* — California Utility

Saves Time and Money:

- Older style disconnectors can cause lock-outs
- Locating problem arresters costs an average of $200
- Actual costs can be much higher
- PDV-100 Optima reliably disconnects a shorted arrester
  - Allows line to be re-energized
  - Provides a visual indication to line crews

How do I make sure I am getting the new Optima design?

Just change the first 6 digits of the catalog number in your order according to the chart below:

Duty Cycle (kv)	MCOV (kV)	Original PDV-100	PDV-100 Optima
3	2.55	217602	213703
6	5.1	217605	213705
9	7.65	217608	213708
10	8.4	217609	213709
12	10.2	213510	213710
15	12.7	213613	213713
18	15.3	213615	213715
21	17	213617	213717
24	19.5	213520	213720
27	22	213622	213722
30	24.4	213624	213724
36	29	213629	213729

Visit us at: www.hubbellpowersystems.com

BULLETIN EU1519

0.625" (16mm) Diameter Rod Deadend Insulators

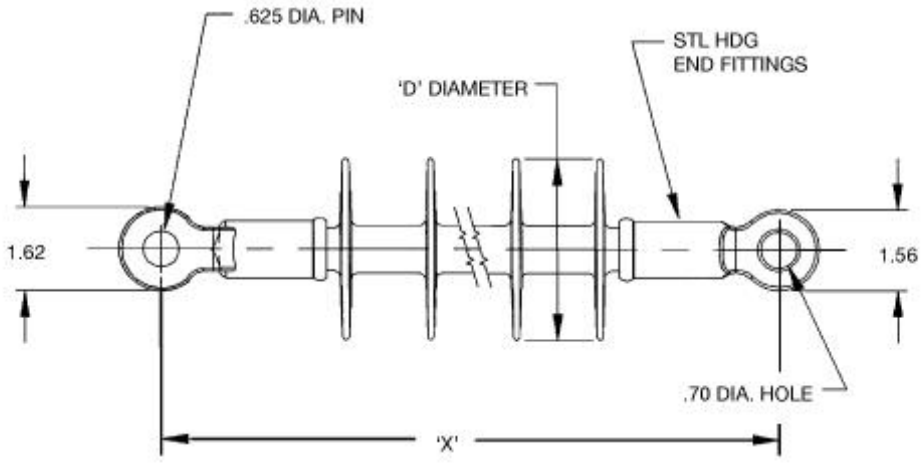

Mechanical Characteristics

Catalog Numbers	No. of Sheds	"X" Length inches (mm)	"D" Diameter Inches (mm)	Net Wt. pounds (kg)	Standard Package Qty. Carton	Standard Package Qty. Pallet	Torsion ft-lb (N-m)	[1]SML pounds (kN)	[2]RTL pounds (kN)	[3]Proof pounds (kN)
4010150215	4	12.50 (318)	3.6 (92)	2.1 (.95)	15	480	35 (47)	15,000 (70)	7,500 (35)	10,000 (44.5)
4010156215	4	12.50 (318)	3.6 (92)	2.1 (.95)	15	480	40 (55)	15,000 (70)	7,500 (35)	10,000 (44.5)
4010280215	8	17.50 (445)	3.0 (76)	2.4 (1.1)	15	360	35 (47)	15,000 (70)	7,500 (35)	10,000 (44.5)
4010286215	8	17.50 (445)	3.0 (76)	2.4 (1.1)	15	360	40 (55)	15,000 (70)	7,500 (35)	10,000 (44.5)
4010250215	8	18.75 (475)	3.5 (89)	2.8 (1.3)	15	360	35 (47)	15,000 (70)	7,500 (35)	10,000 (44.5)
4010256215	8	18.75 (475)	3.5 (89)	2.8 (1.3)	15	360	40 (55)	15,000 (70)	7,500 (35)	10,000 (44.5)
4010350215	8	25.00 (635)	3.0 (76)	3.3 (1.5)	15	300	35 (47)	15,000 (70)	7,500 (35)	10,000 (44.5)

[1]**SML** - Specified Mechanical Load is the tension load that a Veri*Lite insulator can withstand during a 90-second test without failure. SML is comparable to the M&E strength rating of porcelain insulators.

[2]**RTL** - A Routine Test Load value is equal to 50% of the SML value.

[3]**Proof Test** - The mechanical tension load applied at the factory to each insulator for ten (10) seconds.

NOTE: PDI Type insulators are intended for applications which are within 45° of horizontal - to allow proper shed drainage.

0.625" (16mm) Diameter Rod Deadend Insulators

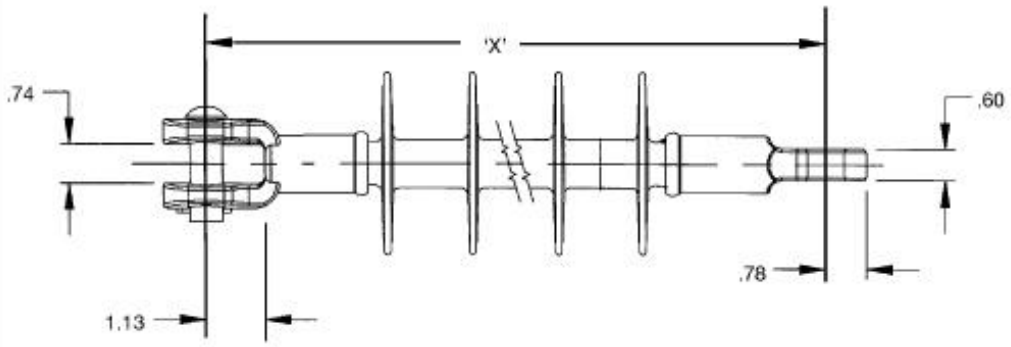

Electrical Characteristics

Catalog Numbers	Type	Leakage Distance Inches (mm)	Dry Arc Distance inches (mm)	Flashover ANSI - kV		Critical Flashover ANSI		RIV		Power Arc kA cycles	SL of # of 4-1/4 Bells	Volt*/ Class
				Dry-kV	Wet-kV	Pos-kV	Neg-kV	Test kV	Max. µV			
4010150215	PDI-15	16 (406)	8 (203)	110	75	140	160	15	<10	150	2	15
4010156215	PDI-15	16 (406)	8 (203)	110	75	140	160	15	<10	150	2	DS-15
4010280215	PDI-28	26 (660)	12¼ (311)	130	110	200	225	20	<10	150	–	25
4010286215	PDI-28	26 (660)	12¼ (311)	130	110	200	225	20	<10	150	–	DS-28
4010250215	PDI-25	31 (787)	14 (356)	150	130	260	280	30	<10	150	3	25 & 35
4010256215	PDI-25	31 (787)	14 (356)	150	130	260	280	30	<10	150	3	DS-35
4010350215	PDI-35	33 (838)	20 (508)	200	160	325	360	30	<10	150	4	35

*Phase-to-Phase voltage.

Key to the Catalog Numbers

401XXXX215

- 0 = Std. Pin
- 3 = Standard Pin Rotated End-fitting
- 5 = ANSI 52-3 B & S
- 6 = IEC 16mm B & S
- Voltage Rating kV
- Ferrous End-fitting
- 0 = Standard Marking
- 6 = LWWG Marking
- SML

Example: Cat. #4013250215 is a Veri*Lite insulator, 25 kV. Rated with standard pin and rotated end-fitting (ferrous) 15,000 lbs. SML, plus standard markings.

3.0 Physical and Electrical Properties

3M™ Cold Shrink Silicone Rubber Termination Kit QT-III, 7640-S, 7650-S and 7660-S series can be used on cables with a rated maximum operating temperature of 105°C and an overload rating of 140°C. QT-III 7640-S, 7650-S and 7660-S Series terminations meet all requirements of IEEE Standard 48-1996, "IEEE Standard Test Procedures and Requirements for High Voltage Alternating-Current Cable Terminations" and are designated Class 1 for outdoor weather-exposed locations. The current rating of these terminations meets or exceeds the current rating of the cables on which they are installed.

Typical Dimensions

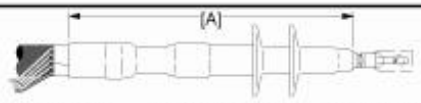

Kit Number	Dimension [A] Max.	Wet Creepage Distance Max.	Arcing Distance Max.
7642-S-2	9.8″ (249 mm)	13.3″ (338 mm)	9.8″ (249 mm)

Table 1

Typical Dimensions

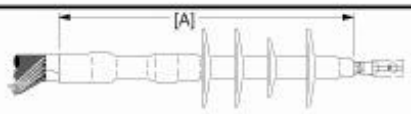

Kit Number	Dimension [A] Max.	Wet Creepage Distance Max.	Arcing Distance Max.
7652-S-4	12.25″ (311 mm)	18.50″ (470 mm)	12.25″ (311 mm)
7653-S-4	12.25″ (311 mm)	18.50″ (470 mm)	12.25″ (311 mm)
7654-S-4	12.25″ (311 mm)	18.50″ (470 mm)	12.25″ (311 mm)
7655-S-4	12.25″ (311 mm)	18.50″ (470 mm)	12.25″ (311 mm)
7656-S-4	13.25″ (337 mm)	19.50″ (495 mm)	13.25″ (337 mm)

Table 2

Typical Dimensions

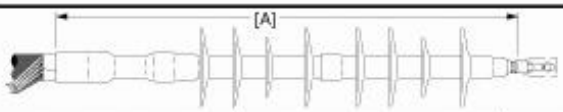

Kit Number	Dimension [A] Max.	Wet Creepage Distance Max.	Arcing Distance Max.
7663-S-8	20.50″ (521 mm)	33.00″ (838 mm)	20.50″ (521 mm)
7664-S-8	20.50″ (521 mm)	33.00″ (838 mm)	20.50″ (521 mm)
7665-S-8	20.50″ (521 mm)	33.00″ (838 mm)	20.50″ (521 mm)
7666-S-8	21.50″ (546 mm)	34.00″ (864 mm)	21.50″ (546 mm)

Table 3

BENEFITS

- Operating eye provides positive hotstick operation. The pulling eye strength exceeds 500 pounds of pull out force.
- Insulation consists of peroxide cured EPDM rubber that offers proven uncompromised reliability and dimensional stability.
- Molded shield of conductive peroxide cured EPDM rubber meets IEEE Standard 592.
- Grounding eye provides a convenient contact point to attach a grounding wire to maintain the shield at ground potential.
- Flexible lead is a No. 4 AWG bare copper rope lay. Available in several standard lengths to suit your application.
- Interface fit provides optimal radial pressure on the IEEE Standard 386 interface.
- The PDE arrester uses the same proven MOV technology utilized in all Ohio Brass arrester products.
- End cap is manufactured from high strength stainless steel.

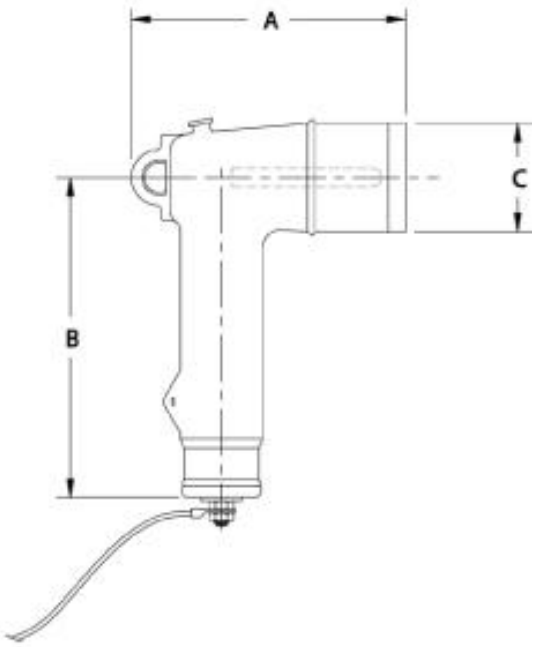

Surge Arrester Selection Chart

IEEE Standard 386 Interface	MCOV Rating (kV)	Rated Voltage (kV)	Dimensions in. (mm)			Elbow Interface	Approximate Shipping Weight		Catalog Number
			A	B	C		(lb.)	(gm.)	
15 kV Class	2.55	3	7.4 (188)	6.6 (168)	2.9 (168)	15kV	3.7	1676	611503
	5.1	6	7.4 (188)	6.6 (168)	2.9 (168)	15kV	3.7	1676	611505
	7.65	9	7.4 (188)	6.6 (168)	2.9 (168)	15kV	3.7	1676	611508
	8.4	10	7.4 (188)	6.6 (168)	2.9 (168)	15kV	3.7	1676	611509
	10.2	12	7.4 (188)	6.6 (168)	2.9 (168)	15kV	3.7	1676	611510
	12.7	15	7.4 (188)	10.2 (259)	2.9 (168)	15kV	5.2	2360	621513
	15.3	18	7.4 (188)	10.2 (259)	2.9 (168)	15kV	5.2	2360	621515
25 kV Class	7.65	9	7.9 (201)	6.6 (168)	3.1 (79)	25/35kV	3.7	1676	612508
	8.4	10	7.9 (201)	6.6 (168)	3.1 (79)	25/35kV	3.7	1676	612509
	10.2	12	7.9 (201)	6.6 (168)	3.1 (79)	25/35kV	3.7	1676	612510
	12.7	15	7.9 (201)	10.2 (259)	3.1 (79)	25/35kV	5.2	2360	622513
	15.3	18	7.9 (201)	10.2 (259)	3.1 (79)	25/35kV	5.2	2360	622515
	17	21	7.9 (201)	10.2 (259)	3.1 (79)	25/35kV	5.2	2360	622517
35 kV Class	19.5	24	7.9 (201)	10.2 (259)	3.1 (79)	25/35kV	5.2	2951	623520
	22	27	7.9 (201)	13.7 (348)	3.1 (79)	25/35kV	6.5	2951	633522
	24.4	30	7.9 (201)	13.7 (348)	3.1 (79)	25/35kV	6.5	2951	633524

Loadbreak Apparatus Connectors

COOPER Power Systems

Electrical Apparatus

200 A 15 kV Class Loadbreak Elbow Connector – Canadian Standard Edition

500-10C

GENERAL

The Cooper Power Systems Loadbreak Elbow Connector is a fully-shielded, insulated plug-in termination for connecting underground cable to transformers, switching cabinets and junctions equipped with loadbreak bushings. The Cooper Elbow Connector is a fully rated 200 A switching device, designed in accordance with IEEE 386-latest revision.

Cooper Power Systems Loadbreak Elbows are molded using high quality peroxide cured EPDM rubber. Standard features include a coppertop connector, tin-plated copper loadbreak probe with an ablative arc-follower tip, and stainless steel reinforced pulling-eye. An optional capacitive test point is available for use with Cooper Power Systems TPR Fault Indicators (see Catalog Section 320-40).

Cable ranges are sized to accept a wider range of cable diameter for a given size elbow. The wider cable ranges increase installation flexibility.

INSTALLATION

Cable stripping and scoring tools, available from various tool manufacturers, are recommended for use when installing loadbreak elbows. After preparing the cable, the elbow housing is pushed onto the cable. The loadbreak probe is threaded into the coppertop connector using the supplied installation tool or an approved equivalent. Use a hotstick to perform loadmake and loadbreak operations. See Installation Instruction Sheet S500-10-1 (5000050751) for details.

Figure 1.
Loadbreak Elbow Connector with test point; also available without test point.

PRODUCTION TESTS

Tests conducted in accordance with IEEE Standard 386:

- AC 60 Hz 1 Minute Withstand – 34 kV
- Minimum Corona Voltage Level – 11 kV
- Test Point Voltage Test

TABLE 1
Voltage Ratings and Characteristics

Description	kV
Standard Voltage Class	15
Maximum Rating Phase-to-Phase	14.4
Maximum Rating Phase-to-Ground	8.3
AC 60 Hz 1 Minute Withstand	34
DC 15 Minute Withstand	53
BIL and Full Wave Crest	95
Minimum Corona Voltage Level	11

Voltage ratings and characteristics are in accordance with IEEE Standard 386.

Tests conducted in accordance with Cooper Power Systems requirements:

- Physical Inspection
- Periodic Dissection
- Periodic Fluoroscopic Analysis

TABLE 2
Current Ratings and Characteristics

Description	Amperes
Continuous	200 A rms
Switching	10 operations at 200 A rms at 14.4 kV
Fault Closure	10,000 A rms symmetrical at 14.4 kV for 0.17 s after 10 switching operations
Short Time	10,000 A rms symmetrical for 0.17 s 3,500 A rms symmetrical for 3.0 s

Current ratings and characteristics are in accordance with IEEE Standard 386.

Solid Copper Air Terminals

Class I Solid Copper
3/8" Diameter Air Terminals

Length	Plain Copper	In-Stock Item	Blunt Tip	In-Stock Item	Weight
12"	330	★	330-BT	★	.52
18"	330A	★	330A-BT	★	.60
24"	330B	★	330B-BT	★	.80
36"	330C		330C-BT	★	1.26
48"	330D		330D-BT		1.68
60"	330E		330E-BT		2.10
72"	330F		330F-BT		2.52

Class II Solid Copper
1/2" Diameter Air Terminals

Length	Plain Copper	In-Stock Item	Blunt Tip	In-Stock Item	Weight
12"	331	★	331BT		.62
18"	331A	★	331A-BT		1.00
24"	331B	★	331B-BT		1.38
36"	331C		331C-BT		2.14
48"	331D		331D-BT		2.88
60"	331E		331E-BT		3.66
72"	331F		331F-BT		4.44

Class II Solid Copper
5/8" Diameter Air Terminals

Length	Plain Copper	In-Stock Item	Blunt Tip	In-Stock Item	Weight
12"	332	★	332-BT		.90
18"	332A	★	332A-BT		1.46
24"	332B		332B-BT		2.08
36"	332C		332C-BT		3.24
48"	332D		332D-BT		4.44
60"	332E		332E-BT		5.40
72"	332F		332F-BT		6.48

Note:

Air terminals on this page are furnished plain, no nickel plating, as our standard product.

Independent Protection Co., Inc.
P.O. Box 537
Goshen, IN 46527-0537
Ph: 574.533.4116 or 800.860.8388 Fax: 574.534.3719
Email: info@ipclp.com
Website: www.ipclp.com

Appendix – ACE Pole Standards

The following diagrams were received from ACE and provide dimensional specifications for the necessary riser pole, guy wires and cross-arm spacing.

P-34

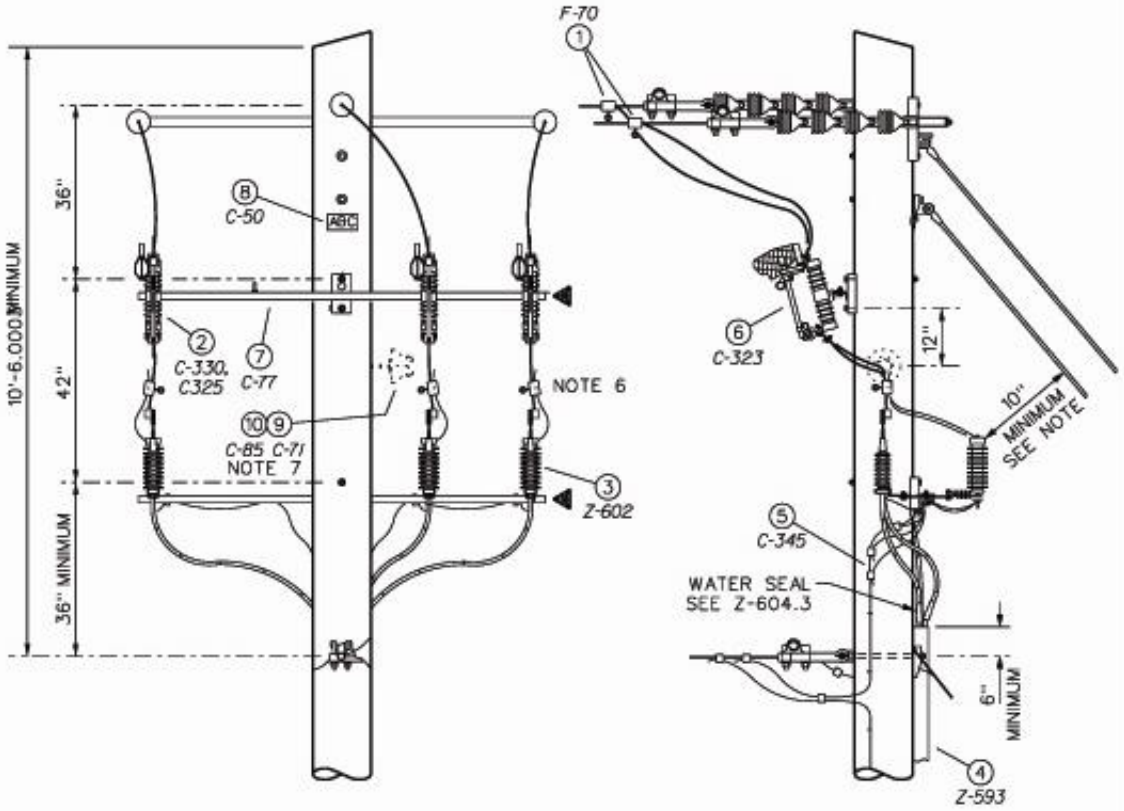

FIELD SIDE VIEW

NOTE:

In order to maintain 10" clearance, a minimum guy lead length of 0.75 x attachment height is required. For more guy information, refer to G-325.

BASIC POLE: G-325

PHI ACE / DP	POWER DISTRIBUTION STANDARDS	THREE PHASE 200 AMP TERMINAL THREE PHASE DEADEND POLE 4, 12, 25 & 35kV

P-54_Sht 2

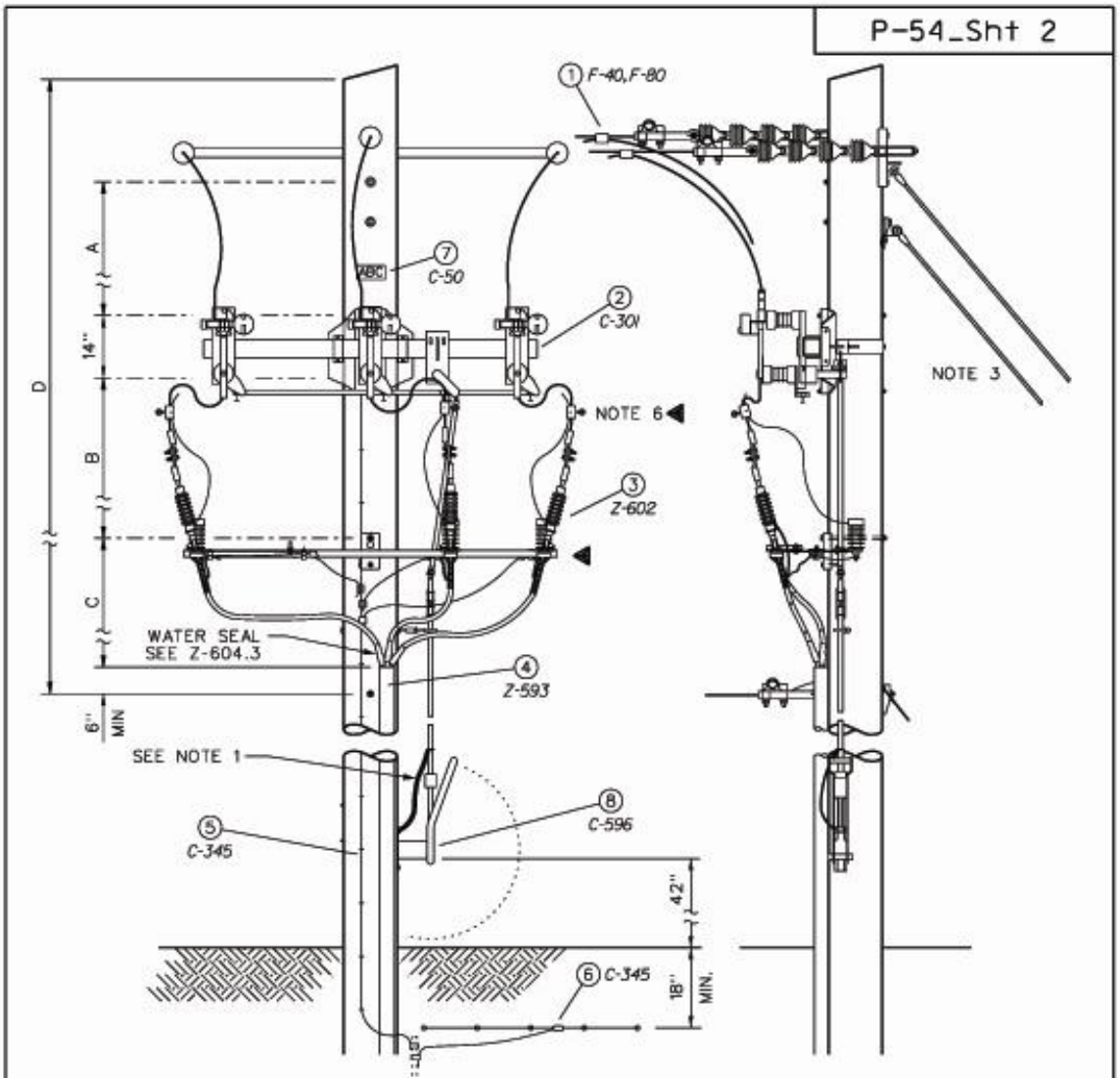

MINIMUM VERTICAL DIMENSIONS (SPACING)

STOCK NO.	CABLE SIZE	VOLT RATING (kV)	VERTICAL SPACING			
			A	B	C	D
3431-5044	1000 kcmil-J	25	60"	54"	54"	16' - 8"
0106-9947	1000 kcmil-J	35	60"	54"	54"	16' - 8"

NOTES:

1. Ground strap and ground connector included with switch handle assembly.
2. Jacketed cables should be STRIPPED BACK to a point 12" above the conduit. This should facilitate the training of the cables and the mounting of the terminators.
3. For guys, refer to G-325.

BASIC POLE: G-325

PHI ACE / DP	POWER DISTRIBUTION STANDARDS	THREE PHASE 600 AMP TERMINAL WITH GANG OPERATED LOADBREAK SWITCH THREE PHASE DEADEND POLE 12, 25 & 35kV

APPENDIX B
3MW Exelon Project AC Single line

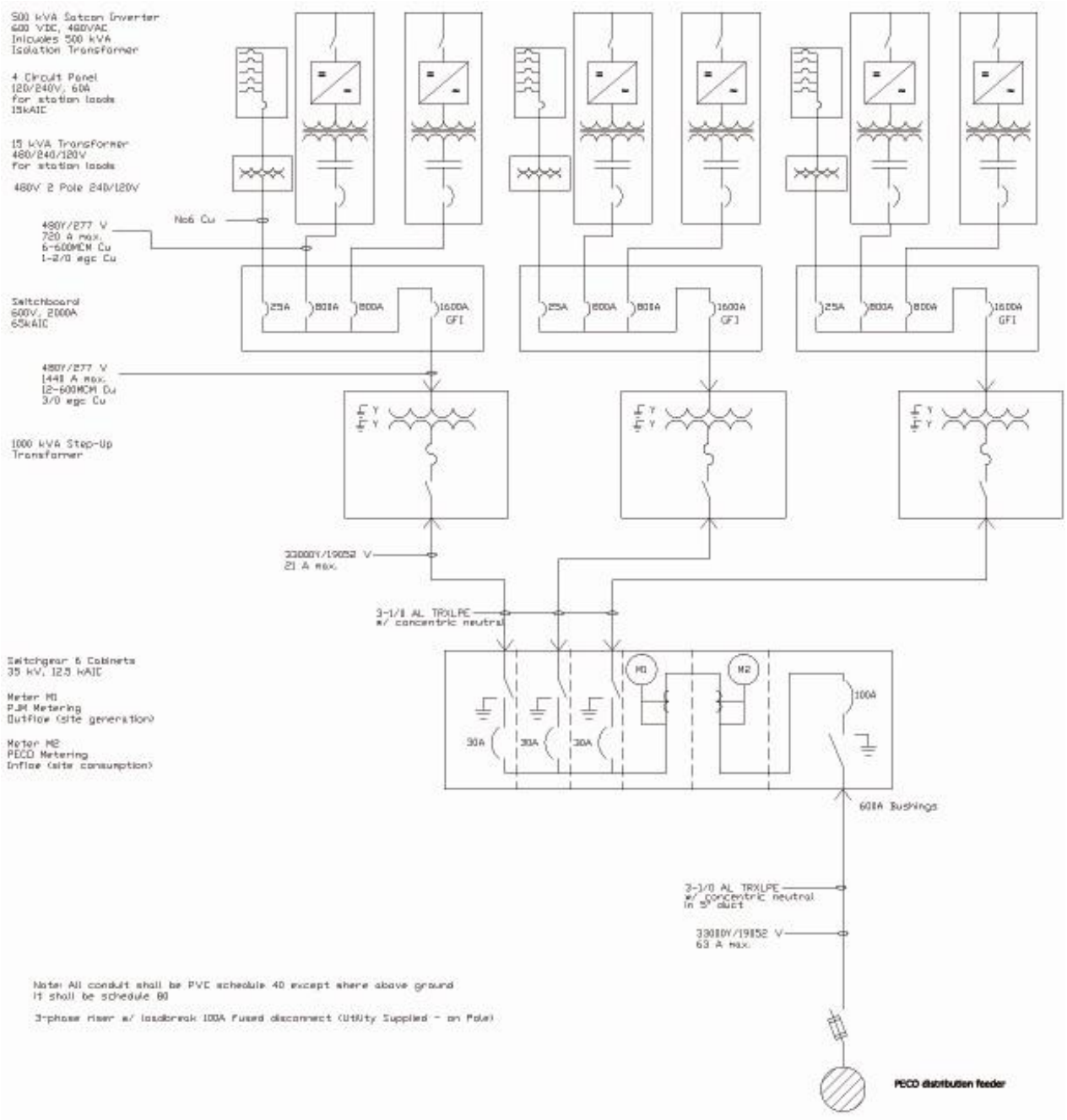

APPENDIX C

2MW Seabrook farms Single Line

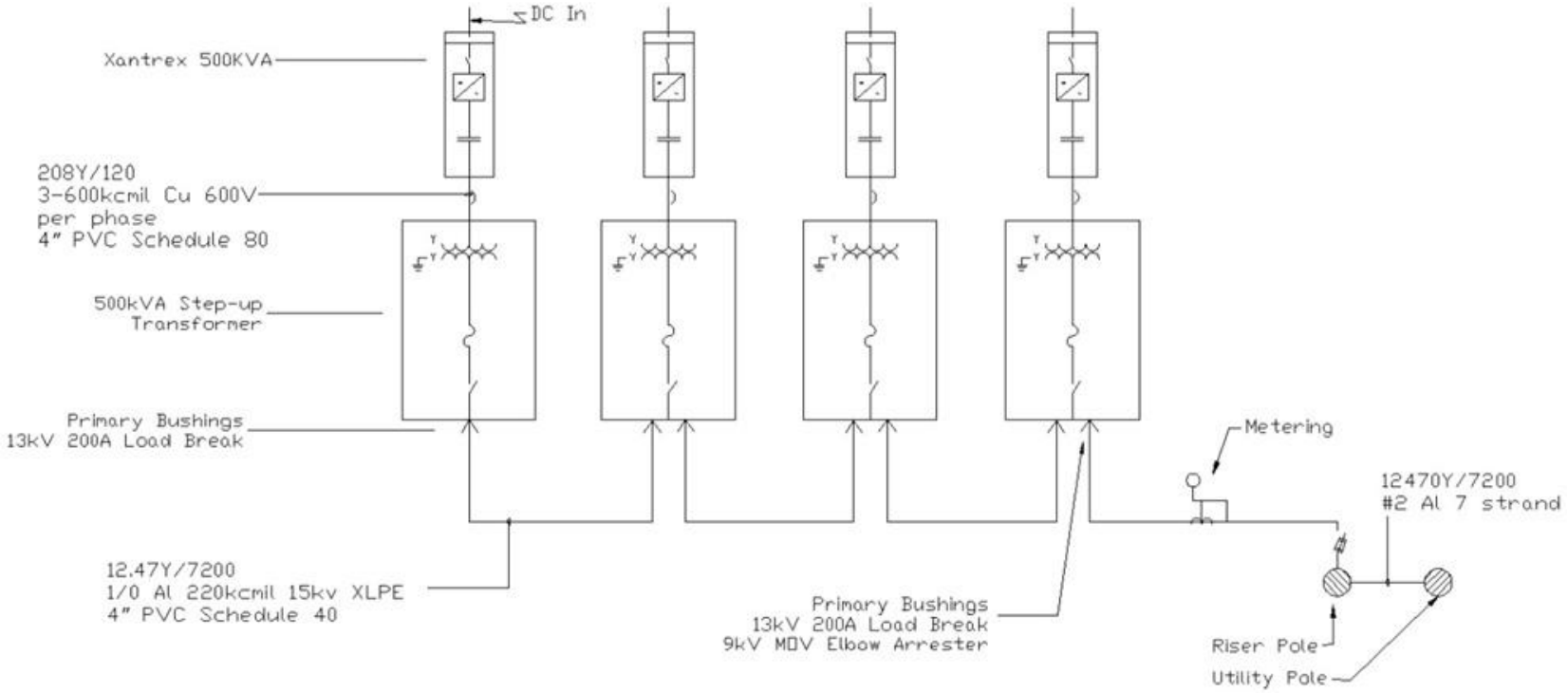

APPENDIX D

PhotoWatt 1650 P-Spice Model

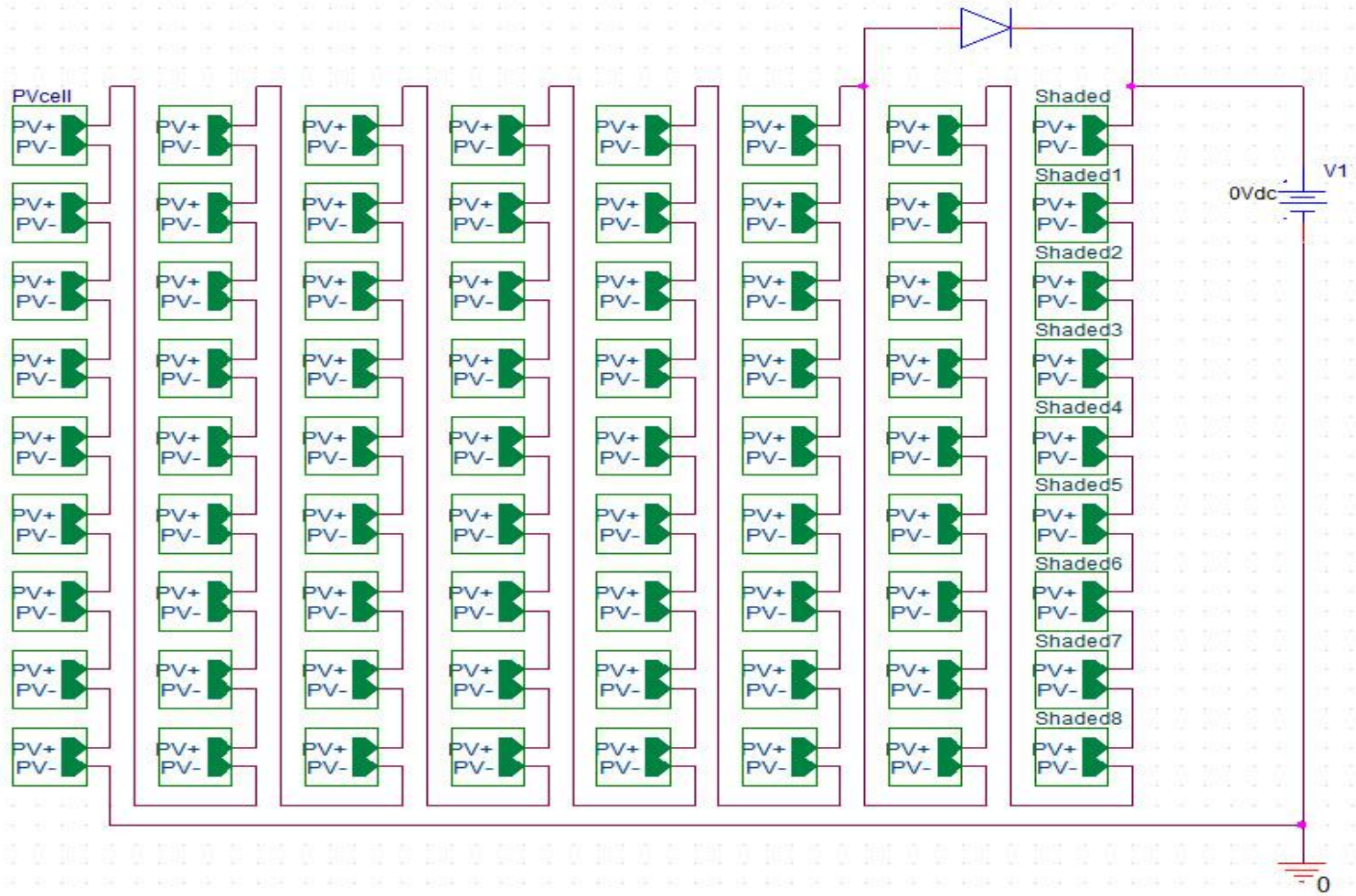

Each green block represents a copy of the circuit seen in Figure 3-17.

APPENDIX E

Incident_Calc MATLAB Program Code

```
function [percent_max, kWh_shaded, shading
,sp]=incident_calc(ModuleAzimuth,alphaDeg,spacing_multiplier,filename)
%Use: shading_calc(Module Azimuth, Module Tilt, Spacing multiplier, ['file
path & name'])
%File path and name are optional, enter string '' to pop dialog to browse.
%Direct insolation calculation program, based on SERI Report:
%Maxwell, E. "A Quasi-Physical Model for Converting Hourly Global Horizontal
%to Direct Normal Insolation", U.S. DoE, SERI, 1987
%Created by Ulrich KW Schwabe @ the CSD, Rowan University, 2009
%Works with NREL TMY data located at
%http://rredc.nrel.gov/solar/old_data/nsrdb/tmy2/


%Modify for different module type:
ModX=1.044;   %Module width in meters
ModY=1.170;   %Module height in meters
ModuleRating=240; %Module Wattage
FrameMargin=0.02; %Module Frame width
CellWidth=5*2.54/100; %5" * 2.54cm/in *1m/100cm.

SystemRating=1000;

%Module installed in Landscape?
LandscapeMode = 1;


%Convert variables to radians for Matlab:
alpha   =   alphaDeg * (pi/180);
% Lat      =   Ldeg * (pi/180);
phi_m   =   ModuleAzimuth * (pi/180);

if(LandscapeMode==1)
    ModHeight=sin(alpha)*ModX;    %Modules in landscape mode
else
    ModHeight=sin(alpha)*ModY;    %Modules in portrait mode
end

spacing=ModHeight*spacing_multiplier;

if (isempty(filename))
    %Load Meteorological Data from NREL for insolation numbers:
    [FileName,PathName,FilterIndex] = uigetfile('*.*');
    dataFile= [PathName,FileName];
else
    dataFile=filename;
end
```

```
fid = fopen(dataFile);
[ID,LocationName,    State,    TimeZone,    Latitude,    Longitude,    NS2]=
textread(dataFile, '%f %s %s %f %f %f %f',1,'delimiter',',');
MeteoData = textscan(fid,['%s %s %f %f %f ' repmat('%*s ', 1 ,35) '%f
%*[^\n]'],'delimiter', ',', 'headerlines',2);
fclose(fid);

Date(1,:)=MeteoData{1}(:);
Time(1,:)=MeteoData{2}(:);
GHI(1,:) =MeteoData{5}(:);
ETRN(1,:)=MeteoData{4}(:);

%Get insolation on collector plane, for each hour of the year:

GHI_reshape=reshape(GHI,24,365)';
GHI_trunc=GHI_reshape(:,4:20);
ETRN_reshape=reshape(ETRN,24,365)';
ETRN_trunc=ETRN_reshape(:,4:20);

Plocation=mean(MeteoData{6}(:));
PC=Plocation/1013.25;

% TimeZone=-5; %-for west of GST
HourofDay(1:365,1:24)=0;
for i=1:365
    HourofDay(i,:)=1:24;
end

%Solar Elevation Angle
SEA=23.45*pi/180;
%Calculate the solar declination for each day of the year
delta = SEA*sin((2*pi/365).*((1:365)-81));

%Convert day into angle of earth's rotation
DayAngle=2*pi*(0:364)/365;

%Equation of time, relate Solar Hour angle to time based on diurnal change
EQT=(7.5E-5    +    (1.868E-3.*cos(DayAngle))    -    (0.032077.*sin(DayAngle))-
(0.014615.* cos(2*DayAngle)) - (0.040849.*sin(2*DayAngle)))*(229.18);

%Calc all solar hour angles throughout the day, for each day of the year
SolarHourAngle(1:365,1:24)  =0;
ZenithAngle(1:365,1:24)     =0;
AM(1:365,1:24)               =0; %Air Mass index, ~ the distance that the sun
travels
for day=1:365
    for hour = 1:24
        SolarHourAngle(day,hour)    =    15*(HourofDay(day,hour)    -12.5    +
EQT(day)/60 + ((Longitude - TimeZone*15)*4)/60);
        ZenithAngle(day,hour) = acos(cos(delta(day)) * cos(deg2rad(Latitude))
*                   cos(deg2rad(SolarHourAngle(day,hour)))                  +
sin(delta(day)).*sin(deg2rad(Latitude)));

        if(ZenithAngle(day,hour)<deg2rad(80))
```

```
            AM(day,hour)=PC*((cos(ZenithAngle(day,hour))+0.15*(93.885        -
ZenithAngle(day,hour))^-1.253)^-1);
        else
            AM(day,hour)=0;
        end
    end
end


% Kn = direct beam transmittance
% Kt effecgtive global horizontal transmittance
% Clearness or Cloudiness Index
K_t(1:365,1:24) =0;
Kn_c(1:365,1:24)=0;
for day = 1:365
    for hour = 1:24
        if(AM(day,hour)>0)
            K_t(day,hour)                                                    =
GHI_reshape(day,hour)/(cos(ZenithAngle(day,hour))*ETRN_reshape(day,hour));
            Kn_c(day,hour)    =             0.866    -    0.122*AM(day,hour)    +
.0121*AM(day,hour)^2   -   0.000653*AM(day,hour)^3   +   0.000014*AM(day,hour)^4;
%Atmospheric
                                %^Correction  on  Page  34  of  "Quasi  Physical
model..."
                                %to .866 from .886
        else
            K_t(day,hour)=0;
            Kn_c(day,hour)=0;
        end
    end
end

a(1:365,1:24)=0;
b(1:365,1:24)=0;
c(1:365,1:24)=0;

for day=1:365
    for hour = 1:24
        %if Kt <= .6
        if(K_t(day,hour)<=0)
            a(day,hour)=0;
            b(day,hour)=0;
            c(day,hour)=0;
        elseif(K_t(day,hour)<=.6)
            a(day,hour) = .512 - 1.56*K_t(day,hour) + 2.286*K_t(day,hour)^2 -
2.222*K_t(day,hour)^3;
            b(day,hour) = .370 + .962*K_t(day,hour);
            c(day,hour) = -.28 + .932*K_t(day,hour) - 2.048*K_t(day,hour)^2;
        elseif(K_t(day,hour)>.6)
            a(day,hour)      =      -5.743      +      21.77*K_t(day,hour)      -
27.49*K_t(day,hour)^2 + 11.56*K_t(day,hour)^3;
            b(day,hour) = 41.40 - 118.5*K_t(day,hour) + 66.05*K_t(day,hour)^2
+ 31.90*K_t(day,hour)^3;
            c(day,hour) = -47.01 + 184.2*K_t(day,hour) - 222*K_t(day,hour)^2
+ 73.81*K_t(day,hour)^3;
        end
```

```
    end
end

%Calculate delta Kn and DNI
delta_Kn(1:365,1:24)=0;
DNI(1:365,1:24)=0;
for day = 1:365;
    for hour = 1 :24
        if(K_t(day,hour)>0)
            delta_Kn(day,hour)            =            a(day,hour)            +
b(day,hour)*exp(c(day,hour)*AM(day,hour));
            DNI(day,hour)=ETRN_reshape(day,hour)*(Kn_c(day,hour)-
delta_Kn(day,hour));
        else
            delta_Kn(day,hour)=0;
            DNI(day,hour)=0;
        end
    end
end

%Calculate solar azimuth and elevation angles based on previous data
phi_s(1:365,1:24)=0;
beta(1:365,1:24)=0;
for day=1:365
    for hour = 1:24
        if(ZenithAngle(day,hour)<deg2rad(80))
            beta(day,hour) = pi/2-ZenithAngle(day,hour);
%                                                          beta(day,hour)     =
asin(cos(deg2rad(Latitude))*cos(delta(day))*cos(deg2rad(SolarHourAngle(day,ho
ur)))+sin(deg2rad(Latitude))*sin(delta(day)));
            phi_s(day,hour)                                                    =
asin((cos(delta(day))*sin(deg2rad(SolarHourAngle(day,hour)))./cos(beta(day,h
our)'));
        end
    end
end

%Calculate the shading length
gamma = ModHeight./tan(beta);
lambda=gamma.*cos(abs(phi_s-phi_m));

sf(1:365,1:24)=0;%shading footprint
%calculate sf, which is the amount of shading under the next row
for day = 1:365
    for hour = 1:24
        if(lambda(day,hour)>spacing)
            sf(day,hour)=lambda(day,hour)-spacing;
        end
    end
end

shading=sf./cos(alpha);%Actual shading on module
sp=shading./ModX; %Percent shading on module surface

sp(sp>1)=1;
```

```
%Estimated module operation under shading. This is based on a 6 row module,
%with three bypass diodes (one for every two rows). Module output is an
%approximate number based on PSPice and empirical testing of modules
for day = 1:365
    for hour = 1:24
        if(shading(day,hour)<ModX/3)
            if(shading(day,hour) > FrameMargin+.5*CellWidth)
                sp(day,hour)=2/3;
            end
        elseif(shading(day,hour)<ModX*(2/3))
            if(shading(day,hour) > FrameMargin+CellWidth*2+.5*CellWidth)
                sp(day,hour)=1/3;
            end
        end
    end
end

%Calculate the amount of insolation incident with the module
incident_direct=DNI.*(cos(beta)*sin(alpha).*cos(phi_s-
phi_m)+sin(beta)*cos(alpha));
%Adjust for shading losses
shaded_incident=incident_direct.*(1-sp);

%Bad method for calculating diffused insolation
diffused=GHI_reshape-DNI;

%Calculate Module specs
ModuleArea=ModX*ModY;
sqm=ModuleRating/ModuleArea;

%Calculate system specs
efficiency=(ModuleRating/ModuleArea)/1000;
systemArea=SystemRating/sqm;

%Calculate system output
Wh_Produced_shaded=shaded_incident*efficiency*systemArea;
Wh_Produced=incident_direct*efficiency*systemArea;
Wh_Produced_diffused=diffused*efficiency*systemArea;

kWh_produced=sum(sum(Wh_Produced))/1000;
kWh_shaded=sum(sum(Wh_Produced_shaded))/1000;

percent_max=kWh_shaded/kWh_produced;
```

APPENDIX F

Various Matlab Scripts utilizing Incident_Calc, used in Chapter 4

```
%Calculate Losses due to Shading for various Azimuth
clear all
close all
clc

j=0;
k=0;

%Load Meteorological Data from NREL for insolation numbers:
[FileName,PathName,FilterIndex] = uigetfile('*.*');
dataFile= [PathName,FileName];

%Set array to run for (in this case Azimuth angles)
min=-45;
step=5;
max=45;
varu=min:step:max;

%run with incident_calc(ModuleAzimuth,alphaDeg,spacing_multiplier,filename)
for i = min:step:max
    j=j+1;
    [percentage(j) kWh(j)]=incident_calc(i,30,2,dataFile);
end

%Plot output!
plot(varu,(1-(percentage))*100)
axis([-45 45 0 8])
xlabel('System Azimuth (°)')
ylabel('Shading losses (%)')
```

```
%Calculate the percentage of maximum output with various spacing multipliers
clear all
close all
clc

j=0;
k=0;

%Load Meteorological Data from NREL for insolation numbers:
[FileName,PathName,FilterIndex] = uigetfile('*.*');
dataFile= [PathName,FileName];

%Set array to run for (in this case Azimuth angles)
min=1.5;
step=.1;
```

```
max=3;
varu=min:step:max;

%run with incident_calc(ModuleAzimuth,alphaDeg,spacing_multiplier,filename)
for i = min:step:max
    j=j+1;
    [percentage(j) kWh(j)]=incident_calc(0,30,i,dataFile);
end

%Plot output!
plot(varu,((percentage))*100)
axis([min max 88 100])
xlabel('Shading Multiplier')
ylabel('Percent max generation')



%Create a Curve to determine spacing multiplier for no more than 2% losses
clear all
close all
clc

j=0;
k=0;

%Load Meteorological Data from NREL for insolation numbers:
[FileName,PathName,FilterIndex] = uigetfile('*.*');
dataFile= [PathName,FileName];

%Set array to run for (in this case Azimuth angles)
min=1.5;
step=2.5;
max=3;
varu=min:step:max;

tilt=0;

out(1:3,1:(45/step)+1)=0;
Azimuth=45;
spacing=0;
i=1;
mult=0;

for tilt=0:step:45
    while(out(3,i)<.98)
        out(3,i)=incident_calc(Azimuth,tilt,mult,dataFile);
        out(1,i)=tilt;
        out(2,i)=mult;
        mult=mult+.01;
    end
    mult=0;
    i=i+1;
end
```

```
%Plot!
plot(out(1,:),out(2,:))
xlabel('Module Tilt (°)');
ylabel('Shading Multiplier');
```

APPENDIX G

Locational Marginal Pricing Compilation

	Jan-08	Feb-08	Mar-08	Apr-08	May-08	Jun-08	Jul-08	Aug-08	Sep-08	Oct-08	Nov-08	Dec-08	Jan-09	Feb-09	Mar-09	Apr-09	May-09	Jun-09	Jul-09	Aug-09	Sep-09	Oct-09	avg
	PJM	PJM	PJM	PJM	PJM	PJM	PJM	PJM	PJM	PJM	PJM	PJM	PJM	PJM	PJM	PJM	PJM	PJM	PJM	PJM	PJM	PJM	
Avg. Energy Cost (PJM)	7.54	7.12	6.84	6.80	5.98	9.36	9.00	7.08	6.50	4.92	5.15	4.93	5.80	4.47	3.91	3.37	3.30	3.27	3.12	3.54	2.98	3.41	5.67
System Total Savings [$]					146.84	293.06	248.03	198.83	140.46	89.96	45.87	39.78	56.89	47.61	56.08	61.56	65.73	61.40	75.76	80.18	50.34	35.12	1490.71
Avg. System Offset (PJM)	7.54	7.12	6.84	6.80	7.93	13.78	12.12	9.44	8.61	5.48	5.40	4.91	5.73	4.14	3.84	3.73	4.02	4.20	3.78	4.46	3.52	3.76	6.86
Avg. Energy Cost during PV Operation [c/kWh]					7.47	11.71	10.77	8.44	7.85	5.50	5.33	4.96	6.00	4.34	4.08	3.64	3.79	3.82	3.51	4.10	3.35	3.76	6.45
Max. Energy Cost during PV Operation [c/kWh]					22.26	48.33	23.65	22.93	25.56	13.45	14.96	14.42	16.71	17.60	16.31	8.81	13.57	10.89	10.43	14.49	10.15	6.99	19.89
Difference					1.94	4.42	3.11	2.36	2.11	0.56	0.25	-0.02	-0.06	-0.33	-0.07	0.36	0.72	0.93	0.66	0.92	0.54	0.35	1.04
																							0.93202

	AECO	AECO	AECO	AECO	AECO	AECO	AECO	AECO	AECO	AECO	AECO	AECO	AECO	AECO	AECO	AECO	AECO	AECO	AECO	AECO	AECO	AECO	
Avg. Energy Cost (¢/kWh)	7.56	6.90	7.66	7.65	9.16	11.98	12.54	8.10	8.20	5.57	5.96	5.46	7.17	4.88	4.26	3.70	3.41	3.37	3.41	3.90	3.17	3.74	6.95
System Total Savings [$]					254.84	379.30	375.26	219.14	181.79	103.80	53.20	44.23	72.84	50.28	60.94	67.63	67.15	60.59	82.32	91.37	53.30	38.16	1930.39
Avg. System Offset (¢/kWh)	7.56	6.90	7.66	7.65	13.76	17.83	18.33	10.40	11.14	6.33	6.26	5.46	7.34	4.37	4.17	4.10	4.11	4.14	4.11	5.08	3.73	4.09	8.74
Avg. Energy Cost during PV Operation [c/kWh]					11.96	15.22	15.75	9.49	9.85	6.26	6.19	5.51	7.62	4.62	4.40	4.02	3.87	3.82	3.84	4.58	3.57	4.14	8.06
Max. Energy Cost during PV Operation [c/kWh]					39.57	50.92	44.61	38.94	48.04	30.29	15.23	16.91	24.70	14.85	18.89	14.78	14.59	15.59	14.19	16.02	11.75	8.83	28.64
Difference					4.59	5.85	5.79	2.31	2.95	0.76	0.30	-0.01	0.17	-0.51	-0.09	0.39	0.69	0.78	0.70	1.18	0.56	0.34	0.42

					May	June	July	August	Septemt	October	Novemb	Decemb	January	Februar	March	April	May	June	July	August	Septemb	October	
kWh Generated					1852.5	2127	2046.87	2106.44	1631.2	1640.2	849.6	810.69	992.3	1151	1461.1	1650.2	1635.2	1462	2002	1798.9	1428.4	933.85	
				(Dates)	######																	######	

Total kWh generated 2008:	13065
Total kWh generated 2009:	14515
Both years:	27579

	PJM	AECO
Total saved 2008:	1202.84	1611.55
Total saved 2009:	590.66	644.58
Both years:	1793.50	2256.13

c/kWh 2008	9.21	12.34
c/kWh 2009	4.07	4.44
c/kWh both years:	6.50	8.18

	Total	2008	2009	Est
PJM				
Average Offset	$6.50	$9.21	$4.07	$8.00
Average Cost	$5.21	$6.99	$3.61	$6.77
Difference	$1.29	$2.21	$0.46	$1.23
Percentage	$0.25	$0.32	$0.13	$0.18
AECO				
Average Offset	$8.18	$12.34	$4.44	$9.94
Average Cost	$6.33	$8.97	$3.61	$8.06
Difference	$1.85	$3.37	$0.83	$1.88
Percentage	$0.29	$0.38	$0.23	$0.23

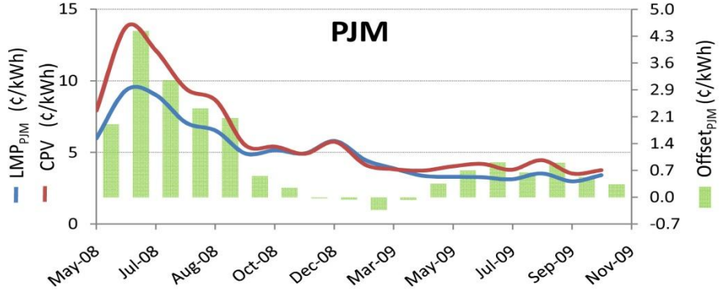

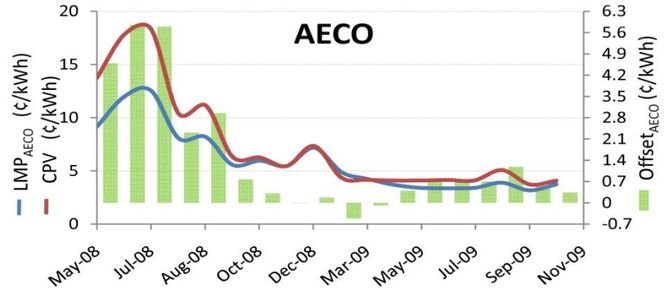

	Outright PV System				
	$4.7/W	$5.38/W	EIA Avg	EIA + PJ	EIA + AECO Offset
2008			14.74¢	16.96¢	18.11¢
2009	15.9¢	18.2¢	14.95¢	15.40¢	15.78¢
Both Ye			14.84¢	16.13¢	16.69¢

APPENDIX H

Worldwide PV Capacity & Wholesale Costs

	Capacity (MW)	Cost ($/W)
1975	0.1	$73.10
1976	0.1	$53.56
1977	0.7	$38.22
1978	2	$30.40
1979	3	$26.06
1980	5	$21.71
1981	9	$20.56
1982	14.7	$16.36
1983	17.4	$15.92
1984	19	$13.32
1985	21	$12.02
1986	25	$10.71
1987	32	$10.13
1988	38	$10.13
1989	43	$10.13
1990	48.4	$9.12
1991	54	$8.83
1992	56	$7.96
1993	61	$7.53
1994	69.4	$6.46
1995	77.6	$6.42
1996	88.6	$5.59
1997	125.8	$5.56
1998	154.9	$5.19
1999	201.3	$4.66
2000	287.7	$4.31
2001	390.5	$4.14
2002	561.8	$4.46
2003	744	$3.70
2004	927	$3.40
2005	1466	$3.50
2006	1744	$3.72
2007	2826	$3.49
2008	5950	$3.60
2009	7300	$2.62

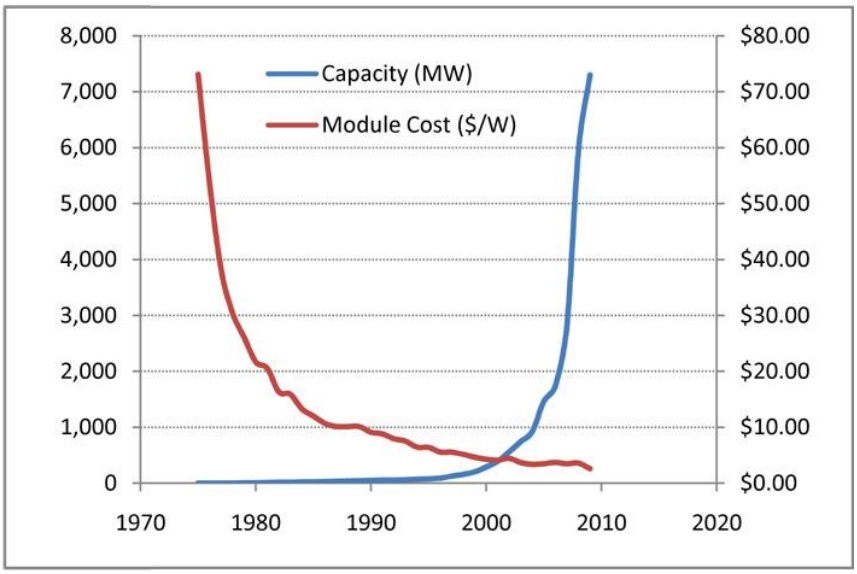

APPENDIX I

Experience Curve Data & Cost Estimates

Year	CPI	1994 Dollars	Nominal Price	2009 Dollars	World Capacity (MW)	US Capacity (MW)	World Cap. (W)	Change in Capacity	Total cumulative produced	Tester	Experience Curve	Min Capacity Est.
1970	38.8											
1971	40.5											
1972	41.8											
1973	44.4											
1974	49.3											
1975	53.8	50.5	18.33	73.1	0.1		100,000		100,000	71.15	69.81	0.1
1976	56.9	37	14.21	53.56	0.1		100,000	0.00%	200,000	71.15	57.93	0.1
1977	60.6	26.4	10.8	38.22	0.7		700,000	600.00%	900,000	39.69	38.63	0.7
1978	65.2	21	9.24	30.4	2		2,000,000	185.70%	2,900,000	28.96	28.19	2
1979	72.6	18	8.82	26.06	3		3,000,000	50.00%	5,900,000	25.65	23.28	3
1980	82.4	15	8.34	21.71	5		5,000,000	66.70%	10,900,000	22.00	19.74	5
1981	90.9	14.2	8.71	20.56	9		9,000,000	80.00%	19,900,000	18.45	16.78	9
1982	96.5	11.3	7.36	16.36	14.7		14,700,000	63.30%	34,600,000	15.92	14.46	14.7
1983	99.6	11	7.39	15.92	17.4		17,400,000	18.40%	52,000,000	10.82	12.96	17.4
1984	103.9	9.2	6.45	13.32	19		19,000,000	9.20%	71,000,000	10.21	11.92	19
1985	107.6	8.3	6.03	12.02	21		21,000,000	10.50%	92,000,000	9.56	11.11	21
1986	109.6	7.4	5.47	10.71	25		25,000,000	19.00%	117,000,000	8.52	10.42	25
1987	113.6	7	5.37	10.13	32		32,000,000	28.00%	149,000,000	7.24	9.76	32
1988	118.3	7	5.59	10.13	38		38,000,000	18.80%	187,000,000	6.46	9.18	38
1989	124	7	5.86	10.13	43	12.83	43,000,000	13.20%	230,000,000	5.95	8.68	43
1990	130.7	6.3	5.56	9.12	48.4	13.84	48,400,000	12.60%	278,400,000	5.51	8.25	48.4
1991	136.2	6.1	5.61	8.83	54	14.94	54,000,000	11.60%	332,400,000	5.12	7.86	54
1992	140.3	5.5	5.21	7.96	56	15.58	56,000,000	3.70%	388,400,000	5.00	7.54	56
1993	144.5	5.2	5.07	7.53	61	20.95	61,000,000	8.90%	449,400,000	4.73	7.25	61
1994	148.2		4.46	6.46	69.4	26.08	69,400,000	13.80%	518,800,000	4.34	6.98	69.4
1995	152.4		4.56	6.42	77.6	31.06	77,600,000	11.80%	596,400,000	4.03	6.72	77.6
1996	156.9		4.09	5.59	88.6	35.46	88,600,000	14.20%	685,000,000	3.69	6.47	88.6
1997	160.5		4.16	5.56	125.8	46.35	125,800,000	42.00%	810,800,000	5.25	6.18	125.8
1998	163		3.94	5.19	154.9	50.56	154,900,000	23.10%	965,700,000	4.99	5.90	154.9
1999	166.6		3.62	4.66	201.3	76.79	201,300,000	30.00%	1,167,000,000	4.68	5.61	201.3
2000	172.2		3.46	4.31	287.7	88.22	287,700,000	42.90%	1,454,700,000	4.28	5.28	287.7
2001	177.1		3.42	4.14	390.5	97.67	390,500,000	35.70%	1,845,200,000	3.97	4.96	390.5
2002	179.9		3.74	4.46	561.8	112.09	561,800,000	43.90%	2,407,000,000	3.63	4.61	561.8
2003	184		3.17	3.7	744	109.36	744,000,000	32.40%	3,151,000,000	3.39	4.29	744
2004	188.9		2.99	3.4	927	181.12	927,000,000	24.60%	4,078,000,000	3.21	4.00	927
2005	195.3		3.19	3.5	1466	226.92	1,466,000,000	58.10%	5,544,000,000	3.65	3.69	1466
2006	201.6		3.5	3.72	1744	337.27	1,744,000,000	19.00%	7,288,000,000	3.56	3.42	1744
2007	207.34		3.37	3.49	2826	517.68	2,826,000,000	62.00%	10,114,000,000	3.33	3.13	2826
2008	215.3		3.59	3.6	5950	986.50	5,950,000,000	110.50%	16,064,000,000	3.00	2.77	5950
2009	214.54			2.62	7300		7,300,000,000	22.70%	23,364,000,000	2.91	2.50	7300
2010												8299.376
2011												9435.568
2012												10727.31
2013												12195.88
2014												13865.51
2015												15763.71
2016												17921.78
2017												20375.28
2018												23164.68
2019												26335.94
2020												29941.35
2021												
2022												
2023												

			Learning Rate	
1983-19	13.69%		-0.27	1550
1997-20	34.11%			
2004-20	51.09%			
total:	26.15%			

Prices			
1975-19	1983-19	1997-20	2004-2009
$68.16			
$57.07			
$38.83			
$28.78			
$23.99			
$20.50			
$17.57			
$15.25			
	$16.25		
	$14.32		
	$12.89		
	$11.69		
	$10.60		
	$9.66		
	$8.89		
	$8.22		
	$7.65		
	$7.18		
	$6.77		
	$6.39		
	$6.04		
	$5.71		
		$5.34	
		$5.06	
		$4.77	
		$4.46	
		$4.15	
		$3.83	
		$3.53	
		$3.26	
			$2.14
			$2.03
			$1.90
			$1.73
			$1.60

Just for Graphs		
Capacity Percent YoY Change	CAGR (Plotting)	Cost Percent YoY Change
18.4%	13.7%	-2.7%
9.2%	13.7%	-16.4%
10.5%	13.7%	-9.8%
19.1%	13.7%	-10.8%
28.0%	13.7%	-5.4%
18.8%	13.7%	0.0%
13.2%	13.7%	0.0%
12.6%	13.7%	-10.0%
11.6%	13.7%	-3.2%
3.7%	13.7%	-9.8%
8.9%	13.7%	-5.5%
13.8%	13.7%	-14.2%
11.8%	13.7%	-0.6%
14.2%	13.7%	-12.9%
42.0%	34.1%	-0.6%
23.1%	34.1%	-6.7%
30.0%	34.1%	-10.1%
42.9%	34.1%	-7.5%
35.7%	34.1%	-3.9%
43.9%	34.1%	7.7%
32.4%	34.1%	-17.1%
24.6%	34.1%	-8.1%
58.1%	51.1%	3.2%
19.0%	51.1%	6.3%
62.0%	51.1%	-6.4%
110.5%	51.1%	3.2%
22.7%	51.1%	-27.2%

	Cumulative Production (MW)						Cost per watt					
	Actual	1983-1996	1997-2004 C	2004-2009 CA	Average CA	PERT	Actual	1983-199	1997-20	2004-20	Average	PERT
1975	0.1						$73.10					
1976	0.2						$53.56					
1977	0.9						$38.22					
1978	2.9						$30.40					
1979	5.9						$26.06					
1980	10.9						$21.71					
1981	19.9						$20.56					
1982	34.6						$16.36					
1983	52						$15.92					
1984	71						$13.32					
1985	92						$12.02					
1986	117						$10.71					
1987	149						$10.13					
1988	187						$10.13					
1989	230						$10.13					
1990	278.4						$9.12					
1991	332.4						$8.83					
1992	388.4						$7.96					
1993	449.4						$7.53					
1994	518.8						$6.46					
1995	596.4						$6.42					
1996	685						$5.59					
1997	810.8						$5.56					
1998	965.7						$5.19					
1999	1167						$4.66					
2000	1454.7						$4.31					
2001	1845.2						$4.14					
2002	2407						$4.46					
2003	3151						$3.70					
2004	4078						$3.40					
2005	5544						$3.50					
2006	7288						$3.72					
2007	10114						$3.49					
2008	16064	16064	16064	16064	16064	16064	$3.60					
2009	23364	23364	23364	23364	23364	23364	$2.62	$2.62	$2.62	$2.62	$2.62	2.62
2010		31,663	33,154	34,394	32,573	32,826		$2.31	$2.28	$2.25	$2.29	$2.28
2011		41,099	46,283	51,059	44,189	45,090		$2.15	$2.08	$2.03	$2.11	$2.10
2012		51,826	63,890	76,240	58,843	60,987		$2.02	$1.91	$1.82	$1.95	$1.93
2013		64,022	87,503	114,287	77,328	81,591		$1.91	$1.75	$1.63	$1.81	$1.79
2014		77,888	119,170	171,773	100,647	108,298		$1.81	$1.61	$1.46	$1.69	$1.66
2015		93,651	161,637	258,632	130,063	142,914		$1.72	$1.49	$1.31	$1.58	$1.54
2016		111,573	218,590	389,872	167,169	187,782		$1.64	$1.37	$1.17	$1.47	$1.43
2017		131,948	294,968	588,167	213,978	245,938		$1.57	$1.26	$1.05	$1.38	$1.33
2018		155,113	397,397	887,779	273,027	321,318		$1.50	$1.17	$0.94	$1.29	$1.24
2019		181,449	534,763	1,340,478	347,514	419,022		$1.44	$1.08	$0.84	$1.21	$1.15
2020		211,390	718,983	2,024,481	441,477	545,662		$1.38	$0.99	$0.75	$1.13	$1.07
2021		245,431	966,037	3,057,971	560,009	709,809		$1.33	$0.92	$0.67	$1.06	$1.00
2022		284,131	1,297,357	4,619,518	709,532	922,570		$1.28	$0.85	$0.60	$1.00	$0.93
2023		328,130	1,741,685	6,978,929	898,151	1,198,342		$1.23	$0.78	$0.54	$0.94	$0.87
2024		378,152	2,337,565	10,543,869	1,136,088	1,555,787		$1.18	$0.72	$0.48	$0.88	$0.81
2025		435,022	3,136,691	15,930,297	1,436,237	2,019,093		$1.14	$0.67	$0.43	$0.83	$0.75
2026		499,678	4,208,384	24,068,893	1,814,866	2,619,613		$1.10	$0.62	$0.39	$0.77	$0.70
2027		573,185	5,645,615	36,365,863	2,292,493	3,397,984		$1.06	$0.57	$0.35	$0.73	$0.65
2028		656,755	7,573,060	54,945,907	2,895,004	4,406,878		$1.02	$0.53	$0.31	$0.68	$0.61
2029		751,767	10,157,925	83,019,329	3,655,052	5,714,568		$0.98	$0.49	$0.28	$0.64	$0.57
2030		859,785	13,624,445	125,436,724	4,613,828	7,409,545		$0.95	$0.45	$0.25	$0.60	$0.53

						Total kWh/	29210.94	29468.5					
	Worldwide Capacity (MW)												
Actual	1983-1996	1997-2004	2004-2009	Average	PERT	BOS	Total Sys	1983-1996	1997-2004	2004-2009	Average	PERT	
0.1													
0.1													
0.7													
2													
3													
5													
9													
14.7													
17.4													
19													
21													
25													
32													
38													
43													
48.4													
54													
56													
61													
69.4													
77.6													
88.6													
125.8													
154.9							$5.31	10.5					
201.3							$6.34	11					
287.7							$4.94	9.25					
390.5							$5.66	9.8					
561.8							$5.34	9.8					
744							$4.55	8.25					
927							$4.60	8					
1466							$4.00	7.5					
1744							$3.88	7.6					
2826							$4.11	7.6					
5950							$3.60	7.2					
7300	7300	7300	7300	7300	7300	$2.94	$5.56	$5.56	$5.56	$5.56	$5.56	$5.56	
	8,299	9,790	11,030	9,209	9,462	$2.91		$5.21	$5.18	$5.16	$5.19	$5.19	
	9,436	13,129	16,666	11,616	12,264	$2.88		$5.03	$4.96	$4.90	$4.99	$4.97	
	10,727	17,607	25,181	14,654	15,896	$2.85		$4.87	$4.76	$4.67	$4.80	$4.78	
	12,196	23,613	38,047	18,485	20,604	$2.82		$4.73	$4.57	$4.45	$4.63	$4.61	
	13,866	31,667	57,487	23,319	26,707	$2.79		$4.60	$4.41	$4.25	$4.48	$4.45	
	15,764	42,468	86,859	29,416	34,616	$2.76		$4.49	$4.25	$4.07	$4.34	$4.30	
	17,922	56,953	131,239	37,107	44,868	$2.74		$4.38	$4.11	$3.91	$4.21	$4.16	
	20,375	76,378	198,295	46,809	58,156	$2.71		$4.28	$3.97	$3.76	$4.09	$4.04	
	23,165	102,429	299,613	59,048	75,380	$2.68		$4.19	$3.85	$3.62	$3.97	$3.92	
	26,336	137,366	452,699	74,487	97,704	$2.66		$4.10	$3.73	$3.50	$3.86	$3.81	
	29,941	184,220	684,003	93,963	126,641	$2.63		$4.01	$3.62	$3.38	$3.76	$3.70	
	34,040	247,054	1,033,490	118,531	164,147	$2.60		$3.93	$3.52	$3.28	$3.67	$3.60	
	38,701	331,320	1,561,547	149,524	212,761	$2.58		$3.85	$3.42	$3.18	$3.57	$3.51	
	43,999	444,328	2,359,411	188,619	275,772	$2.55		$3.78	$3.33	$3.09	$3.49	$3.42	
	50,022	595,880	3,564,940	237,937	357,445	$2.53		$3.71	$3.25	$3.01	$3.40	$3.33	
	56,870	799,125	5,386,428	300,149	463,306	$2.50		$3.64	$3.17	$2.93	$3.33	$3.25	
	64,656	1,071,694	8,138,596	378,628	600,520	$2.47		$3.57	$3.09	$2.86	$3.25	$3.18	
	73,507	1,437,230	12,296,970	477,627	778,371	$2.45		$3.51	$3.02	$2.80	$3.18	$3.10	
	83,570	1,927,446	18,580,044	602,511	1,008,894	$2.43		$3.44	$2.95	$2.74	$3.11	$3.04	
	95,011	2,584,865	28,073,423	760,048	1,307,690	$2.40		$3.38	$2.89	$2.68	$3.04	$2.97	
	108,018	3,466,519	42,417,395	958,776	1,694,977	$2.38		$3.33	$2.83	$2.63	$2.98	$2.91	

Outright System ¢/kWh					LSPV & Optimization Savings Applied ¢/kWh				
Actual	1983-1996	2004-2009	Average	PERT	Actual	1983-1996	2004-2009	Average	PERT
35.95¢					33.93¢				
37.66¢					35.42¢				
31.67¢					29.85¢				
33.55¢					31.55¢				
33.55¢					31.61¢				
28.24¢					26.60¢				
27.39¢					25.76¢				
25.68¢					24.20¢				
26.02¢					24.56¢				
26.02¢					24.52¢				
24.65¢					23.27¢				
19.02¢	19.02¢	19.02¢	19.02¢	19.02¢	17.93¢	17.93¢	17.93¢	17.93¢	17.93¢
	17.69¢	17.48¢	17.62¢	17.61¢		16.64¢	16.44¢	16.58¢	16.56¢
	16.82¢	16.33¢	16.66¢	16.63¢		15.81¢	15.33¢	15.65¢	15.62¢
	16.07¢	15.28¢	15.81¢	15.76¢		15.08¢	14.31¢	14.83¢	14.78¢
	15.40¢	14.32¢	15.05¢	14.98¢		14.43¢	13.38¢	14.08¢	14.02¢
	14.79¢	13.44¢	14.34¢	14.25¢		13.83¢	12.53¢	13.40¢	13.32¢
	14.22¢	12.64¢	13.69¢	13.58¢		13.29¢	11.76¢	12.77¢	12.67¢
	13.70¢	11.91¢	13.08¢	12.96¢		12.78¢	11.05¢	12.18¢	12.06¢
	13.20¢	11.24¢	12.51¢	12.37¢		12.30¢	10.40¢	11.63¢	11.50¢
	12.74¢	10.63¢	11.97¢	11.82¢		11.85¢	9.80¢	11.10¢	10.96¢
	12.30¢	10.06¢	11.46¢	11.31¢		11.42¢	9.26¢	10.61¢	10.46¢
	11.87¢	9.54¢	10.98¢	10.82¢		11.01¢	8.75¢	10.15¢	9.99¢
	11.47¢	9.06¢	10.52¢	10.35¢		10.62¢	8.29¢	9.70¢	9.54¢
	11.09¢	8.62¢	10.09¢	9.91¢		10.25¢	7.86¢	9.28¢	9.11¢
	10.72¢	8.20¢	9.68¢	9.50¢		9.90¢	7.46¢	8.88¢	8.71¢
	10.37¢	7.82¢	9.28¢	9.10¢		9.55¢	7.09¢	8.50¢	8.33¢
	10.03¢	7.47¢	8.91¢	8.73¢		9.23¢	6.74¢	8.14¢	7.96¢
	9.70¢	7.14¢	8.55¢	8.37¢		8.91¢	6.42¢	7.80¢	7.62¢
	9.39¢	6.83¢	8.21¢	8.03¢		8.60¢	6.13¢	7.47¢	7.29¢
	9.08¢	6.54¢	7.89¢	7.70¢		8.31¢	5.85¢	7.16¢	6.97¢
	8.79¢	6.27¢	7.58¢	7.40¢		8.03¢	5.58¢	6.86¢	6.68¢
	8.51¢	6.01¢	7.29¢	7.10¢		7.76¢	5.34¢	6.57¢	6.39¢

ITC Applied ¢/kWh						SRECs Applied ¢/kWh				SRECs (with 1250kWh)		
Actual	1983-1996	2004-2009	Average	PERT	ITC %	Actual	1983-1996	2004-2009	Average			
35.95¢						35.95¢						
37.66¢						37.66¢						
31.67¢						31.67¢						
33.55¢						33.55¢						
33.55¢						33.55¢						
28.24¢						28.24¢						
27.39¢						27.39¢						
25.68¢						25.68¢						
26.02¢						26.02¢						
26.02¢						26.02¢						
17.25¢					30%	6.37¢	6.37¢	6.37¢	6.37¢	$5,339.66		
13.31¢	13.31¢	13.31¢	13.31¢	13.31¢	30%	3.01¢	3.01¢	3.01¢	3.01¢	$4,677.37		
	12.38¢	12.23¢	12.33¢	12.32¢	30%		3.91¢	3.80¢	3.69¢	$4,025.99		
	11.78¢	11.43¢	11.66¢	11.64¢	30%		5.23¢	4.99¢	4.74¢	$3,385.69		
	11.25¢	10.69¢	11.07¢	11.03¢	30%		6.64¢	6.24¢	5.84¢	$2,755.82		
	10.78¢	10.02¢	10.53¢	10.48¢	30%		8.08¢	7.55¢	7.00¢	$2,136.53		
	10.35¢	9.41¢	10.04¢	9.98¢	30%		9.56¢	8.88¢	8.21¢	$1,527.00		
	9.96¢	8.85¢	9.58¢	9.51¢	30%		11.05¢	10.24¢	9.47¢	$927.37		
	9.59¢	8.34¢	9.15¢	9.07¢	30%		12.54¢	11.61¢	10.76¢	$336.81		
	13.20¢	11.24¢	12.51¢	12.37¢	0%		12.29¢	11.24¢	10.33¢	$267.14		
	12.74¢	10.63¢	11.97¢	11.82¢	0%		12.06¢	10.91¢	9.95¢	$198.52		
	12.30¢	10.06¢	11.46¢	11.31¢	0%		11.85¢	10.61¢	9.61¢	$130.97		
	11.87¢	9.54¢	10.98¢	10.82¢	0%		11.65¢	10.33¢	9.32¢	$64.80		
	11.47¢	9.06¢	10.52¢	10.35¢	0%		11.47¢	10.08¢	9.06¢			
	11.09¢	8.62¢	10.09¢	9.91¢	0%		11.09¢	9.64¢	8.62¢			
	10.72¢	8.20¢	9.68¢	9.50¢	0%		10.72¢	9.22¢	8.20¢			
	10.37¢	7.82¢	9.28¢	9.10¢	0%		10.37¢	8.82¢	7.82¢			
	10.03¢	7.47¢	8.91¢	8.73¢	0%		10.03¢	8.44¢	7.47¢			
	9.70¢	7.14¢	8.55¢	8.37¢	0%		9.70¢	8.08¢	7.14¢			
	9.39¢	6.83¢	8.21¢	8.03¢	0%		9.39¢	7.75¢	6.83¢			
	9.08¢	6.54¢	7.89¢	7.70¢	0%		9.08¢	7.42¢	6.54¢			
	8.79¢	6.27¢	7.58¢	7.40¢	0%		8.79¢	7.12¢	6.27¢			
	8.51¢	6.01¢	7.29¢	7.10¢	0%		8.51¢	6.83¢	6.01¢			

SRECs + ITC Applied ¢/kWh				All Applied ¢/kWh			
Actual	1983-1996	2004-2009	Average	Actual	1983-1996	2004-2009	Average
35.95¢				33.93¢			
37.66¢				35.42¢			
31.67¢				29.85¢			
33.55¢				31.55¢			
33.55¢				31.61¢			
28.24¢				26.60¢			
27.39¢				25.76¢			
25.68¢				24.20¢			
26.02¢				24.56¢			
26.02¢				24.52¢			
-1.03¢				-1.48¢			
-2.70¢	-2.70¢	-2.70¢	-2.70¢	-3.10¢	-3.10¢	-3.09¢	-3.09¢
	-1.40¢	-1.55¢	-1.45¢		-1.83¢	-1.97¢	-1.88¢
	0.19¢	-0.16¢	0.07¢		-0.29¢	-0.63¢	-0.40¢
	1.82¢	1.26¢	1.64¢		1.29¢	0.75¢	1.11¢
	3.47¢	2.71¢	3.22¢		2.88¢	2.15¢	2.64¢
	5.12¢	4.18¢	4.81¢		4.49¢	3.58¢	4.19¢
	6.78¢	5.68¢	6.41¢		6.10¢	5.02¢	5.73¢
	8.44¢	7.18¢	8.00¢		7.70¢	6.49¢	7.28¢
	12.29¢	10.33¢	11.59¢		11.43¢	9.53¢	10.75¢
	12.06¢	9.95¢	11.29¢		11.21¢	9.16¢	10.46¢
	11.85¢	9.61¢	11.01¢		11.00¢	8.84¢	10.19¢
	11.65¢	9.32¢	10.76¢		10.81¢	8.55¢	9.95¢
	11.47¢	9.06¢	10.52¢		10.64¢	8.30¢	9.72¢
	11.09¢	8.62¢	10.09¢		10.27¢	7.87¢	9.30¢
	10.72¢	8.20¢	9.68¢		9.91¢	7.47¢	8.90¢
	10.37¢	7.82¢	9.28¢		9.57¢	7.10¢	8.52¢
	10.03¢	7.47¢	8.91¢		9.24¢	6.76¢	8.16¢
	9.70¢	7.14¢	8.55¢		8.92¢	6.44¢	7.81¢
	9.39¢	6.83¢	8.21¢		8.62¢	6.14¢	7.48¢
	9.08¢	6.54¢	7.89¢		8.33¢	5.86¢	7.17¢
	8.79¢	6.27¢	7.58¢		8.04¢	5.60¢	6.87¢
	8.51¢	6.01¢	7.29¢		7.77¢	5.35¢	6.58¢

APPENDIX J

LMP Data Extractor & Calc

```
%Program to extract PJM LMP data and combine it with recorded data from
%SMA's SunnyPortal Website.
%Calculates difference between PV electricity costs with LMP and standard
%rates. Created by Ulrich KW Schwabe 2009 at the Rowan University CSD
%

clear all; close all;
clc;
%Load File, rename it and create a results folder.
[FileName,PathName,FilterIndex] = uigetfile('*.*');
name = [PathName,FileName];
% Sheet1 = load(name, 'v1');

max_num_col = 85;
format = ['%s %s %s %s %s %s %s',repmat('%f',1,max_num_col)];
fid = fopen(name);
tester = textscan(fid,format,'delimiter',',');
fclose(fid);

%Find the start of the data we need:
i=1;
StartOfData=1;
while i==1,
   if(ischar(tester{1}{StartOfData}))
       if(isempty(tester{1}{StartOfData}))
       else
            if(strcmp(tester{1}{StartOfData}(1:4),'Date'))
                i=0;
            end
       end
   end
   StartOfData = StartOfData+1;
end

fid = fopen(name);
max_num_col = 85;   %Max Columns, adjust if necessary!!!
format = ['%s %s %s %s %s %s %s',repmat('%f',1,max_num_col)];
LMPdata      =      textscan(fid,      format,      'delimiter',      ',',
'headerlines',StartOfData+2);

%Extract only the PJM and AECO data we want
countPJM=0;
for i = 1:length(LMPdata{3})
    if(strcmp(LMPdata{3}(i), 'PJM'))
        countPJM=countPJM+1;
        date{countPJM}=[LMPdata{1}{i}(1:4)    '/'    LMPdata{1}{i}(5:6)    '/'
LMPdata{1}{i}(7:8)];
        namePJM{countPJM}='PJM';
```

```
        k=1;
        for j = 8:3:79
            LMPcostPJM(countPJM,k)=LMPdata{j}(i);
            k=k+1;
        end
    end
end
countAECO=0;
for i = 1:length(LMPdata{3})
    if(strcmp(LMPdata{3}(i), 'AECO'))
        countAECO=countAECO+1;
        nameAECO{countAECO}='AECO';
        k=1;
        for j = 8:3:79
            LMPcostAECO(countAECO,k)=LMPdata{j}(i);
            k=k+1;
        end
    end
end

PJMsize=size(LMPcostPJM);
PJMLMP=reshape(LMPcostPJM',PJMsize(1)*PJMsize(2),1);

%Fix hours
h=0;
for i=1:PJMsize(1)*PJMsize(2)
    h=h+1;
    if(h==25)
        h=1;
    end
    hours(i)=h;
end

AECOsize=size(LMPcostAECO);
AECOLMP=reshape(LMPcostAECO',AECOsize(1)*AECOsize(2),1);

h=0;
for i=1:AECOsize(1)*AECOsize(2)
    h=h+1;
    if(h==25)
        h=1;
    end
    hoursAECO(i)=h;
end

%Create a giant Cell Array of all data in the correct format
datecount=1;
for i = 1:length(PJMLMP)
    plop{1}(i)=date(datecount);
    plop{2}(i)=hours(i);
    plop{3}(i)=PJMLMP(i);
    plop{4}(i)=AECOLMP(i);

    if(mod(i,24)==0)
        datecount=datecount+1;
```

```
    end
end


%%%%%%%%%%%%%Load kWh sheet%%%%%%%%%%%%%%%

%Load File, rename it and create a results folder.
[FileName2,PathName2,FilterIndex2] = uigetfile('*.*');
name2 = [PathName2,FileName2];

fid2 = fopen(name2);
kWhdata    =    textscan(fid2,    '%s    %f    %f    %f    %f',    'delimiter',    ';',
'headerlines',1);

%Convert NaNs to 0s
rmnan=isnan(kWhdata{2});
kWhdata{2}(rmnan)=0;
clear rmnan;
rmnan=isnan(kWhdata{3});
kWhdata{3}(rmnan)=0;
clear rmnan;
rmnan=isnan(kWhdata{4});
kWhdata{4}(rmnan)=0;
clear rmnan;
rmnan=isnan(kWhdata{5});
kWhdata{5}(rmnan)=0;
clear rmnan;


%%%%%%%%%%%%%Load Temp/Insolation sheet%%%%%%%%%%%%%%%

%Load File, rename it and create a results folder.
[FileName3,PathName3,FilterIndex3] = uigetfile('*.*');
name3 = [PathName3,FileName3];

fid3 = fopen(name3);
tempData    =    textscan(fid3,    '%s    %f    %f    %f    %f',    'delimiter',    ';',
'headerlines',1);

%Convert NaNs to 0s
rmnan=isnan(tempData{2});
tempData{2}(rmnan)=0;
clear rmnan;
rmnan=isnan(tempData{3});
tempData{3}(rmnan)=0;
clear rmnan;
rmnan=isnan(tempData{4});
tempData{4}(rmnan)=0;
clear rmnan;
rmnan=isnan(tempData{5});
tempData{5}(rmnan)=0;
clear rmnan;

%Pre-initialize everything
```

```
STPkWhTotal = zeros(length(PJMLMP),1);
TotalkWh = zeros(length(PJMLMP),1);
PJMckWh = zeros(length(PJMLMP),1);
AECOckWh = zeros(length(PJMLMP),1);
TotalSavedPJM= zeros(length(PJMLMP),1);
TotalSavedAECO=zeros(length(PJMLMP),1);
    kWhDuringPVOperationPJM=0;
    kWhDuringPVOperationAECO=0;

%Calculate various information
HourCounter=0;
for i = 1:length(PJMLMP)
    STPkWhTotal(i) = kWhdata{3}(i)+ kWhdata{4}(i) + kWhdata{5}(i); %Total
SunTechPower System kWh
    TotalkWh(i) = STPkWhTotal(i)+ kWhdata{2}(i); %Total kWh for both systems
    PJMckWh(i) = (plop{3}(i)*100)/1000; %PJM costs per kWh
    AECOckWh(i) = (plop{4}(i)*100)/1000; %AECO costs per kWh
    TotalSavedPJM(i)= PJMckWh(i) * TotalkWh(i); %Total money saved on PJM
with both systems
    TotalSavedAECO(i)= AECOckWh(i) * TotalkWh(i); %Total money saved on AECO
with both systems
    if (TotalkWh(i)>0.01)
        kWhDuringPVOperationPJM = kWhDuringPVOperationPJM + PJMckWh(i);
        kWhDuringPVOperationAECO = kWhDuringPVOperationAECO + AECOckWh(i);
        HourCounter=HourCounter+1;
    end
end


%%%%%%%%%%%%%%Print Data to new File%%%%%%%%%%%%%%%
new_file=fopen([name(1:length(name)-4) '_processed.csv'],'w');
fprintf(new_file,'Date, Hour, SPDate_kWh, SPDate_Temps, PJM, AECO, Kaneka
kWh, ST kWh, Total kWh, Pyranometer Insolation [W/m^2], Sensorbox Insolation
[W/m^2], Ambient T [C], Module T [C],Total Saved PJM, Total Saved AECO,,,
PJM, AECO\r\n');

for i = 1:length(PJMLMP)
    %Add Time/Dates for each sheet (for comparison purposes)
    fprintf(new_file,'%s',plop{1}{i}); %Date
    fprintf(new_file,',');
    fprintf(new_file,'%d',plop{2}(i)); %Hour
    fprintf(new_file,',');
    fprintf(new_file,'%s',kWhdata{1}{i}); %SPDate
    fprintf(new_file,',');
    fprintf(new_file,'%s',tempData{1}{i}); %SPDate2
    fprintf(new_file,',');

    %Add LMP Data
    fprintf(new_file,'%g',plop{3}(i)); %PJM $/MWh
    fprintf(new_file,',');
    fprintf(new_file,'%g',plop{4}(i)); %AECO $/MWh
    fprintf(new_file,',');

    %Add production Data
    fprintf(new_file,'%g',kWhdata{2}(i)); %Kaneka kWh
```

```
fprintf(new_file,',');
fprintf(new_file,'%g',STPkWhTotal(i)); %Total STP kWh
fprintf(new_file,',');
fprintf(new_file,'%g',TotalkWh(i)); %Total kWh (both systems)
fprintf(new_file,',');

%Add temp/insolation Data
fprintf(new_file,'%g',tempData{2}(i)); %Pyranometer Insol
fprintf(new_file,',');
fprintf(new_file,'%g',tempData{3}(i)); %Sensorbox Insol
fprintf(new_file,',');
fprintf(new_file,'%g',tempData{4}(i)); %Ambient T
fprintf(new_file,',');
fprintf(new_file,'%g',tempData{5}(i)); %Module T
fprintf(new_file,',');

%Add totals
fprintf(new_file,'%g',TotalSavedPJM(i));
fprintf(new_file,',');
fprintf(new_file,'%g',TotalSavedAECO(i));
fprintf(new_file,',');

% Print Special Info
if(i==1)
    fprintf(new_file,',');
    fprintf(new_file,'Average Energy Cost [c/kWh]');
    fprintf(new_file,',');
    fprintf(new_file,'%g', mean(PJMckWh));
    fprintf(new_file,',');
    fprintf(new_file,'%g', mean(AECOckWh));
    fprintf(new_file,',');
end
if(i==2)
    fprintf(new_file,',');
    fprintf(new_file,'System Total Savings [$]');
    fprintf(new_file,',');
    fprintf(new_file,'%g', sum(TotalSavedPJM)/100);
    fprintf(new_file,',');
    fprintf(new_file,'%g', sum(TotalSavedAECO)/100);
    fprintf(new_file,',');
end
if(i==3)
    fprintf(new_file,',');
    fprintf(new_file,'Avg. System Offset [c/kWh]');
    fprintf(new_file,',');
    fprintf(new_file,'%g', sum(TotalSavedPJM)/(sum(TotalkWh)));
    fprintf(new_file,',');
    fprintf(new_file,'%g', sum(TotalSavedAECO)/(sum(TotalkWh)));
    fprintf(new_file,',');
end
if(i==4)
    fprintf(new_file,',');
    fprintf(new_file,'Avg. Energy Cost during PV Operation [c/kWh]');
    fprintf(new_file,',');
    fprintf(new_file,'%g', kWhDuringPVOperationPJM/HourCounter);
    fprintf(new_file,',');
```

```
            fprintf(new_file,'%g', kWhDuringPVOperationAECO/HourCounter);
            fprintf(new_file,',');
        end
        if(i==5)
            fprintf(new_file,',');
            fprintf(new_file,'Max. Energy Cost during PV Operation [c/kWh]');
            fprintf(new_file,',');
            fprintf(new_file,'%g', max(PJMLMP(TotalkWh>.01))/10);
            fprintf(new_file,',');
            fprintf(new_file,'%g', max(AECOLMP(TotalkWh>.01))/10);
            fprintf(new_file,',');
        end

        fprintf(new_file,'\r\n');
    end

    fclose(new_file);

        disp(['Done! Output file: ' [name(1:length(name)-4) '_processed.csv']])
```

APPENDIX K

Financial Data Sets

System Capacity:	1,000,000W	
Cost of System:	5	$ 5,000,000
ITC (of 80% dep):	30%	$ 1,200,000
Financing:	50%	
Bonus Depreciation:	0%	
Interest Rate:	8%	
Length of loan:	6Yr	
Tax Rate:	45%	
25yr dep. property basis	20%	
5yr dep. property basis	80%	$ 1,000,000
Initial Fees&O&M	4%	$ 3,400,000
Fees& O&M	1%	
kWh Generated over life	27,687,000	
IRR:	9.88%	

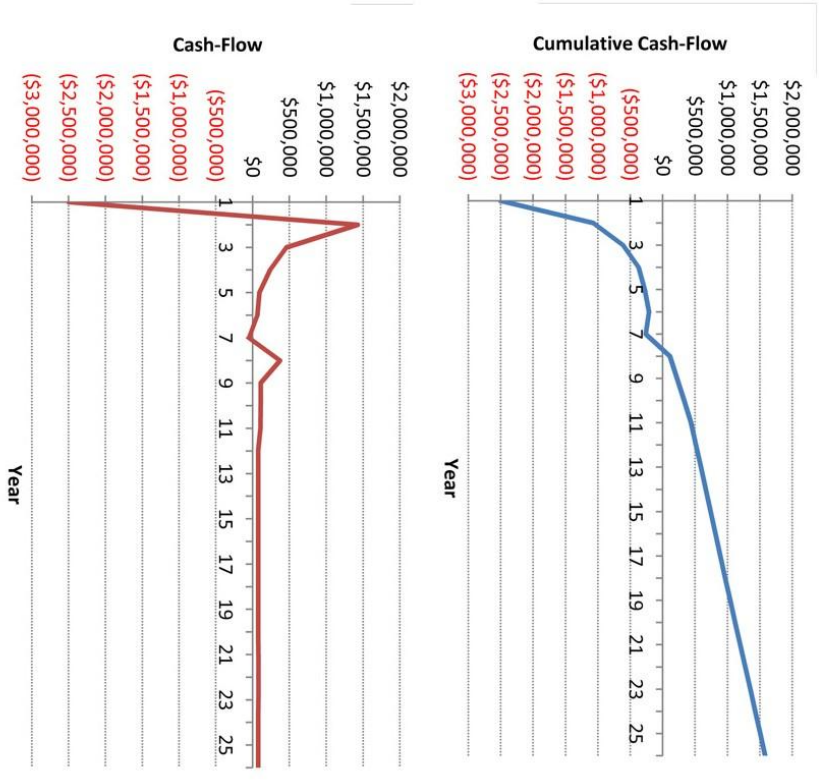

Year	SREC	Electricity	Revenue	Maintenance, Insurance, Legal	Operating Income
0					
1	668,250	179,043	847,293	($200,000)	647,293
2	644,350	163,884	808,234	($50,000)	758,234
3	620,800	163,472	784,272	($50,000)	734,272
4	600,000	160,717	760,717	($50,000)	710,717
5	578,313	159,219	737,532	($50,000)	687,532
6	558,125	157,369	715,494	($50,000)	665,494
7	538,238	156,213	694,450	($50,000)	644,450
8	63,250	155,216	218,466	($50,000)	168,466
9	60,288	154,542	214,830	($50,000)	164,830
10	57,375	154,180	211,555	($50,000)	161,555
11	0	154,862	154,862	($50,000)	104,862
12	0	154,857	154,857	($50,000)	104,857
13	0	153,366	153,366	($50,000)	103,366
14	0	152,689	152,689	($50,000)	102,689
15	0	152,810	152,810	($50,000)	102,810
16	0	154,028	154,028	($50,000)	104,028
17	0	155,684	155,684	($50,000)	105,684
18	0	156,825	156,825	($50,000)	106,825
19	0	157,772	157,772	($50,000)	107,772
20	0	158,529	158,529	($50,000)	108,529
21	0	158,488	158,488	($50,000)	108,488
22	0	158,731	158,731	($50,000)	108,731
23	0	157,440	157,440	($50,000)	107,440
24	0	156,149	156,149	($50,000)	106,149
25	0	154,857	154,857	($50,000)	104,857
Total:	**$4,388,987.50**	**$3,940,941.80**	**$8,329,929.30**	**($1,400,000.00)**	**$6,929,929.30**

ome & Expenditures		
25 yr MACRS	MACRS	Total Dep Deduction
(40,000)	(680,000)	(720,000)
(40,000)	(1,088,000)	(1,128,000)
(40,000)	(652,800)	(692,800)
(40,000)	(391,680)	(431,680)
(40,000)	(391,680)	(431,680)
(40,000)	(195,840)	(235,840)
(40,000)		(40,000)
(40,000)		(40,000)
(40,000)		(40,000)
(40,000)		(40,000)
(40,000)		(40,000)
(40,000)		(40,000)
(40,000)		(40,000)
(40,000)		(40,000)
(40,000)		(40,000)
(40,000)		(40,000)
(40,000)		(40,000)
(40,000)		(40,000)
(40,000)		(40,000)
(40,000)		(40,000)
(40,000)		(40,000)
(40,000)		(40,000)
(40,000)		(40,000)
($1,000,000.00)	($3,400,000.00)	($4,400,000.00)

			Taxes		
EBIntT	Interest	EBT	Income tax	Tax Credits	Tax Total
(72,707)	(200,000)	(272,707)	122,718	1,200,000	1,322,718
(369,766)	(172,737)	(542,503)	244,126		244,126
41,472	(143,293)	(101,821)	45,820		45,820
279,037	(111,493)	167,544	(75,395)		(75,395)
255,852	(77,150)	178,702	(80,416)		(80,416)
429,654	(40,058)	389,596	(175,318)		(175,318)
604,450	0	604,450	(272,003)		(272,003)
128,466	0	128,466	(57,810)		(57,810)
124,830	0	124,830	(56,173)		(56,173)
121,555	0	121,555	(54,700)		(54,700)
64,862	0	64,862	(29,188)		(29,188)
64,857	0	64,857	(29,186)		(29,186)
63,366	0	63,366	(28,515)		(28,515)
62,689	0	62,689	(28,210)		(28,210)
62,810	0	62,810	(28,265)		(28,265)
64,028	0	64,028	(28,813)		(28,813)
65,684	0	65,684	(29,558)		(29,558)
66,825	0	66,825	(30,071)		(30,071)
67,772	0	67,772	(30,497)		(30,497)
68,529	0	68,529	(30,838)		(30,838)
68,488	0	68,488	(30,820)		(30,820)
68,731	0	68,731	(30,929)		(30,929)
67,440	0	67,440	(30,348)		(30,348)
66,149	0	66,149	(29,767)		(29,767)
64,857	0	64,857	(29,186)		(29,186)
$2,529,929.30	**($744,730.79)**	**$1,785,198.51**	**($803,339.33)**	**$1,200,000.00**	**$396,660.67**

Non-tax deductible depr.	Net Income	Principal Payment	Depreciation	Cash Flow Annual	Cash Flow Cumulative
				(2,500,000)	(2,500,000)
(24,000)	1,026,011	(340,788)	744,000	1,429,223	(1,070,777)
(24,000)	(322,377)	(368,052)	1,152,000	461,572	(609,206)
(24,000)	(80,002)	(397,496)	716,800	239,303	(369,903)
(24,000)	68,149	(429,295)	455,680	94,534	(275,369)
(24,000)	74,286	(463,639)	455,680	66,327	(209,042)
(24,000)	190,278	(500,730)	259,840	(50,613)	(259,654)
(24,000)	308,448	0	64,000	372,448	112,793
(24,000)	46,656	0	64,000	110,656	223,450
(24,000)	44,656	0	64,000	108,656	332,106
(24,000)	42,855	0	64,000	106,855	438,961
(24,000)	11,674	0	64,000	75,674	514,635
(24,000)	11,671	0	64,000	75,671	590,307
(24,000)	10,851	0	64,000	74,851	665,158
(24,000)	10,479	0	64,000	74,479	739,637
(24,000)	10,546	0	64,000	74,546	814,183
(24,000)	11,216	0	64,000	75,216	889,398
(24,000)	12,126	0	64,000	76,126	965,525
(24,000)	12,753	0	64,000	76,753	1,042,278
(24,000)	13,274	0	64,000	77,274	1,119,552
(24,000)	13,691	0	64,000	77,691	1,197,244
(24,000)	13,668	0	64,000	77,668	1,274,912
(24,000)	13,802	0	64,000	77,802	1,352,714
(24,000)	13,092	0	64,000	77,092	1,429,806
(24,000)	12,382	0	64,000	76,382	1,506,188
(24,000)	11,672	0	64,000	75,672	1,581,859
($600,000.00)	**$1,581,859.18**	**($2,500,000.00)**	**$5,000,000.00**	**$1,581,859.18**	

				MACRS (%)				
	SRECs per MW	Utility Cost	kWh/kW	5yr	25yr	25yr (non Tax	Bonus Depreciati	kWh Generated
1	540.00	14.47	1238	20.00%	4.00%	2.00%	0.00%	1,237,500
2	526.00	13.38	1225	32.00%	4.00%	2.00%		1,225,000
3	512.00	13.48	1213	19.20%	4.00%	2.00%		1,212,500
4	500.00	13.39	1200	11.52%	4.00%	2.00%		1,200,000
5	487.00	13.41	1188	11.52%	4.00%	2.00%		1,187,500
6	475.00	13.39	1175	5.76%	4.00%	2.00%		1,175,000
7	463.00	13.44	1163		4.00%	2.00%		1,162,500
8	55.00	13.50	1150		4.00%	2.00%		1,150,000
9	53.00	13.59	1138		4.00%	2.00%		1,137,500
0	51.00	13.70	1125		4.00%	2.00%		1,125,000
	0.00	13.87	1117		4.00%	2.00%		1,116,663
	0.00	13.97	1108		4.00%	2.00%		1,108,325
	0.00	13.94	1100		4.00%	2.00%		1,099,988
	0	13.99	1092		4.00%	2.00%		1,091,650
	0	14.11	1083		4.00%	2.00%		1,083,313
	0	14.33	1075		4.00%	2.00%		1,074,975
	0	14.60	1067		4.00%	2.00%		1,066,638
	0	14.82	1058		4.00%	2.00%		1,058,300
	0	15.03	1050		4.00%	2.00%		1,049,963
	0	15.22	1042		4.00%	2.00%		1,041,625
	0	15.34	1033		4.00%	2.00%		1,033,288
	0	15.49	1025		4.00%	2.00%		1,024,950
	0	15.49	1017		4.00%	2.00%		1,016,613
	0	15.49	1008		4.00%	2.00%		1,008,275
	0	15.49	1000		4.00%	2.00%		999,938